University of Nevada, Reno

Application of Hydrothermal Carbonization, Membrane Distillation, and Algae Cultivation for Sustainable Dairy Manure Treatment

A dissertation submitted in partial fulfillment of the requirement for the degree of

Doctor of Philosophy in Chemical Engineering

By

Nicholas Silva

Dr. Sage R. Hiibel/Dissertation Advisor

May 2023

THE GRADUATE SCHOOL

We recommend that the dissertation
prepared under our supervision by

Nicholas Silva

entitled

Application of Hydrothermal Carbonization, Membrane Distillation, and Algae Cultivation for Sustainable Dairy Manure Treatment

be accepted in partial fulfillment of the
requirements for the degree of

Doctor of Philosophy

Sage R. Hiibel, Ph. D.
Advisor

Charles J. Coronella, Ph. D.
Committee Member

David C. Cantu, Ph. D.
Committee Member

Jeffrey LaCombe, Ph. D.
Committee Member

David Hanigan, Ph. D.
Graduate School Representative

Markus Kemmelmeier, Ph.D., Dean
Graduate School

May, 2023

ABSTRACT

Dairy production has grown more efficient as the number of cows on each facility increases; however, this expansion has also increased the concentration of localized manure that can lead to environmental concerns such as greenhouse gas emissions or eutrophication. This dissertation investigates a sustainable alternative to conventional dairy manure treatment methods that incorporates hydrothermal carbonization (HTC), algae cultivation, and membrane distillation (MD). HTC converts dairy manure into a low-grade coal that can be used as an energy source, while expelling nutrients into the HTC aqueous product (HAP). The algae can be cultivated on the HAP, where they consume the nutrients, reduce eutrophication risk, and when harvested, can be used as a protein supplement for the cattle on-site. The algal supernatant can be treated with MD to produce clean water and replace conventional reverse osmosis systems. The parts of the project investigated in this work include the potential to remediate the HAP, cultivate the algae, and treat the supernatant using MD.

Arthrospira maxima, *Chlamydomonas reinhardtii*, *Chlorella vulgaris*, and *Scenedesmus obliquus* were microalgae strains selected for this work due to their high protein content or potential to be cultivated on wastewater. All four species are capable of heterotrophic growth. The screening process revealed dilution to 5% HAP was required for successful cultivation, with little growth observed at higher concentrations. *A. maxima* remediated the most COD, TN, TP, and NH_3 in the HAP, followed by *C. reinhardtii*; both strains averaged 43% protein content. The other strains removed fewer nutrients and had lower protein content when grown on HAP. Of the four species, *A. maxima* had the highest growth rate but required a bicarbonate pH buffer that introduced other environmental

complications. Both *A. maxima* and *C. reinhardtii* were moved forward as the preferred candidates for nutrient utilization and dietary supplements as buffered and non-buffered species.

The supernatants of the two strains were treated using MD and compared to their respective HAP controls to assess the effects of algae cultivation and the buffer on membrane operation and distillate quality. The water flux of both supernatants resembled the flux of the unbuffered HAP control. The flux of the buffered HAP control was greatly reduced compared to unbuffered HAP, but was restored after cultivation with *A. maxima*. The distillate produced from the *A. maxima* supernatant had reduced COD, TN, TP, and NH_3 concentrations while the distillate produced from the *C. reinhardtii* supernatant had increased concentrations of COD and NH_3 compared to their respective controls. Fluorescence was used to characterize the types of organic species removed during algae cultivation or MD treatment revealing the detected distillate species shared properties with simple aromatics or biological byproducts. A simplified *A. maxima* regrowth experiment revealed the buffer can be recycled back into cultivation if extra nutrients were provided, but a second growth cycle on the supernatant is not possible.

A. maxima was shown to successfully reduced eutrophication or greenhouse gas risks compared to traditional dairy manure management methods. Future work should focus on further improving the system by reducing water usage and alleviating complications associated with the bicarbonate buffer.

ACKNOWEDGEMENTS

It has been a long journey with many hiccups and challenges, but I had an excellent support group of family and friends that could assist me with this accomplishment. I am grateful to all the labmates, classmates, and mentors I met over the last seven years for all the help they could provide whether it was for classes, research, or just to have fun. I would like to give a special thanks to Dr. Sage Hiibel and my committee for their support and guidance over the course of my PhD.

This material is based on work supported by the National Science Foundation under NSF Award #1856009.

TABLE OF CONTENTS

LIST OF TABLES

LIST OF FIGURES

LIST OF EQUATIONS

LIST OF ACRONYMS

AD	Anaerobic Digestion
AGMD	Air Gap Membrane Distillation
BDL	Below Detection Limits
CAFO	Concentrated Animal Feeding Operation
CF	Concentration Factor
COD	Chemical Oxygen Demand
DCMD	Direct Contact Membrane Distillation
DI	Distilled
DOM	Dissolved Organic Matter
EEM	Excitation Emission Matrix
EPA	Environmental Protection Agency
EPS	Extracellular Polymeric Substance
FI	Fluorescence Index
FO	Forward Osmosis
FRI	Fluorescence Regional Integration
GHG	Greenhouse Gas
HAP	Hydrothermal Carbonization (HTC) Aqueous Product
HHV	Higher Heating Value
HIS	Hydrophilic Substance
HIX	Humification Index
HOA	Hydrophobic Acid
HOB	Hydrophobic Base

HTC	Hydrothermal Carbonization
HTL	Hydrothermal Liquefaction
IFE	Inner Filter Effect
LCA	Life Cycle Assessment
LEP	Liquid Entry Pressure
LMH	L/m^2*h
LR	Low Range
MD	Membrane Distillation
NEWIR	Nutrient, Energy, and Water Innovations for Resource Recovery
NIST	National Institute of Standards and Technology
NSF	National Science Foundation
OD	Optical Density
PARAFAC	Parallel Factor Analysis
PP	Polypropylene
PTFE	Polytetrafluoroethylene
PVDF	Polyvinylidene Fluoride
RO	Reverse Osmosis
SGMD	Sweeping Gas Membrane Distillation
TN	Total Nitrogen
TOC	Total Organic Carbon
TP	Total Phosphorus
ULR	Ultra Low Range
VFA	Volatile Fatty Acid

VMD	Vacuum Membrane Distillation
ZLD	Zero Liquid Discharge

1 INTRODUCTION

1.1 Motivation

As the global population continues to increase, the demand for food, energy, and water continues to grow. These highly connected resources are crucial to support society and life, and are often referred to as the food-energy-water nexus. The key to a sustainable future is to improve the production, management, and usage of these resources.

The agricultural industry has been adopting a more streamlined model for milk production. Over the recent decades, the number of dairy cows located on concentrated animal feeding operations (CAFOs) has been increasing. In 1992, the fraction of dairy cows in facilities with >1000 cattle only accounted for 10% of the population [1]. By 2012, this fraction increased to 49% [1] and it further increased to 55% by 2017 [2]. CAFOs are more efficient and have made milk production more economical than on smaller farms. The production cost per head in dairy facilities with >2000 cattle were on average 16% lower than farms with 1000 - 2000 cattle, which were also lower than facilities with fewer animals [1]. The higher density of cattle has made dairy production more cost-effective but has introduced other concerns such as the environmental consequences of the increase in localized dairy manure.

Historically small dairy farms could apply manure as fertilizer and recycle the nutrients locally. Manure applied more frequently also results in fewer greenhouse gas emissions [3]; however, CAFOs cannot spread to nearby cropland in fear of over-application that may lead to pollution or eutrophication into nearby bodies of water [4]. The most frequent manure management methods involve long-term storage such as an anaerobic lagoon [5]. These lagoons require a large footprint but need little maintenance

and passively treat the waste. As the non-degradable material settles to the bottom, a layer of sludge accumulates. Eventually, the sludge is removed and can be applied to nearby cropland; however, large dairies are still restricted with how much could be applied to nearby cropland [6]. During long-term storage, the manure emits methane, which is a more harmful greenhouse gas than carbon dioxide since it has x25 the warming potential [7]. Liquid manure is a major methane emission source because microorganisms under anaerobic conditions will reduce volatile solids into methane [8].

In a California survey, other methods of manure storage and treatment included solid-liquid separators, scrapers, or pond additives (enzymatic or microbial). The same survey revealed farmers are interested in learning about newer manure management techniques such as anaerobic digestion [9]. Anaerobic digestion is a process where microorganisms reduce organic waste in the absence of oxygen to produce biogas that is primarily composed of methane and carbon dioxide. Since this occurs within a controlled environment, the methane is not released into the atmosphere and can be collected to be used as an energy source where the methane is combusted into carbon dioxide. The liquid product (digestate) contains most of the nutrients present in the manure and can be applied to cropland as a fertilizer but is still subject to the limited application challenge associated with CAFOs. As the size of CAFOs continues to grow, manure management methods that can remediate the dairy manure nutrients or improve on other environmental aspects become of more interest.

1.2 NEWIR Manure Project

The work in this dissertation describes in part the work conducted for the Nutrient, Energy, and Water Innovations for Resource Recovery (NEWIR) Manure project that investigates a sustainable alternative for dairy manure treatment. The general schematic for the project is summarized in Figure 1.1 and involves a combination of processes such as hydrothermal carbonization (HTC), algae cultivation, and membrane distillation (MD) to extract value from dairy manure.

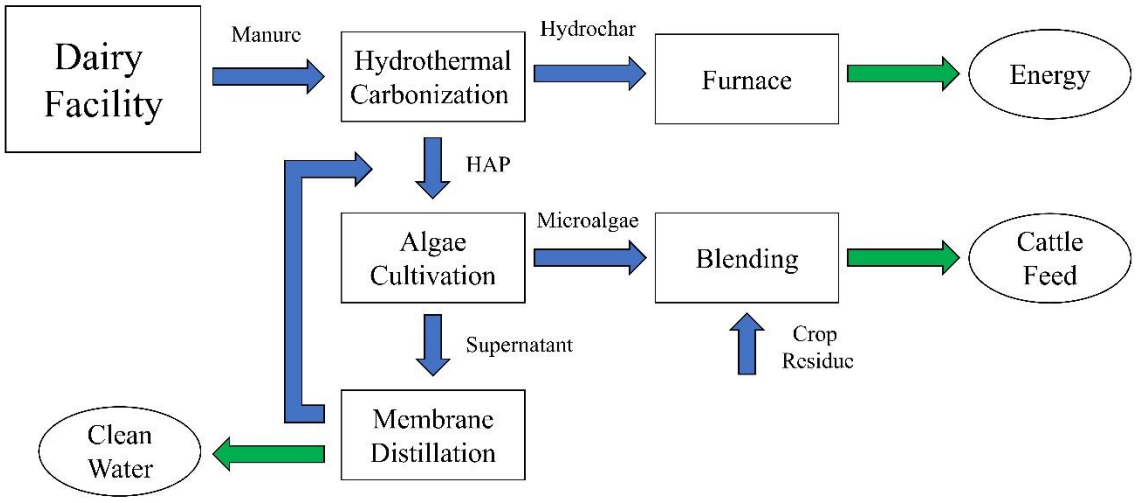

Figure 1.1: Outline of the NEWIR Manure project.

HTC is a thermal treatment process that uses the unique properties of water at high temperatures and pressures to convert organic wastes into a low grade-coal called hydrochar. Water is a crucial element for HTC, so the wet dairy manure can immediately be treated with HTC and reduce methane emissions. The HTC process creates a hydrochar while simultaneously expelling some nutrients into an aqueous solution [10]. The hydrochar can be burned as an additional energy source and offset the energy requirements

of the system [11]; however, one branch of the project aims to valorize the hydrochar and create a high-value activated carbon.

The HTC aqueous product (HAP) contains some of the nitrogen and phosphorus from the dairy manure and was used to cultivate protein-rich algae. Algal strains investigated in this work have high protein content and are capable of heterotrophic growth. The protein-rich algae would remediate the nutrients in the HAP and serve as a dietary supplement for the dairy cattle, offsetting demand of traditional supplements like soybean or canola. The lagoons used for traditional manure treatment could be repurposed into raceway ponds for algae cultivation and reduce the required capital investment. The heterotrophic capability of the algae suggests the species would thrive in the nutrient- and carbon-rich environment of the HAP.

After algal cultivation, the remediated HAP, also referred to as the algal supernatant, can be treated with MD. MD is a thermal separation process that can harness low-grade waste heat to produce clean water [12]. The higher temperature heat associated with the freshly produced HAP will be used to preheat the HTC feedstock, but MD can use the remaining low temperature heat to drive the separation of clean water from HAP. MD has already been demonstrated potential to treat HAP, with >98% rejection of carbon, nitrogen, and phosphorus [13]. The removal of nitrogen and carbon species during algae cultivation suggests the MD distillate produced from the supernatant will be of higher quality than the distillate produced from HAP. This dissertation focuses on the assessment of algae cultivation on the HAP and the treatment of HAP algal supernatant using MD.

1.3 Hydrothermal Carbonization

The HTC process is a crucial unit operation as the research discussed in this dissertation targets remediating and treating the HAP it produces. Common feedstocks for HTC include organic wastes such as agricultural or biological wastes. Many biofuel studies have investigated using algae as a feedstock where the organic material can be turned into a fuel and the nutrients could be recycled to cultivate more algae [11,14]. The HTC process requires a high-water content, so dairy manure, which naturally has a high-water concentration, is an ideal feedstock.

HTC occurs between 180 and 250 °C with autogenous pressure produced by water [15]. At higher temperatures, starting around 250 °C, hydrothermal liquefaction (HTL) occurs [15]. While HTL primarily produces bio-oil, the main product of HTC is a low-grade coal with properties resembling lignite coal. Under HTC operating temperatures, water simultaneously acts as a mild acid and mild base, triggering a series of chemical reactions to degrade and reform lignocellulosic material to a hydrochar [16,17]. The reactions in the HTC process include hydrolysis, dehydration, decarboxylation, aromatization, and polymerization [18–20]. Hydrolysis reactions break the cellulose into monosaccharides, the hemicellulose into hexoses and polysaccharides, and the lignin into phenolic species. The dehydration reactions convert pentoses and hexoses into furfurals and the hexoses into organic acids. Decarboxylation produces carbon dioxide from organic acids. Aromatization converts furfurals into aromatics as a precursor to polymerization where it condenses into a hydrochar and releases water. The operating temperature affects the types of reactions that will occur as well as which types of lignocellulosic material will

be broken down. For example, hemicellulose begins decomposing near 180 °C and cellulose around 220 °C [21,22].

The hydrochar can be burned as an energy source, where its energy is dependent on the HTC operating conditions and feedstock properties. Hydrochar produced from sugarcane or Leucaena wood has a higher heating value (HHV) of 18-29 MJ/kg [23] while the HHV of hydrochar from dairy manure is 19-22 MJ/kg [16]. Generally, the hydrochar produced at higher temperatures has higher HHV and is more hydrophobic. The increase in hydrophobicity makes it easier to separate the hydrochar from the water, which is advantageous for scale up. Many studies have investigated alternative applications of the hydrochar, including its use in fuel cells [24], as a catalyst [25], or as a soil amendment [26].

The majority of HTC research is focused on the production, analysis, and application of the hydrochar while the HAP is less studied. The operating conditions of the HTC affect the nutrient concentration as well as the carbon speciation in the HAP since different lignocellulosic materials are affected at different temperatures. Higher HTC operating temperatures and longer operating times result in a reduced phosphorus concentration in the HAP, while these parameters had less effect on the nitrogen concentration [13,27]. Adding acids like citric acid into the HTC process also increases the amount of phosphorus that solubilize in HAP [27]; however, the acidic environment makes algae cultivation more challenging. Increasing HTC operating temperature increased the concentration of phenolic and ketone species as the polysaccharides broke down [28]. To promote algal growth with more nutrients and fewer potential toxic compounds, the algae

cultivation in these studies were predominantly done on HAP produced at 200 °C with no acidic additives.

1.4 Microalgae and Cyanobacteria

Algae are photosynthetic microorganisms that live in fresh or saltwater environments. The term “microalgae” scientifically refers to eukaryotic species but is sometimes used as an encompassing term to include cyanobacteria, which have the common name “blue-green algae”. Cyanobacteria are prokaryotic species but grow under similar environmental conditions to microalgae. Of the investigated strains in this work, *Chlorella vulgaris*, *Chlamydomonas reinhardtii*, and *Scenedesmus obliquus* are microalgae while *Arthrospira maxima* is a cyanobacteria. Algae cells can take various shapes and can grow individually or group up. *A. maxima* (Fig. 1.2A) groups up and grows in S-shaped chains while *C. reinhardtii* (Fig. 1.2B) and *C. vulgaris* are commonly singular and spherical.

Most algae grow autotrophically, meaning they produce their organic material from carbon dioxide and use sunlight as the energy source. However, some species are capable of heterotrophic growth, meaning the algae use organic compounds as both the carbon and energy source. As a result, the heterotrophic species can grow in environments where light is limited. Mixotrophic growth refers to the combination of autotrophic and heterotrophic growth pathways. Depending on the growth environment and mode of growth, the composition of the algae may change. Some algal strains have high lipid content, which is further enhanced when cultivated under stressed conditions, while others may have high protein content or produce other valuable biochemicals. The diversity of existing algae

leads to a large range of potential applications. The four strains investigated in this work were selected because they are capable of heterotrophic growth and because they are known to have high protein content, making them ideal candidates for a dietary supplement.

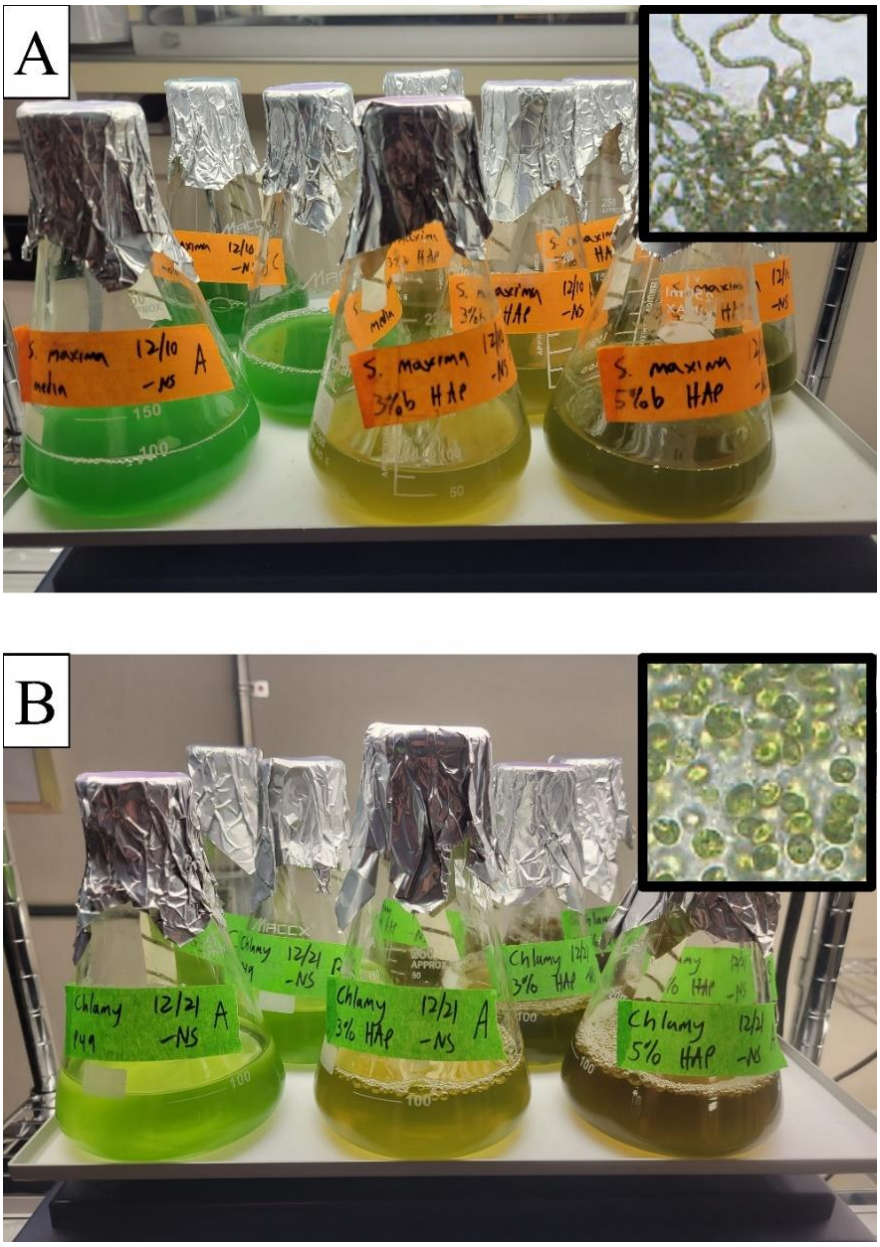

Figure 1.2: Experimental images of (A) *Arthrospira maxima* and (B) *Chlamydomonas reinhardtii* cultivated on UTEX media, 3% HAP, and 5% HAP (left to right). Microscope images for each species are modified from [29]. No scale available.

1.4.1 Growth Factors

Various factors affect the growth rates of algae including operational conditions such as lighting or agitation, or media selection. Photosynthetic species require light to grow. Generally, higher intensities of light will increase productivity and increasing specific wavelengths of light may affect algae composition, such as increase lipid content [30]. Excess light may result in photoinhibition where the photosynthetic capabilities of the algae is be reduced [31]. If trying to force the heterotrophic growth pathway, less light should be used.

Agitation is not required to cultivate algae, since they often grow in natural stagnant waters; however, incorporating a form of agitation can increase algae growth rates. In general, agitation prevents the algae from sedimenting and promotes a uniform distribution of light and nutrients for cultivation. The type of agitation (mixing, aeration, or circulation) depends on the bioreactor type and geometry. The shear stress associated with excess agitation potentially results in lysis of the algae cell [32].

Scaling up algae cultivation commonly occurs in either a raceway pond or photobioreactor. Raceway ponds (Fig. 1.3A) are media pools, typically outside, with baffles and risers to promote mixing. Since they do not occur in a controlled environment, the evaporative loss is significant, contamination is more likely, and fluctuations in weather conditions have a greater effect on biomass quality [33]. Photobioreactors (Fig 1.4B) are controlled, isolated systems that offer reduced evaporative loss, lower contamination risk, and more consistent biomass quality in exchange for a greater capital investment and higher operational costs when compared to the raceway ponds [34]. Photobioreactors come in a variety of geometries aiming to improve light uniformity, mixing, CO_2 and O_2 gas transfer,

temperature management, or ease of cleaning [33]. Both raceway ponds and photobioreactors operate as a batch, but some studies have investigated hybrid systems to obtain a continuous operation type or a compromise between costs and consistency [35].

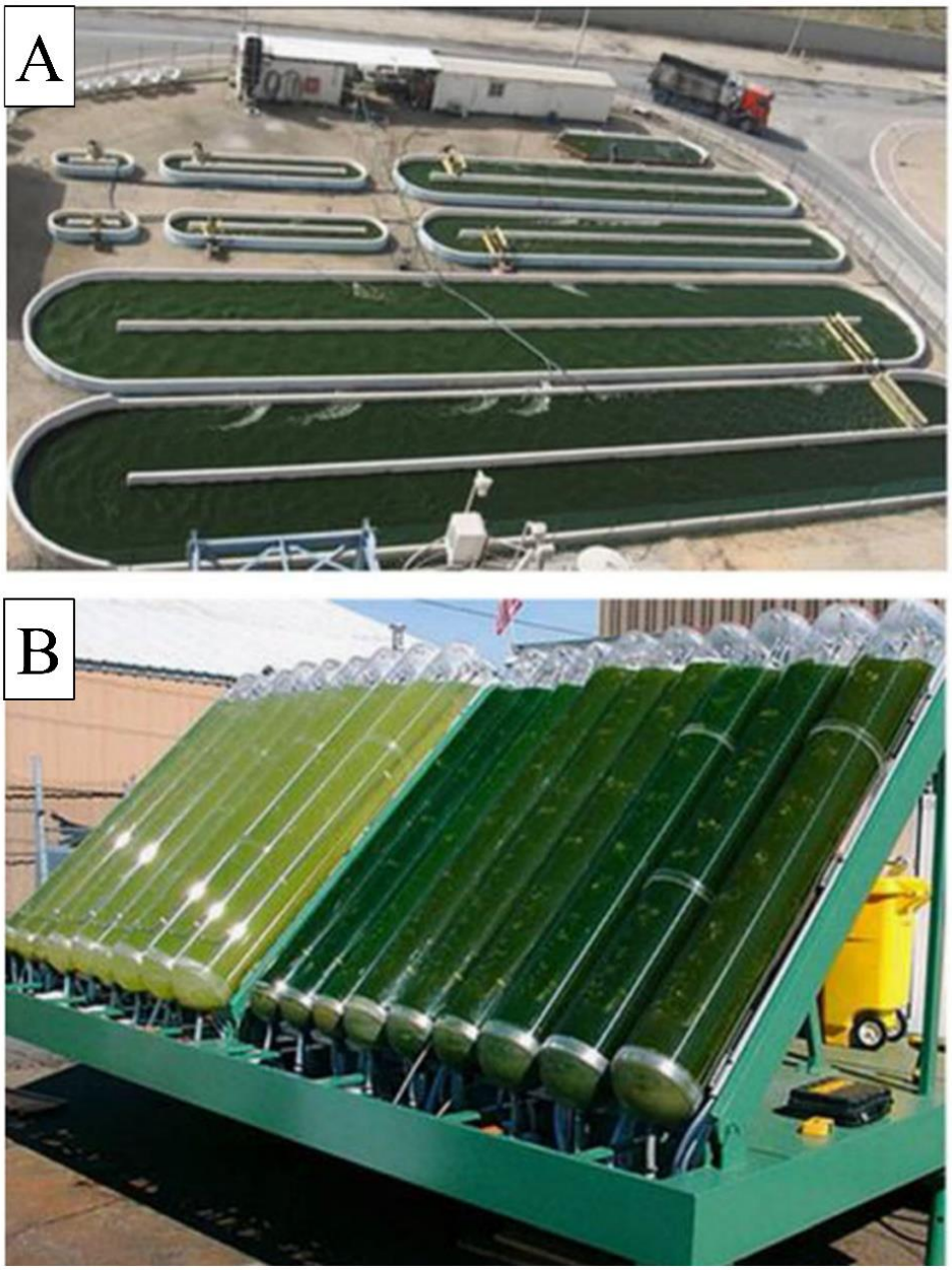

Figure 1.3: Examples of (A) raceway ponds and (B) photobioreactors. Image modified from [33].

Algae are robust species that grow where nutrients and light are available, which is why unwarranted algal blooms from nutrient eutrophication can be a major concern [36]. The algae medium refers to the solution where the culture grows. A viable medium includes a viable nitrogen source, phosphorus, vitamins, trace metals, and micronutrients. Nitrate is frequently used in synthetic media as the nitrogen source. Ammonia can also be used but has been demonstrated to be toxic or inhibitory at high concentrations [37,38]. The pH of the media can also have a significant effect on algae growth rates, so use of a buffer or CO_2 aeration should be considered as forms of pH control. In general, pH increases during the day due to the uptake of CO_2 through photosynthesis and decreases at night because of the release of CO_2 by respiration [39].

Synthetic media optimization is challenging due to the number of potential control and objective variables where the results are algae specific. Early optimization can be conducted by comparing biomass growth to various named media (such as BG 11 medium, Bold's medium, etc.) where the types of solutes differ [40]. More rigorous optimizations are performed by varying the concentrations of select solutes to see how they affect the growth rates and composition [41]. Since some algae are capable of heterotrophic growth, glucose or acetate can be added to the media to enhance growth rates [42].

One of the major limitations for algae cultivation is the nutrient supply, so algae growth on various wastewaters, such as olive oil mill wastewater [43], landfill leachate [44], sewage [45], or anaerobic digestates [46], has been evaluated. In the biofuel industry, cultivation of algae on HAP produced from algae has been investigated, where the nutrients can be recycled into the cultivation process while producing lipids for biofuels [14,47]. If a waste stream has a sufficiently high nutrient concentration, algae growth may be viable.

It has been seen that dairy manure [48] and the anaerobic digestate of dairy manure [49] can both stimulate algae growth, resulting insubstantial removal of the nutrients and chemical oxygen demand (COD) in both cases. Over time, the algae strains can also acclimate to a specific wastewater, growing faster and remediating more of the nitrogen after becoming acclimated [50].

1.4.2 Algal Biomass Applications

Algae produce a large range of organic and chemical species that make them of interest to a wide range of industries. Algae cultivation can be used to remediate nutrients or treat wastewater, but the biomass and byproducts can be used in a variety of potential applications as well (Fig. 1.4).

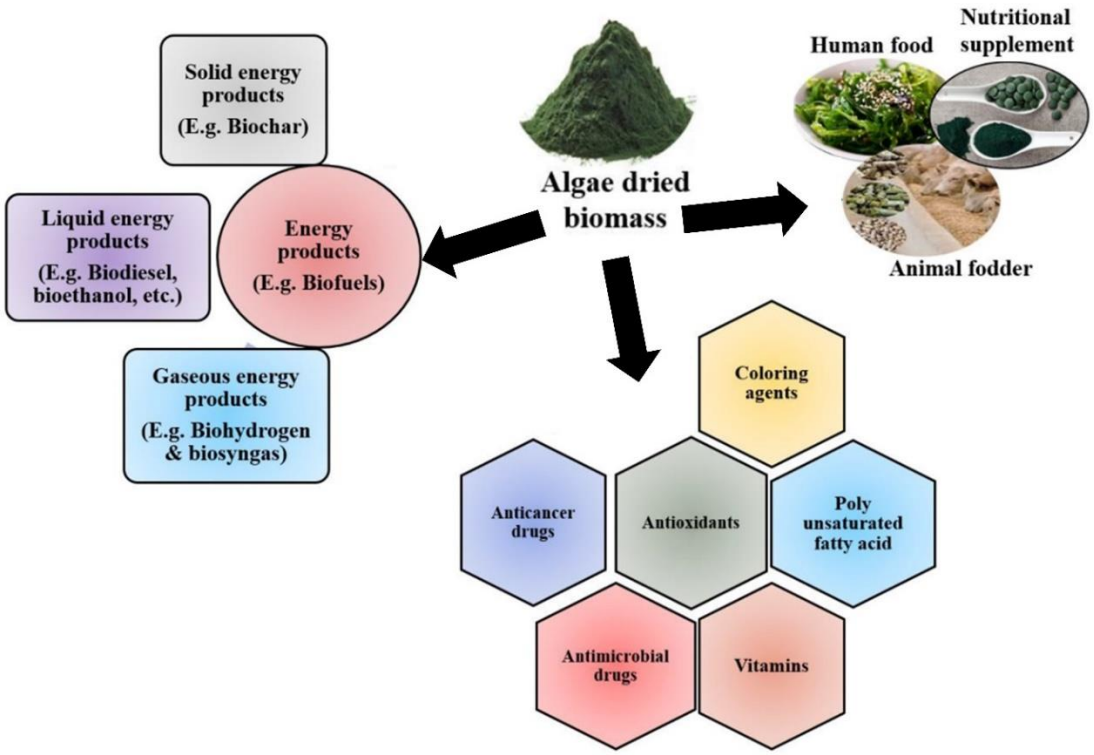

Figure 1.4: Potential applications of algal biomass including use as biofuels, dietary supplements, and valuable byproducts. Image modified from [51].

Various parts of the algae can be used as a potential fuel source. Generally, algae with high lipid content are of interest to the biofuel industry, where the lipids can be used in various ways to produce a biofuel, not limited to transesterification. As mentioned in Section 1.4.1, the biomass can be used as a feedstock for HTC to produce a low-grade coal [11,14], and some studies have investigated using multi-cellular macroalgae as a feedstock in anaerobic digestion to produce biogas [52]. Some algae species, such as *C. reinhardtii*, produce H_2 gas that can be gathered as another energy source [53]. When the algae are cultivated in a stressful environment, such as nitrogen starvation, their lipid content increases further as they stop dividing and accumulate more triacylglycerols [54]. Other operating parameters such as temperature, light, and pH will alter algae composition, but the effects are strain specific. For example, increasing the temperature from 25 to 30 °C reduced the lipid content of *Chlorella vulgaris* but increased the lipid content of *Nannochloropsis oculata* [55]. Some studies have also looked towards genetic engineering to further enhance the lipid or carbohydrate content of algae to make them more viable for the biofuel industry [56].

One of the major challenges for using algae in the biofuel industry is the trade-off between cell growth and lipid accumulation [57]. A two-staged cultivation approach is often used to combat this [58]. In the first stage, the algae are grown in a nutrient-rich culture to maximize biomass. In the second stage, the dense culture is grown under stressful conditions to increase lipid accumulation. The transfer of the biomass from a nutrient-rich culture to a nutrient-limited culture strains economic viability, so other stress conditions in the second stage, such as the use of green light [59] or addition of NaCl [60], have been investigated.

Microalgae and cyanobacteria are high-nutrient food sources and have been a part of human diet for thousands of years dating back to the Aztecs [61]. As global demand for food production increases, the use of algae is viewed as a potential sustainable alternative to crop production. Algae are rich in protein, carbohydrates, lipids, and various vitamins that are crucial for the human diet. *Arthrospira* (Spirulina) and *Chlorella* contain up to 70% protein and are already commercially available as protein supplements for human consumption. Microalgae and cyanobacteria are excellent sources of various micronutrients vitamins including β-carotene as they exceed conventional rich foods [62]. *Arthrospira* also produces several pigments such as phycocyanin, myxoxanthophyl, and zeaxanthin [63]. For medical applications, phycocyanin has been reported to have anti-oxidative, anti-inflammatory, anti-cancer, and immune enhancement properties [64].

The primary objective of the algae was to remediate the nutrients in the HAP while simultaneously serving as a protein dietary supplement for the cattle. The investigated algal strains are capable of heterotrophic growth, so the organic carbon in HAP may be used for their growth. *A. maxima* and *C. vulgaris* have high protein content and it has been seen that *C. reinhardtii* can have a competitive protein content [65]. *S. obliquus* may not be as protein rich as the three previous species but has demonstrated potential to treat various wastewaters, including raw sewage [45,66].

1.5 Membrane Distillation

Membranes are common separation tools used in water and wastewater treatment, and are frequently defined as a semipermeable barrier. Each membrane process has its unique driving force. Ultrafiltration, nanofiltration, and reverse osmosis (RO) are pressure-

driven processes and require large pumps for operation. Forward osmosis (FO) uses osmotic pressure to draw water from a dirty feed. Other membrane processes like electrodialysis may be driven by a charge gradient or electric potential. The driving force for MD is a chemical species' partial pressure, so it is often thought of as a thermal separation process. In MD (Fig. 1.5), a hydrophobic, microporous membrane is used to separate a warm feed stream and a cool distillate stream [67]. The membrane hydrophobicity prevents liquid water from entering the pores and the temperature difference of the two streams creates a partial pressure difference across the membrane, facilitating the passage of vapor through the membrane pores.

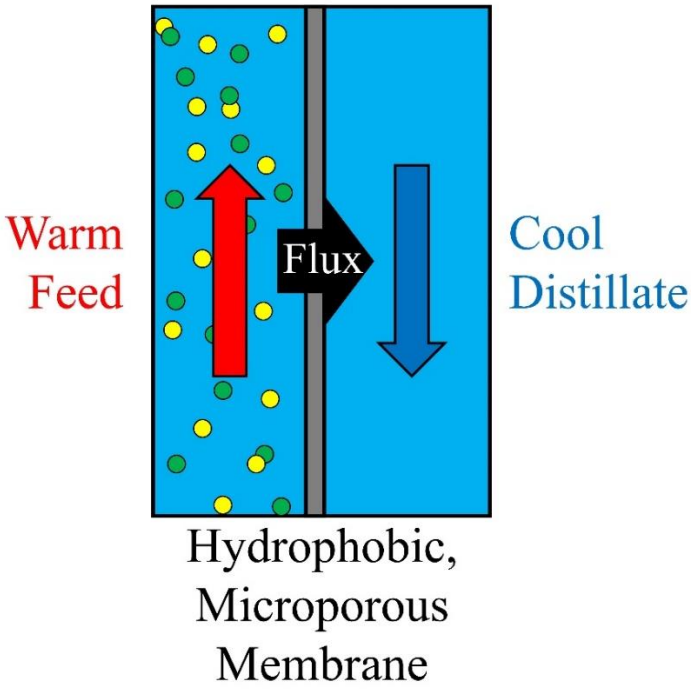

Figure 1.5: Simplified graphic for demonstrating the MD treatment process.

The water flux rate through the membrane is proportional to the induced partial pressure difference. A species' partial pressure is dependent on its concentration and

temperature. Methods such as Raoult's Law and Henry's Law can be used to estimate the partial pressures from solution concentrations. For near pure substances, the vapor pressure can be used to estimate partial pressures. The vapor pressure, P_v, can be estimated using Antoine's Equation (Eq. 1.1) that requires three species-dependent constants (A, B, and C) and temperature (T) for the modelled temperature range.

$$P_v = \exp\left(A + \frac{B}{C + T}\right) \tag{1.1}$$

The exponential nature of the vapor pressure, as demonstrated in Figure 1.6, shows that a small temperature difference can cause a large driving force that can drive separation. which is why MD excels when low-grade heat is available [68].

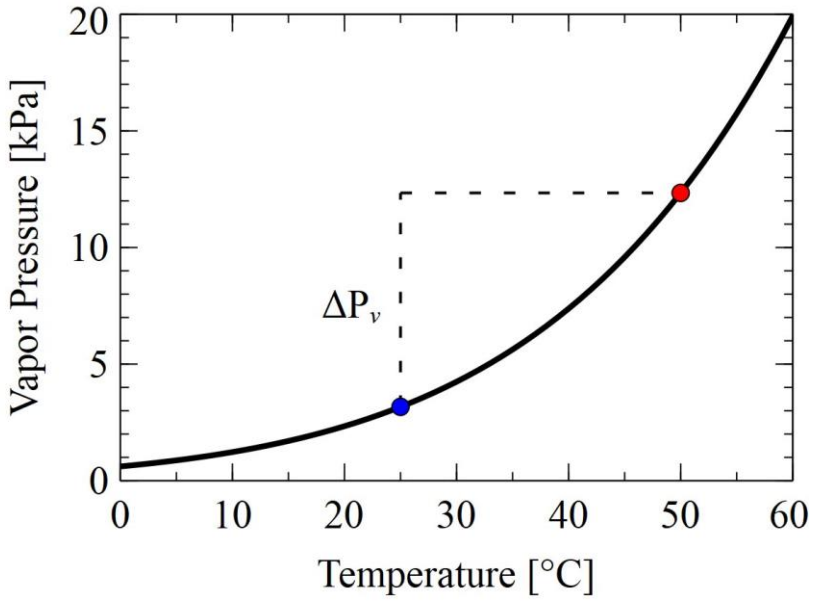

Figure 1.6: Graphic of the vapor pressure of water calculated from Antoine's Equation demonstrating the MD driving force associated with distillate and feed temperatures of 25 °C and 50 °C, respectively. Antoine constant values obtained from National Institute of Standards and Technology (NIST).

MD is often used for desalination and has demonstrated near 100% rejection of salts [69]. Under typical MD operating conditions for water treatment (< 70 °C), ions have negligible vapor pressure resulting in negligible transport across the membrane. The high removal of ions demonstrates MD can produce high-quality water and rival RO under certain operating conditions. Many studies investigate coupling MD with RO to treat water further and pursue a zero liquid discharge (ZLD) system [70–72]. RO uses hydraulic pressure to treat saltwater and its byproduct is a highly concentrated salt brine. To treat the brine further, RO must operate at a higher pressure than the brine's osmotic pressure. The salt concentration in the brine has a strong effect on the solution's osmotic pressure, while the water vapor pressure is significantly less affected. MD can treat the brine further once RO becomes infeasible [71].

Water treatment using MD is typically conducted by producing clean water on the distillate side; however, due to the flexibility of the driving force, removal of contaminants from the feed may also be performed. If the contaminants are more volatile than the solvent, they pass through the membrane more readily. This has been demonstrated when extracting volatile aromas from fruit juices [73] and removing alcohols from solution [74].

1.5.1 MD Configurations

The configuration of the membranes and the two streams greatly affect the outcome and efficiency of MD operation. The four most common MD configurations are direct contact membrane distillation (DCMD), air gap membrane distillation (AGMD), sweeping gas membrane distillation (SGMD), and vacuum membrane distillation (VMD).

The simplest configuration is DCMD where the membrane is in direct contact with the warm feed and cool distillate streams (Fig. 1.7A). This design has the lowest capital costs of any MD design because it does not require special equipment such as a vacuum or a compressor. The major concerns with DCMD are membrane fouling and the high energy loss due to heat transfer that often make it infeasible for scale-up. The other variations of MD aim to improve upon these properties. The most common uses of the DCMD configuration are at the bench scale to test model accuracy or assess MD feasibility when energy use is not a concern.

AGMD is a configuration developed to reduce the heat transfer through the membrane. In this design, a thin, stagnant layer of air on the distillate side (Fig. 1.7B) is present as an additional transport resistance. Feed side vapor passes through the membrane and must diffuse through the stagnant air before it can condense, typically on a cooled surface. This extra resistance reduces heat transfer, but consequently also reduces mass transfer. During the scale-up process, AGMD is commonly preferred to DCMD because it is more energy efficient. With implemented energy recovery at the pilot scale, it also demonstrated higher water flux than DCMD [75].

SGMD is another variation that reduces the heat transfer through the membrane. Instead of having clean water circulating on the distillate side of the membrane, an inert gas stream is used (Fig. 1.7C). Heat transfer through gases is significantly lower than liquids; thus, the overall heat transfer is reduced. The amount of air that must be condensed to recover the species that pass through the membrane makes SGMD impracticable for desalination. This configuration is most appealing when removing volatile components from the feed side water, such as ammonia [76]. It is also useful when the distillate does

not need to be recovered, such as when concentrating ethylene glycol from a watery mixture [77].

VMD is another MD configuration (Fig. 1.3D) where the distillate side is under vacuum, significantly reducing heat transfer across the membrane. Since the reverse driving force is reduced, the mass flux is enhanced as well. Although VMD saves energy due to reduced heat transfer, it is the most energy intensive of the four configurations because of the vacuum energy requirements. Much like SGMD, a compressor is required to recover the distillate. VMD is often compared to SGMD because the preferred applications are similar [73]. Volatile organic components can be removed from the wastewater [78] or the feed can be concentrated by removing unrecovered water [79].

The four configurations mentioned are the most frequently studied, but other more complex variations have been investigated. Material gap membrane distillation follows the same principle as AGMD but with a material such as sand to replace the air gap to improve the mass transfer [80]. Vacuum-enhanced AGMD or DCMD are variations of AGMD and DCMD where the distillate side operates below atmospheric conditions to increase water flux [81]. Alternatively, negative pressure DCMD is when the feed side operates under negative gauge pressure to provide higher scaling resistance to $CaSO_4$ [82]. The selected configuration is dependent on the feed and the treatment objective and should be considered alongside the properties of the membrane itself.

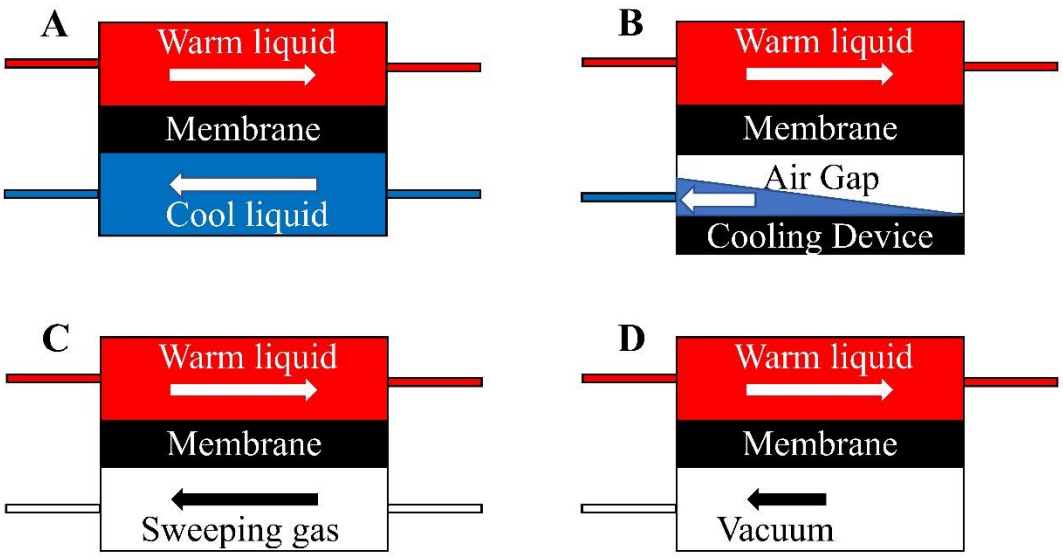

Figure 1.7: Common membrane distillation configurations from various studies: (A) direct contact MD, (B) air gap MD, (C) sweeping gas MD, and (D) vacuum MD.

1.5.2 Membrane Properties

Hydrophobicity is the most important property of MD membrane since it prevents liquid water from entering the pores. MD membranes are commonly fabricated from polytetrafluoroethylene (PTFE), polypropylene (PP), or polyvinylidene fluoride (PVDF). In addition to being hydrophobic, these polymers are thermally stable and chemically resistant to common water solutes. As MD does not operate under significant hydraulic pressure, the membrane material does not require the strength of RO membranes. A support layer may be added for extra strength, but it also adds another transport resistance and reduces water flux. Recently, ceramic membranes have been investigated for applications in MD [83–85]. Ceramic membranes have properties ideal for MD efficiency, such as high thermal resistance, chemical resistance, and mechanical strength [86]; however, ceramics

tend to be hydrophilic, so surface modification such as chemical vapor deposition [87,88] is required.

Surface modification is a powerful technique to adjust the properties of the membrane and change its performance. It has been demonstrated that membranes with higher hydrophobicity have increased flux [89] and improved wetting resistance [90]. Membrane surfaces can be modified to become superhydrophobic to further increase the flux [91]. If treating oily substances, the surface can be modified to become omniphobic, retaining hydrophobicity to repel liquid water, but gain oleophobic properties to repel organics and reduce fouling [92]. The distillate side could be selectively modified to become hydrophilic, reducing the intensity of the distillate boundary layer and increase flux [93]. A proper balance during membrane fabrication and modification is needed to improve flux and prevent pore wetting, which will be further discussed in Section 1.5.3. Membrane physical properties that manifest during fabrication affect membrane performance such as pore size (r), porosity (ϵ), tortuosity (τ), and thickness (δ).

Large pore sizes increase mass flux, but also make the membrane more susceptible to pore wetting. Common MD membrane pore sizes range from 0.1 to 0.6 μm [12] and follow a size distribution. When modeling MD transport, an average pore size is traditionally used since the effect of the pore distribution is outweighed by the uncertainties associated with modeling or lab practice [94].

The liquid entry pressure (LEP) is the hydraulic pressure difference that will result in pore wetting [95] and can be calculated using the surface tension (γ_L) and contact angle (θ_c) between the liquid and membrane (Eq. 1.2).

$$\text{LEP} = -\frac{2\gamma_L}{r}\cos(\theta_c) \tag{1.2}$$

The membrane porosity refers to the fraction of a membrane volume that is void space. Membranes with higher porosity have higher transmembrane fluxes and lower thermal conductivities [96].

Tortuosity is defined as the ratio of the actual path length within the pore structure to the straight-line path length. Therefore, an ideal path has a tortuosity of 1 with actual membranes having values >1. Measuring the tortuosity of a membrane is difficult, so it can be estimated as a function of the membrane porosity as shown in Equation 1.3 [97].

$$\tau = \frac{(2-\epsilon)^2}{\epsilon} \tag{1.3}$$

The membrane thickness is inversely related to the heat and mass flux through it, and optimal thickness value ranges from 30 to 60 μm when accounting for the thermal conductivity of common MD polymers [98].

1.5.3 Membrane Fouling and Wetting

MD is traditionally run as a multi-pass system. This means it is more resistant to fouling than dead-end flow; however, much like any membrane process, fouling is still a major concern. Membrane fouling results in reduced performance and diminished efficiency as an extra layer of resistance forms on the membrane surface and pores get clogged. The major consequence of fouling is a reduced transmembrane flux. Types of fouling are often defined by the species that adhere to the membrane. Organic fouling

occurs when organic species adhere to the membrane surface. These components may be dissolved organic matter (DOM) or colloidal particles. Biological fouling refers to the microorganisms and their extracellular polymeric substance (EPS) on the membrane. This type of fouling is only introduced if MD is in contact with a biological culture such as in a membrane bioreactor [99]. Inorganic fouling, also known as scaling, occurs when salts precipitate on the membrane surface, and is the predominant fouling mechanism during desalination [71]. If the fouling substances are hydrophobic, only reduced flux would be observed; however, if the fouling causes the surface to become more hydrophilic, pore wetting may occur.

Pore wetting (Fig. 1.8) is a phenomenon that occurs when the membrane surface loses its hydrophobicity and no longer prevents liquid water from entering the pores. The membrane is no longer selective, and the feed stream can freely flow through the pore and into the distillate. Surfactants and other amphiphilic species are the frequent causes of pore wetting. The hydrophobic end fouls the membrane surface, while the hydrophilic head reduces the surface tension such that liquid water can enter the membrane pores. Methods for early detection of pore wetting are important for MD operation [100]. One such method involves real-time monitoring of the distillate conductivity where sudden increases in conductivity is a sign a wetted membrane [101].

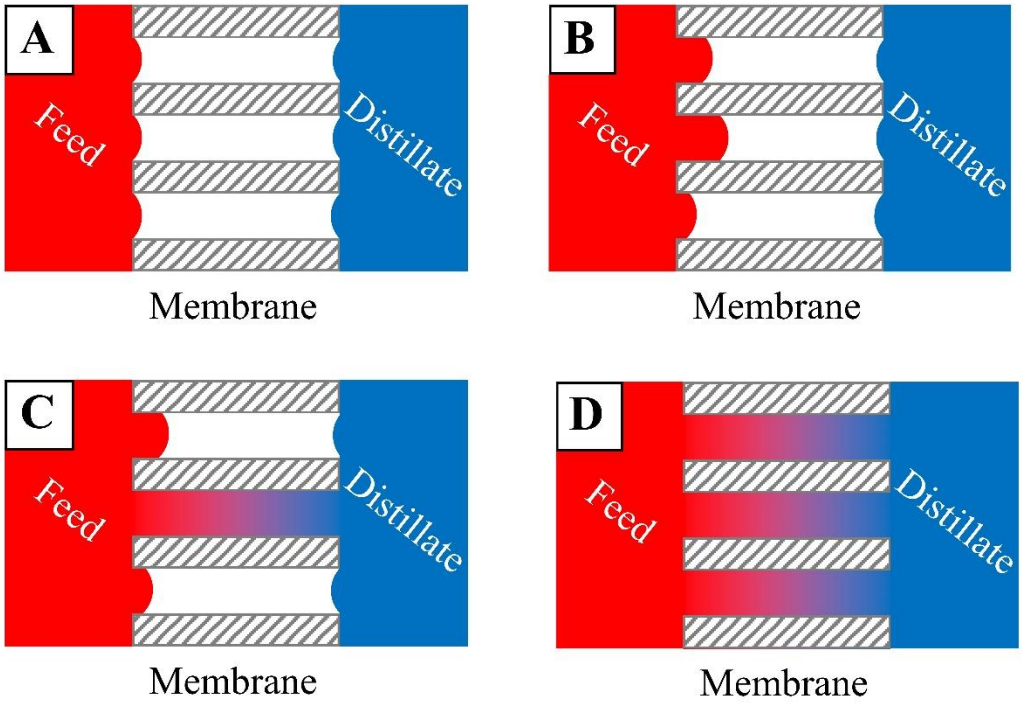

Figure 1.8: Different phases of membrane wetting for MD treatment: (A) not wetted, (B) surface wetted, (C) partially wetted, and (D) fully wetted.

1.6 Fluorescence Characterization

During the HTC process, many different reactions occur creating many products in the HAP. The chemicals in the HAP may include sugars, amino acids, volatile fatty acids, alcohols, phenols, and/or furfurals [16,102,103], so descript analysis such chromatography is difficult. In this work, fluorescence analysis was used as a "fingerprint" characterization for HAP batches and treatments to characterize the types of chemical species that were removed or treated.

Fluorescence occurs when an excited electron emits a photon and falls to a lower electron energy level. A Jablonski diagram (Fig. 1.9) demonstrates the potential energies emitted for specific transitions that are always the same and dependent on the chemical

species. A photon's energy is inversely proportional to its wavelength. An excitation emission matrix (EEM) is a 3-D plot of intensities against the wavelengths of the excited and emitted light. These wavelengths commonly fall in the ultraviolet to visible light range of light. Unlike traditional UV-vis spectroscopy, which can be used to determine the wavelengths a species absorbs light, fluorescence is used to determine the wavelengths a species emits when excited by a specific wavelength [104]. Once an EEM is obtained from spectrofluorometer, the data can be analyzed in several ways including peak-picking, fluorescent ratios, fluorescence regional integration (FRI), or parallel factor analysis (PARAFAC), but some corrections or normalization may be necessary.

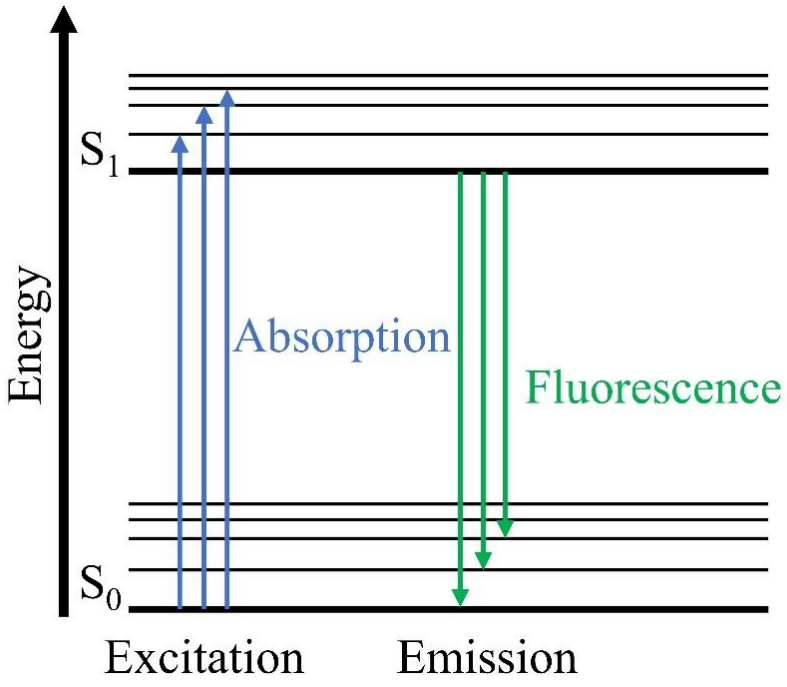

Figure 1.9: A simplified Jablonski diagram demonstrating potential absorption/excitation and fluorescence/emission energies for two electronic states, S_0 and S_1.

1.6.1 Fluorescence Corrections

Several corrections to the spectrofluorometer EEM spectra are needed before proper analysis. The general outline of corrections follows (1) spectral corrections, (2) inner-filter corrections, and (3) intensity calibrations [105].

Rayleigh and Raman scatter are the most prominent spectral corrections. Rayleigh scatter refers to the elastic scatter where the excitation and emission wavelengths are near equal [106]. First-order Rayleigh scattering appears as a large diagonal interference where the excitation and emission wavelengths are similar. Higher levels of Rayleigh scatter exist and occur where the emission wavelengths are near 2x or 1/2x the excitation wavelength. Raman scatter is a non-elastic scatter and is related to the energy loss associated with vibration [107]. For pure water, this results in an energy loss of approximately 3400 cm^{-1} [108]. First-order Raman scatter occurs to a lesser degree than Rayleigh scattering and occurs at the diagonal with this energy difference from the Rayleigh scattering line. Higher levels of Raman scattering can be estimated with integer factors like Rayleigh scatter. Rayleigh and Raman scatter have been handled in various ways, in some cases simply ignoring the data of the regions, or in other cases applying a curved correction. If the data within the scatter region is not of interest, the area could simply be removed from presentation and analysis. Some of the methods for correction include subtracting an EEM scan of the pure sample solvent, commonly pure water, from the sample data [109] or removing a best-fit of a normal distribution at the interference region [110]. Often these methods are not sufficient if the interference is too large relative to the sample data, so the regions can be zeroed before conducting a curved fit. A shape-preserving cubic polynomial

can be used instead of a spline function to preserve the local extrema of the data and prevent the formation of artifacts [111].

The inner-filter effect (IFE) occurs when the sample absorbs light at both the excitation and emission wavelength resulting in a systematic skew of the intensities. Many of the methods to reduce this effect occur during or prior to data collection, with the most trusted being dilution. If a sample has low absorbance values across the investigated wavelengths (< 0.05), postprocessing IFE corrections are not necessary [112]. To help reduce IFE, a thinner cuvette or other methods to decrease the path length can be used. Particularly for in-line measurements, these actions are not always possible, so methods of post-processing corrections have been investigated. One of the simplest methods assumes the average path of absorption is half of the cuvette size. The initial intensities (I_0) of the EEM spectra are scaled by a factor dependent on the absorbances at the excitation (A_{ex}) and emission (A_{em}) wavelength, mathematically resulting in Eq. 1.4.

$$I_{cor} = I_0 * 10\text{^}\left(\frac{1}{2}(A_{ex} + A_{em})\right) \tag{1.4}$$

Though this correction is simple, it requires accurate measurement of the absorbances and the use of a UV-vis spectrophotometer. Some spectrofluorometers are equipped with an additional sensor to measure and apply an IFE correction. More advanced techniques for IFE correction have been investigated accounting for cuvette geometry or taking measurements at different locations of the cuvette [113]. Another method investigated using Raman peak intensities to scale the spectra, thus avoiding required dilution or absorbance measurements [114].

Lastly, the intensities provided by the instrument are arbitrary and dependent on instrumental settings so they cannot be used for quantitative comparison across different studies or instruments. The instrumental-dependent properties of the scan can be removed by normalizing the data to the Raman peak of pure water [105]. Therefore, a separate fluorescent scan of pure water with the same instrumental parameters, best run the same day as the samples, is required to normalize the data. The Raman peak at 350 nm is commonly used where the band occurs from approximately 371 to 428 nm [105]. By normalizing an EEM spectra with the area under the pure water Raman peak, quantitative comparisons to other samples normalized to the same Raman scatter can be conducted even if analyzed on a different instrument or with different settings.

1.6.2 Fluorescence Analysis

Peak-picking is the analytical technique where single indices of the spectra are compared across samples. As this is point-wise comparison, it requires significantly less data and processing than other analytical techniques. Selection of which indices depends on the sample and can be chosen by the localized maxima [115]. Sgyoi et al. [116] provided excitation and emission wavelengths that follow the discretization done for FRI performed by Chen et. al [117]. The excitation and emission indices for the Regions I-V in Figure 1.10A are 225/290, 225/340, 245/440, 275/345, and 345/440 (Ex/Em) respectively.

Internal fluorescent ratios, which do not require the full EEM, can also be used to characterize the samples. The Fluorescence Index (FI) is the ratio of the emission intensities at 450 nm to 500 nm with an excitement wavelength of 370 nm. The intensity of the FI can be used to determine the source of the isolated aquatic fulvic acid [109]. The

extent of humification of the organic matter can be determined using the humification index (HIX). The HIX is determined using the 2-D spectra of 254 nm light. It is calculated as the ratio of the area under emissions 435-480 nm to the area under emissions 300-345 nm [118].

FRI is an analytical technique first described by Chen et al. [117] that separates the EEM into different regions for integration to assess the composition of the sample. This analytical technique uses the full spectra and data to make composition conclusions unlike peak picking or the fluorescent ratios. During the example, the EEM spectra was divided into five regions based on common general properties of chemical species (Fig 1.10A). Regions I and II correspond to simple aromatic species such as tyrosine, Region III corresponds to fulvic-like substances, Region IV corresponds to biological byproduct-like substances, and Region V corresponds to humic-like substances. The FRI technique can be applied to any type of regional separation of the EEM by following a similar process, though the regionalization done in the example is traditionally used. An alternative approach has been to regionalize species by their hydrophobicity (Fig. 1.10B) and separate species into hydrophobic acids (HOA), hydrophobic bases (HOB) or hydrophilic substances (HIS) [119].

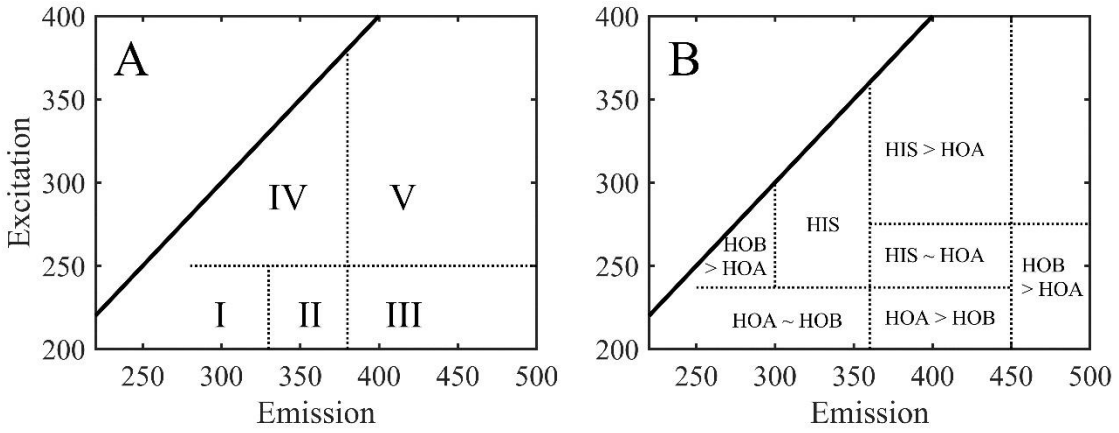

Figure 1.10: Analytical regions for FRI analysis: (A) classical separation by general chemical properties and (B) separation by hydrophobicity.

PARAFAC modeling is potentially the strongest tool for EEM analysis, but is also the most quantitatively rigorous. Each chemical produces a specific EEM signal and when there is a mixture, the signals overlap. In PARAFAC, the sample's EEM is decomposed into a linear combination of a set collection of signals to determine what species or types of species are present in the sample. The results are heavily dependent on signal availability and the number of signals used for decomposition. OpenFluor is a database containing hundreds of PARAFAC spectra obtained from published works to aid in this analysis [120]. The potential for component identification will continue to grow as the database continues to expand.

1.7 Dissertation Outline

The work discussed in this dissertation focuses on the cultivation of several microalgae species on HAP and the subsequent treatment of the HAP algal supernatant using MD. In Chapter 2, *A. maxima, C. reinhardtii, C. vulgaris,* and *S. obliquus* were

cultivated on various HAP dilutions and assessed for their growth rates, nutrient remediation potential, and protein content. In Chapter 3, the supernatant produced from the two highest performing algae were treated with MD, with the water production rate and distillate quality evaluated. In Chapter 4, the results of the two previous chapters are reviewed alongside the potential future steps for the NEWIR Manure project.

1.8 Works Cited

[1] J. MacDonald, D. Newton, Milk Production Continues Shifting to Large-Scale Farms, USDA Economic Research Service. (2014) 1–5.

[2] J.M. Macdonald, J. Law, R. Mosheim, United States Department of Agriculture Consolidation in U.S. Dairy Farming United States Department of Agriculture, 2020. www.ers.usda.gov.

[3] A. Naranjo, A. Johnson, H. Rossow, E. Kebreab, Greenhouse gas, water, and land footprint per unit of production of the California dairy industry over 50 years, J Dairy Sci. 103 (2020) 3760–3773. https://doi.org/10.3168/jds.2019-16576.

[4] J.A. Burkholder, B. Libra, P. Weyer, S. Heathcote, D. Kolpin, P.S. Thorne, M. Wichman, Impacts of waste from concentrated animal feeding operations on water quality, Environ Health Perspect. 115 (2007) 308–312. https://doi.org/10.1289/ehp.8839.

[5] M.T. Niles, S. Wiltshire, Tradeoffs in US dairy manure greenhouse gas emissions, productivity, climate, and manure management strategies, Environ Res Commun. 1 (2019) 075003. https://doi.org/10.1088/2515-7620/ab2dec.

[6] D.L. Pfost, D. Rastorfer, Anaerobic lagoons for storage/treatment of livestock manure, University of Missouri-Extension. (2000).

[7] R.W. Todd, N.A. Cole, K.D. Casey, R. Hagevoort, B.W. Auvermann, Methane emissions from southern High Plains dairy wastewater lagoons in the summer, Anim Feed Sci Technol. 166–167 (2011) 575–580. https://doi.org/10.1016/j.anifeedsci.2011.04.040.

[8] J.A.D.R.N. Appuhamy, L.E. Moraes, C. Wagner-Riddle, D.P. Casper, E. Kebreab, Predicting manure volatile solid output of lactating dairy cows, J Dairy Sci. 101 (2018) 820–829. https://doi.org/10.3168/jds.2017-12813.

[9] D. Meyer, P.L. Price, H.A. Rossow, N. Silva-del-Rio, B.M. Karle, P.H. Robinson, E.J. DePeters, J.G. Fadel, Survey of dairy housing and manure management practices in California, J Dairy Sci. 94 (2011) 4744–4750. https://doi.org/10.3168/jds.2010-3761.

[10] M. Heidari, A. Dutta, B. Acharya, S. Mahmud, A review of the current knowledge and challenges of hydrothermal carbonization for biomass conversion, Journal of the Energy Institute. 92 (2019) 1779–1799. https://doi.org/10.1016/j.joei.2018.12.003.

[11] J.A. Libra, K.S. Ro, C. Kammann, A. Funke, N.D. Berge, Y. Neubauer, M.-M. Titirici, C. Fühner, O. Bens, J. Kern, K.-H. Emmerich, Hydrothermal carbonization of biomass residuals, Biofuels. 2 (2011) 89–124. https://doi.org/10.4155/bfs.10.81.

[12] A. Alkhudhiri, N. Darwish, N. Hilal, Membrane distillation: A comprehensive review, Desalination. 287 (2012) 2–18. https://doi.org/10.1016/j.desal.2011.08.027.

[13] N.A. Silva, S.R. Hiibel, Nutrient recovery of the hydrothermal carbonization aqueous product from dairy manure using membrane distillation, Environ Technol. 0 (2021) 1–10. https://doi.org/10.1080/09593330.2021.1995785.

[14] M. Tsarpali, N. Arora, J.N. Kuhn, G.P. Philippidis, Beneficial use of the aqueous phase generated during hydrothermal carbonization of algae as nutrient source for algae cultivation, Algal Res. 60 (2021) 102485. https://doi.org/10.1016/j.algal.2021.102485.

[15] D. Lachos-Perez, P. César Torres-Mayanga, E.R. Abaide, G.L. Zabot, F. de Castilhos, Hydrothermal carbonization and Liquefaction: differences, progress, challenges, and opportunities, Bioresour Technol. 343 (2022). https://doi.org/10.1016/j.biortech.2021.126084.

[16] M. Toufiq Reza, A. Freitas, X. Yang, S. Hiibel, H. Lin, C.J. Coronella, Hydrothermal carbonization (HTC) of cow manure: Carbon and nitrogen distributions in HTC products, Environ Prog Sustain Energy. 35 (2016) 1002–1011. https://doi.org/10.1002/ep.12312.

[17] A. v. Bandura, S.N. Lvov, The ionization constant of water over wide ranges of temperature and density, J Phys Chem Ref Data. 35 (2006) 15–30. https://doi.org/10.1063/1.1928231.

[18] L. Wang, Y. Chang, A. Li, Hydrothermal carbonization for energy-efficient processing of sewage sludge: A review, Renewable and Sustainable Energy Reviews. 108 (2019) 423–440. https://doi.org/10.1016/j.rser.2019.04.011.

[19] G. Ischia, L. Fiori, Hydrothermal Carbonization of Organic Waste and Biomass: A Review on Process, Reactor, and Plant Modeling, Waste Biomass Valorization. 12 (2021) 2797–2824. https://doi.org/10.1007/s12649-020-01255-3.

[20] A. Kruse, A. Funke, M.M. Titirici, Hydrothermal conversion of biomass to fuels and energetic materials, Curr Opin Chem Biol. 17 (2013) 515–521. https://doi.org/10.1016/j.cbpa.2013.05.004.

[21] T. Wang, Y. Zhai, Y. Zhu, C. Li, G. Zeng, A review of the hydrothermal carbonization of biomass waste for hydrochar formation: Process conditions, fundamentals, and physicochemical properties, Renewable and Sustainable Energy Reviews. 90 (2018) 223–247. https://doi.org/10.1016/j.rser.2018.03.071.

[22] S. Yu, X. Yang, Q. Li, Y. Zhang, H. Zhou, Breaking the temperature limit of hydrothermal carbonization of lignocellulosic biomass by decoupling temperature and pressure, Green Energy and Environment. (2023). https://doi.org/10.1016/j.gee.2023.01.001.

[23] J. Parnthong, S. Nualyai, W. Kraithong, A. Jiratanachotikul, P. Khemthong, K. Faungnawakij, S. Kuboon, Higher heating value prediction of hydrochar from sugarcane leaf and giant leucaena wood during hydrothermal carbonization process, J Environ Chem Eng. 10 (2022) 1DUMMY. https://doi.org/10.1016/j.jece.2022.108529.

[24] M.M. Titirici, M. Antonietti, Chemistry and materials options of sustainable carbon materials made by hydrothermal carbonization, Chem Soc Rev. 39 (2010) 103–116. https://doi.org/10.1039/b819318p.

[25] R. Demir-Cakan, P. Makowski, M. Antonietti, F. Goettmann, M.M. Titirici, Hydrothermal synthesis of imidazole functionalized carbon spheres and their application in catalysis, Catal Today. 150 (2010) 115–118. https://doi.org/10.1016/j.cattod.2009.05.003.

[26] M.T. Reza, J. Andert, B. Wirth, D. Busch, J. Pielert, J.G. Lynam, J. Mumme, Hydrothermal Carbonization of Biomass for Energy and Crop Production, Applied Bioenergy. 1 (2014) 11–29. https://doi.org/10.2478/apbi-2014-0001.

[27] S. v. Qaramaleki, J.A. Villamil, A.F. Mohedano, C.J. Coronella, Factors Affecting Solubilization of Phosphorus and Nitrogen through Hydrothermal Carbonization of Animal Manure, ACS Sustain Chem Eng. 8 (2020) 12462–12470. https://doi.org/10.1021/acssuschemeng.0c03268.

[28] K. Wu, Y. Gao, G. Zhu, J. Zhu, Q. Yuan, Y. Chen, M. Cai, L. Feng, Characterization of dairy manure hydrochar and aqueous phase products generated by hydrothermal carbonization at different temperatures, J Anal Appl Pyrolysis. 127 (2017) 335–342. https://doi.org/10.1016/j.jaap.2017.07.017.

[29] P.B. Kós, Biomedical potential of cyanobacteria and algae, n.d. www.kazusa.or.jp/.

[30] M.N. Metsoviti, G. Papapolymerou, I.T. Karapanagiotidis, N. Katsoulas, Effect of light intensity and quality on growth rate and composition of Chlorella vulgaris, Plants. 9 (2020). https://doi.org/10.3390/plants9010031.

[31] B.-P. Han, M. Virtanen, J. Koponen, M. Stras ˇkraba, Effect of photoinhibition on algal photosynthesis: a dynamic model, 2000. https://academic.oup.com/plankt/article/22/5/865/1475631.

[32] C. Wang, C.Q. Lan, Effects of shear stress on microalgae – A review, Biotechnol Adv. 36 (2018) 986–1002. https://doi.org/10.1016/j.biotechadv.2018.03.001.

[33] I. Branyikova, S. Lucakova, Technical and physiological aspects of microalgae cultivation and productivity—spirulina as a promising and feasible choice, Organic Agriculture. 11 (2021) 269–276. https://doi.org/10.1007/s13165-020-00323-1.

[34] J.-S. Chang, P.-L. Show, T.-C. Ling, C.-Y. Chen, S.-H. Ho, C.-H. Tan, D. Nagarajan, W.-N. Phong, 11 - Photobioreactors, in: C. Larroche, M.Á. Sanromán, G. Du, A. Pandey (Eds.), Current Developments in Biotechnology and Bioengineering, Elsevier, 2017: pp. 313–352. https://doi.org/https://doi.org/10.1016/B978-0-444-63663-8.00011-2.

[35] R.R. Narala, S. Garg, K.K. Sharma, S.R. Thomas-Hall, M. Deme, Y. Li, P.M. Schenk, Comparison of microalgae cultivation in photobioreactor, open raceway pond, and a two-stage hybrid system, Front Energy Res. 4 (2016). https://doi.org/10.3389/fenrg.2016.00029.

[36] D.M. Anderson, J.M. Burkholder, W.P. Cochlan, P.M. Glibert, C.J. Gobler, C.A. Heil, R.M. Kudela, M.L. Parsons, J.E.J. Rensel, D.W. Townsend, V.L. Trainer, G.A. Vargo, Harmful algal blooms and eutrophication: Examining linkages from selected coastal regions of the United States, Harmful Algae. 8 (2008) 39–53. https://doi.org/10.1016/j.hal.2008.08.017.

[37] A. Abeliovich, Y. Azov, Toxicity of ammonia to algae in sewage oxidation ponds, Appl Environ Microbiol. 31 (1976) 801–806. https://doi.org/10.1128/aem.31.6.801-806.1976.

[38] Q. Lu, P. Chen, M. Addy, R. Zhang, X. Deng, Y. Ma, Y. Cheng, F. Hussain, C. Chen, Y. Liu, R. Ruan, Carbon-dependent alleviation of ammonia toxicity for algae cultivation and associated mechanisms exploration, Bioresour Technol. 249 (2018) 99–107. https://doi.org/10.1016/j.biortech.2017.09.175.

[39] K. Gao, Approaches and involved principles to control pH/pCO2 stability in algal cultures, J Appl Phycol. 33 (2021) 3497–3505. https://doi.org/10.1007/s10811-021-02585-y.

[40] A. Ilavarasi, D. Mubarakali, R. Praveenkumar, E. Baldev, N. Thajuddin, Optimization of various growth media to freshwater microalgae for biomass production, Biotechnology. 10 (2011) 540–545. https://doi.org/10.3923/biotech.2011.540.545.

[41] A. Udayan, N. Sreekumar, M. Arumugam, Statistical optimization and formulation of microalga cultivation medium for improved omega 3 fatty acid production, Systems Microbiology and Biomanufacturing. 2 (2022) 369–379. https://doi.org/10.1007/s43393-021-00069-1.

[42] H.S. Yun, Y.S. Kim, H.S. Yoon, Effect of Different Cultivation Modes (Photoautotrophic, Mixotrophic, and Heterotrophic) on the Growth of Chlorella sp. and Biocompositions, Front Bioeng Biotechnol. 9 (2021). https://doi.org/10.3389/fbioe.2021.774143.

[43] G. Pinto, A. Pollio, L. Previtera, M. Stanzione, F. Temussi, Removal of low molecular weight phenols from olive oil mill wastewater using microalgae, 2003.

[44] S.F.L. Pereira, A.L. Gonçalves, F.C. Moreira, T.F.C.V. Silva, V.J.P. Vilar, J.C.M. Pires, Nitrogen removal from landfill leachate by microalgae, Int J Mol Sci. 17 (2016). https://doi.org/10.3390/ijms17111926.

[45] S. Yewalkar-Kulkarni, G. Gera, S. Nene, K. Pandare, B. Kulkarni, S. Kamble, Exploiting Phosphate-Starved cells of Scenedesmus sp. for the Treatment of Raw Sewage, Indian J Microbiol. 57 (2017) 241–249. https://doi.org/10.1007/s12088-016-0626-0.

[46] L. Zuliani, N. Frison, A. Jelic, F. Fatone, D. Bolzonella, M. Ballottari, Microalgae cultivation on anaerobic digestate of municipalwastewater, sewage sludge and agro-waste, Int J Mol Sci. 17 (2016). https://doi.org/10.3390/ijms17101692.

[47] S.Z. Tarhan, A.T. Koçer, D. Özçimen, İ. Gökalp, Cultivation of green microalgae by recovering aqueous nutrients in hydrothermal carbonization process water of biomass wastes, Journal of Water Process Engineering. 40 (2021). https://doi.org/10.1016/j.jwpe.2020.101783.

[48] L. Wang, L. Chen, S. (Xiao) Wu, Microalgae Cultivation Using Screened Liquid Dairy Manure Applying Different Folds of Dilution: Nutrient Reduction Analysis with Emphasis on Phosphorus Removal, Appl Biochem Biotechnol. 192 (2020) 381–391. https://doi.org/10.1007/s12010-020-03316-8.

[49] L. Wang, Y. Li, P. Chen, M. Min, Y. Chen, J. Zhu, R.R. Ruan, Anaerobic digested dairy manure as a nutrient supplement for cultivation of oil-rich green microalgae Chlorella sp., Bioresour Technol. 101 (2010) 2623–2628. https://doi.org/10.1016/j.biortech.2009.10.062.

[50] R. Rezaei, A. Akbulut, S.L. Sanin, Effect of algae acclimation to the wastewater medium on the growth kinetics and nutrient removal capacity, Environ Monit Assess. 191 (2019). https://doi.org/10.1007/s10661-019-7856-7.

[51] X. Wang, Y. Zhang, C. Xia, A. Alqahtani, A. Sharma, A. Pugazhendhi, A review on optimistic biorefinery products: Biofuel and bioproducts from algae biomass, Fuel. 338 (2023). https://doi.org/10.1016/j.fuel.2022.127378.

[52] M.E. Montingelli, S. Tedesco, A.G. Olabi, Biogas production from algal biomass: A review, Renewable and Sustainable Energy Reviews. 43 (2015) 961–972. https://doi.org/10.1016/j.rser.2014.11.052.

[53] X. Li, S. Huang, J. Yu, Q. Wang, S. Wu, Improvement of hydrogen production of Chlamydomonas reinhardtii by co-cultivation with isolated bacteria, Int J Hydrogen Energy. 38 (2013) 10779–10787. https://doi.org/10.1016/j.ijhydene.2013.02.102.

[54] G. Breuer, P.P. Lamers, D.E. Martens, R.B. Draaisma, R.H. Wijffels, The impact of nitrogen starvation on the dynamics of triacylglycerol accumulation in nine microalgae strains, Bioresour Technol. 124 (2012) 217–226. https://doi.org/10.1016/j.biortech.2012.08.003.

[55] A. Converti, A.A. Casazza, E.Y. Ortiz, P. Perego, M. Del Borghi, Effect of temperature and nitrogen concentration on the growth and lipid content of Nannochloropsis oculata and Chlorella vulgaris for biodiesel production, Chemical Engineering and Processing: Process Intensification. 48 (2009) 1146–1151. https://doi.org/10.1016/j.cep.2009.03.006.

[56] A. Brar, M. Kumar, T. Soni, V. Vivekanand, N. Pareek, Insights into the genetic and metabolic engineering approaches to enhance the competence of microalgae as biofuel resource: A review, Bioresour Technol. 339 (2021). https://doi.org/10.1016/j.biortech.2021.125597.

[57] Z. Zhu, J. Sun, Y. Fa, X. Liu, P. Lindblad, Enhancing microalgal lipid accumulation for biofuel production, Front Microbiol. 13 (2022). https://doi.org/10.3389/fmicb.2022.1024441.

[58] V.C. Liyanaarachchi, M. Premaratne, T.U. Ariyadasa, P.H.V. Nimarshana, A. Malik, Two-stage cultivation of microalgae for production of high-value compounds and biofuels: A review, Algal Res. 57 (2021). https://doi.org/10.1016/j.algal.2021.102353.

[59] C.H. Ra, C.H. Kang, J.H. Jung, G.T. Jeong, S.K. Kim, Effects of light-emitting diodes (LEDs) on the accumulation of lipid content using a two-phase culture process with three microalgae, Bioresour Technol. 212 (2016) 254–261. https://doi.org/10.1016/j.biortech.2016.04.059.

[60] L. Xia, H. Ge, X. Zhou, D. Zhang, C. Hu, Photoautotrophic outdoor two-stage cultivation for oleaginous microalgae Scenedesmus obtusus XJ-15, Bioresour Technol. 144 (2013) 261–267. https://doi.org/10.1016/j.biortech.2013.06.112.

[61] J.L. García, M. de Vicente, B. Galán, Microalgae, old sustainable food and fashion nutraceuticals, Microb Biotechnol. 10 (2017) 1017–1024. https://doi.org/10.1111/1751-7915.12800.

[62] J. Fabregas, C. Herrero, Vitamin content of four marine microalgae. Potential use as source of vitamins in nutrition, 1990. https://academic.oup.com/jimb/article/5/4/259/5940467.

[63] S. Mobin, F. Alam, Some Promising Microalgal Species for Commercial Applications: A review, in: Energy Procedia, Elsevier Ltd, 2017: pp. 510–517. https://doi.org/10.1016/j.egypro.2017.03.177.

[64] L. Jiang, Y. Wang, Q. Yin, G. Liu, H. Liu, Y. Huang, B. Li, Phycocyanin: A potential drug for cancer treatment, J Cancer. 8 (2017) 3416–3429. https://doi.org/10.7150/jca.21058.

[65] R. Darwish, M.A. Gedi, P. Akepach, H. Assaye, A.S. Zaky, D.A. Gray, Chlamydomonas reinhardtii Is a Potential Food Supplement with the Capacity to Outperform Chlorella and Spirulina, Applied Sciences. 10 (2020). https://doi.org/10.3390/app10196736.

[66] Y. Ling, L. ping Sun, S. ying Wang, C.S.K. Lin, Z. Sun, Z. gang Zhou, Cultivation of oleaginous microalga Scenedesmus obliquus coupled with wastewater treatment for enhanced biomass and lipid production, Biochem Eng J. 148 (2019) 162–169. https://doi.org/10.1016/j.bej.2019.05.012.

[67] E. Balis, J.C. Griffin, S.R. Hiibel, Membrane Distillation-Crystallization for inland desalination brine treatment, Sep Purif Technol. 290 (2022). https://doi.org/10.1016/j.seppur.2022.120788.

[68] R.D. Gustafson, S.R. Hiibel, A.E. Childress, Membrane distillation driven by intermittent and variable-temperature waste heat: System arrangements for water production and heat storage, Desalination. 448 (2018) 49–59. https://doi.org/10.1016/j.desal.2018.09.017.

[69] K.A. Salls, D. Won, E.P. Kolodziej, A.E. Childress, S.R. Hiibel, Evaluation of semi-volatile contaminant transport in a novel, gas-tight direct contact membrane distillation system, Desalination. 427 (2018) 35–41. https://doi.org/10.1016/j.desal.2017.11.001.

[70] O. Alrehaili, F. Perreault, S. Sinha, P. Westerhoff, Increasing net water recovery of reverse osmosis with membrane distillation using natural thermal differentials between brine and co-located water sources: Impacts at large reclamation facilities, Water Res. 184 (2020) 116134. https://doi.org/10.1016/j.watres.2020.116134.

[71] Z. Yan, H. Yang, F. Qu, H. Yu, H. Liang, G. Li, J. Ma, Reverse osmosis brine treatment using direct contact membrane distillation: Effects of feed temperature and velocity, Desalination. 423 (2017) 149–156. https://doi.org/10.1016/j.desal.2017.09.010.

[72] G. Naidu, S. Jeong, Y. Choi, S. Vigneswaran, Membrane distillation for wastewater reverse osmosis concentrate treatment with water reuse potential, J Memb Sci. 524 (2017) 565–575. https://doi.org/10.1016/j.memsci.2016.11.068.

[73] R. Bagger-Jørgensen, A.S. Meyer, M. Pinelo, C. Varming, G. Jonsson, Recovery of volatile fruit juice aroma compounds by membrane technology: Sweeping gas versus vacuum membrane distillation, Innovative Food Science and Emerging Technologies. 12 (2011) 388–397. https://doi.org/10.1016/j.ifset.2011.02.005.

[74] A. Kujawska, J.K. Kujawski, M. Bryjak, M. Cichosz, W. Kujawski, Removal of volatile organic compounds from aqueous solutions applying thermally driven membrane processes. 2. Air gap membrane distillation, J Memb Sci. 499 (2016) 245–256. https://doi.org/10.1016/j.memsci.2015.10.047.

[75] L. Eykens, I. Hitsov, K. De Sitter, C. Dotremont, L. Pinoy, B. Van der Bruggen, Direct contact and air gap membrane distillation: Differences and similarities between lab and pilot scale, Desalination. 422 (2017) 91–100. https://doi.org/10.1016/j.desal.2017.08.018.

[76] Z. Xie, T. Duong, M. Hoang, C. Nguyen, B. Bolto, Ammonia removal by sweep gas membrane distillation, Water Res. 43 (2009) 1693–1699. https://doi.org/10.1016/j.watres.2008.12.052.

[77] P.M. Duyen, P. Jacob, R. Rattanaoudom, C. Visvanathan, Feasibility of sweeping gas membrane distillation on concentrating triethylene glycol from waste streams, Chemical Engineering and Processing: Process Intensification. 110 (2016) 225–234. https://doi.org/10.1016/j.cep.2016.10.015.

[78] G.C. Sarti, C. Gostoli, S. Bandini, Extraction of organic components from aqueous streams by vacuum membrane distillation, J Memb Sci. 80 (1993) 21–33. https://doi.org/10.1016/0376-7388(93)85129-K.

[79] A. Criscuoli, E. Drioli, Vacuum membrane distillation for the treatment of coffee products, Sep Purif Technol. 209 (2019) 990–996. https://doi.org/10.1016/j.seppur.2018.09.058.

[80] L. Francis, N. Ghaffour, A.A. Alsaadi, G.L. Amy, Material gap membrane distillation: A new design for water vapor flux enhancement, J Memb Sci. 448 (2013) 240–247. https://doi.org/10.1016/j.memsci.2013.08.013.

[81] G. Naidu, W.G. Shim, S. Jeong, Y.K. Choi, N. Ghaffour, S. Vigneswaran, Transport phenomena and fouling in vacuum enhanced direct contact membrane distillation: Experimental and modelling, Sep Purif Technol. 172 (2017) 285–295. https://doi.org/10.1016/j.seppur.2016.08.024.

[82] Y. Liu, T. Horseman, Z. Wang, H.A. Arafat, H. Yin, S. Lin, T. He, Negative Pressure Membrane Distillation for Excellent Gypsum Scaling Resistance and Flux Enhancement, Environ Sci Technol. 56 (2022) 1405–1412. https://doi.org/10.1021/acs.est.1c07144.

[83] S. Cong, X. Liu, F. Guo, Membrane distillation using surface modified multi-layer porous ceramics, Int J Heat Mass Transf. 129 (2019) 764–772. https://doi.org/10.1016/j.ijheatmasstransfer.2018.10.011.

[84] S. Abdulhamid Alftessi, M. Hafiz Dzarfan Othman, M. Ridhwan Bin Adam, T. Mohamed Farag, Z. Sheng Tai, Y. Olabode Raji, M.A. Rahman, J. Jaafar, A. Fauzi Ismail, S. Abu Bakar, Hydrophobic silica sand ceramic hollow fiber membrane for desalination via direct contact membrane distillation, Alexandria Engineering Journal. 61 (2022) 9609–9621. https://doi.org/10.1016/j.aej.2022.03.044.

[85] K. Bin Bandar, M.D. Alsubei, S.A. Aljlil, N. Bin Darwish, N. Hilal, Membrane distillation process application using a novel ceramic membrane for Brackish water desalination, Desalination. 500 (2021). https://doi.org/10.1016/j.desal.2020.114906.

[86] N.M.A. Omar, M.H.D. Othman, Z.S. Tai, T.A. Kurniawan, T. El-badawy, P.S. Goh, N.H. Othman, M.A. Rahman, J. Jaafar, A.F. Ismail, Bottlenecks and recent improvement strategies of ceramic membranes in membrane distillation applications: A review, J Eur Ceram Soc. 42 (2022) 5179–5194. https://doi.org/10.1016/j.jeurceramsoc.2022.06.019.

[87] E. Balis, A. Sapalidis, G. Pilatos, E. Kouvelos, C. Athanasekou, C. Veziri, P. Boutikos, K.G. Beltsios, G. Romanos, Enhancement of vapor flux and salt rejection efficiency induced by low cost-high purity MWCNTs in upscaled PVDF and PVDF-HFP hollow fiber modules for membrane distillation, Sep Purif Technol. 224 (2019) 163–179. https://doi.org/10.1016/j.seppur.2019.04.067.

[88] M. Miao, T. Liu, J. Bai, Y. Wang, Engineering the wetting behavior of ceramic membrane by carbon nanotubes via a chemical vapor deposition technique, J Memb Sci. 648 (2022). https://doi.org/10.1016/j.memsci.2022.120357.

[89] J. Liu, Q. Wang, H. Shan, H. Guo, B. Li, Surface hydrophobicity based heat and mass transfer mechanism in membrane distillation, J Memb Sci. 580 (2019) 275–288. https://doi.org/10.1016/j.memsci.2019.01.057.

[90] M. Rezaei, D.M. Warsinger, J.H. Lienhard V, W.M. Samhaber, Wetting prevention in membrane distillation through superhydrophobicity and recharging an air layer on the membrane surface, J Memb Sci. 530 (2017) 42–52. https://doi.org/10.1016/j.memsci.2017.02.013.

[91] W. Qing, J. Wang, X. Ma, Z. Yao, Y. Feng, X. Shi, F. Liu, P. Wang, C.Y. Tang, One-step tailoring surface roughness and surface chemistry to prepare superhydrophobic polyvinylidene fluoride (PVDF) membranes for enhanced membrane distillation performances, J Colloid Interface Sci. 553 (2019) 99–107. https://doi.org/10.1016/j.jcis.2019.06.011.

[92] X. Li, H. Shan, M. Cao, B. Li, Facile fabrication of omniphobic PVDF composite membrane via a waterborne coating for anti-wetting and anti-fouling membrane distillation, J Memb Sci. 589 (2019) 117262. https://doi.org/10.1016/j.memsci.2019.117262.

[93] S. Ragunath, S. Roy, S. Mitra, Selective hydrophilization of the permeate surface to enhance flux in membrane distillation, Sep Purif Technol. 170 (2016) 427–433. https://doi.org/10.1016/j.seppur.2016.07.001.

[94] J. Woods, J. Pellegrino, J. Burch, Generalized guidance for considering pore-size distribution in membrane distillation, J Memb Sci. 368 (2011) 124–133. https://doi.org/10.1016/j.memsci.2010.11.041.

[95] A.C.M. Franken, J.A.M. Nolten, M.H.V. Mulder, D. Bargeman, C.A. Smolders, Wetting criteria for the applicability of membrane distillation, J Memb Sci. 33 (1987) 315–328. https://doi.org/10.1016/S0376-7388(00)80288-4.

[96] L. Eykens, K. De Sitter, C. Dotremont, L. Pinoy, B. Van Der Bruggen, How to Optimize the Membrane Properties for Membrane Distillation: A Review, Ind Eng Chem Res. 55 (2016) 9333–9343. https://doi.org/10.1021/acs.iecr.6b02226.

[97] S. Srisurichan, R. Jiraratananon, A.G. Fane, Mass transfer mechanisms and transport resistances in direct contact membrane distillation process, J Memb Sci. 277 (2006) 186–194. https://doi.org/10.1016/j.memsci.2005.10.028.

[98] F. Laganà, G. Barbieri, E. Drioli, Direct contact membrane distillation: Modelling and concentration experiments, J Memb Sci. 166 (2000) 1–11. https://doi.org/10.1016/S0376-7388(99)00234-3.

[99] S. Goh, J. Zhang, Y. Liu, A.G. Fane, Fouling and wetting in membrane distillation (MD) and MD-bioreactor (MDBR) for wastewater reclamation, Desalination. 323 (2013) 39–47. https://doi.org/10.1016/j.desal.2012.12.001.

[100] C.R. Taylor, P. Ahmadiannamini, S.R. Hiibel, Identifying pore wetting thresholds of surfactants in direct contact membrane distillation, Sep Purif Technol. 217 (2019) 17–23. https://doi.org/10.1016/j.seppur.2019.01.061.

[101] N.G.P. Chew, S. Zhao, C.H. Loh, N. Permogorov, R. Wang, Surfactant effects on water recovery from produced water via direct-contact membrane distillation, J Memb Sci. 528 (2017) 126–134. https://doi.org/10.1016/j.memsci.2017.01.024.

[102] Z. Zhu, Z. Liu, Y. Zhang, B. Li, H. Lu, N. Duan, B. Si, R. Shen, J. Lu, Recovery of reducing sugars and volatile fatty acids from cornstalk at different hydrothermal treatment severity, Bioresour Technol. 199 (2016) 220–227. https://doi.org/10.1016/j.biortech.2015.08.043.

[103] L.P. Xiao, Z.J. Shi, F. Xu, R.C. Sun, Hydrothermal carbonization of lignocellulosic biomass, Bioresour Technol. 118 (2012) 619–623. https://doi.org/10.1016/j.biortech.2012.05.060.

[104] J.R. Lakowicz, ed., Introduction to Fluorescence, in: Principles of Fluorescence Spectroscopy, Springer US, Boston, MA, 2006: pp. 1–26. https://doi.org/10.1007/978-0-387-46312-4_1.

[105] A.J. Lawaetz, C.A. Stedmon, Fluorescence intensity calibration using the Raman scatter peak of water, Appl Spectrosc. 63 (2009) 936–940. https://doi.org/10.1366/000370209788964548.

[106] L. Tan, W. Du, Y. Zhang, L.J. Tang, J.H. Jiang, R.Q. Yu, Rayleigh scattering correction for fluorescence spectroscopy analysis, Chemometrics and Intelligent Laboratory Systems. 203 (2020). https://doi.org/10.1016/j.chemolab.2020.104028.

[107] M.A. Linne, Spectroscopic Measurement : An Introduction to the Fundamentals, Elsevier Science & Technology, San Diego, UNITED KINGDOM, 2002. http://ebookcentral.proquest.com/lib/knowledgecenter/detail.action?docID=299535.

[108] G.W. Faris, R.A. Copeland, Wavelength dependence of the Raman cross section for liquid water, 1997.

[109] D.M. McKnight, E.W. Boyer, P.K. Westerhoff, P.T. Doran, T. Kulbe, D.T. Andersen, Spectrofluorometric characterization of dissolved organic matter for indication of precursor organic material and aromaticity, Limnol Oceanogr. 46 (2001) 38–48. https://doi.org/10.4319/lo.2001.46.1.0038.

[110] P.H.C. Eilers, P.M. Kroonenberg, Modeling and correction of Raman and Rayleigh scatter in fluorescence landscapes, Chemometrics and Intelligent Laboratory Systems. 130 (2014) 1–5. https://doi.org/10.1016/j.chemolab.2013.09.002.

[111] M. Bahram, R. Bro, C. Stedmon, A. Afkhami, Handling of Rayleigh and Raman scatter for PARAFAC modeling of fluorescence data using interpolation, J Chemom. 20 (2006) 99–105. https://doi.org/10.1002/cem.978.

[112] J.R. Lakowicz, ed., Instrumentation for Fluorescence Spectroscopy, in: Principles of Fluorescence Spectroscopy, Springer US, Boston, MA, 2006: pp. 27–61. https://doi.org/10.1007/978-0-387-46312-4_2.

[113] T. Weitner, T. Friganović, D. Šakić, Inner Filter Effect Correction for Fluorescence Measurements in Microplates Using Variable Vertical Axis Focus, Anal Chem. (2022). https://doi.org/10.1021/acs.analchem.2c01031.

[114] T. Larsson, M. Wedborg, D. Turner, Correction of inner-filter effect in fluorescence excitation-emission matrix spectrometry using Raman scatter, Anal Chim Acta. 583 (2007) 357–363. https://doi.org/10.1016/j.aca.2006.09.067.

[115] B. Liu, L. Gu, X. Yu, G. Yu, H. Zhang, J. Xu, Dissolved organic nitrogen (DON) profile during backwashing cycle of drinking water biofiltration, Science of the Total Environment. 414 (2012) 508–514. https://doi.org/10.1016/j.scitotenv.2011.10.049.

[116] M. Sgroi, P. Roccaro, G. v. Korshin, V. Greco, S. Sciuto, T. Anumol, S.A. Snyder, F.G.A. Vagliasindi, Use of fluorescence EEM to monitor the removal of emerging contaminants in full scale wastewater treatment plants, J Hazard Mater. 323 (2017) 367–376. https://doi.org/10.1016/j.jhazmat.2016.05.035.

[117] W. Chen, P. Westerhoff, J.A. Leenheer, K. Booksh, Fluorescence Excitation-Emission Matrix Regional Integration to Quantify Spectra for Dissolved Organic Matter, Environ Sci Technol. 37 (2003) 5701–5710. https://doi.org/10.1021/es034354c.

[118] A. Zsolnay, E. Baigar, M. Jimenez, B. Steinweg, F. Saccomandi, Differentiating with fluorescence spectroscopy the sources of dissolved organic matter in soils subjected to drying, Chemosphere. 38 (1999) 45–50. https://doi.org/https://doi.org/10.1016/S0045-6535(98)00166-0.

[119] K. Xiao, Y. Shen, S. Liang, J. Tan, X. Wang, P. Liang, X. Huang, Characteristic Regions of the Fluorescence Excitation-Emission Matrix (EEM) to Identify Hydrophobic/Hydrophilic Contents of Organic Matter in Membrane Bioreactors, Environ Sci Technol. 52 (2018) 11251–11258. https://doi.org/10.1021/acs.est.8b02684.

[120] K.R. Murphy, C.A. Stedmon, P. Wenig, R. Bro, OpenFluor- An online spectral library of auto-fluorescence by organic compounds in the environment, Analytical Methods. 6 (2014) 658–661. https://doi.org/10.1039/c3ay41935e.

2 NUTRIENT RECOVERY BY MICROALGAE IN AQUEOUS PRODUCT OF HYDROTHERMAL CARBONIZATION OF DAIRY MANURE

Silva, N. A., Glover, C. J., and Hiibel, S. R. (in revision). *Cleaner Waste Systems*.

Approximate contributions of each author are as follows:

N.A. Silva performed 60% of experimental data collection, 40% of manuscript preparation, and 100% of manuscript revision.
C.J. Glover performed 40% of experimental data collection and 60% of manuscript preparation.
S.R. Hiibel assisted with experimental design, project management, and manuscript review.

2.1 Abstract

Hydrothermal carbonization (HTC) is an emerging technology for energy recovery from wet biomass waste streams, including dairy manure. The HTC aqueous product (HAP) contains organic compounds and nutrients, requiring further treatment prior to environmental discharge. The goal of this study was to evaluate nutrient removal from dairy manure HAP using four species of microalgae: *Chlamydomonas reinhardtii, Chlorella vulgaris, Arthrospira maxima,* and *Scenedesmus obliquus*. The optimal HAP concentration for all species was 5% with little to no growth observed at lower dilutions. The highest nutrient removal occurred with *A. maxima* with >93%, 33%, 81%, and 50% removal of NH_3, NO_3^-, total nitrogen (TN), and total phosphorus (TP), respectively. Nutrient removal with the other species ranged from 35-82% of NH_3, 29-35% of NO_3^-, 12-34% of TN, and 8-78% of TP. Integrating HTC and microalgae cultivation is a promising treatment method for combined energy and nutrient recovery from dairy manure.

2.2 Introduction

Recent widespread growth in the US dairy industry has led to larger farm sizes, with the median farm size increasing from 80 to 900 cows between 1987 and 2012 [1]. While larger farms are more cost-effective and able to meet growing demand for dairy products, the concentrated production of large quantities of manure has led to environmental concerns and challenges. The EPA reports that a significant portion of manure nutrients (60-70%) cannot be absorbed by the cropland where farms are located [2], leading to soil nutrient buildup and water quality concerns. Manure management is also responsible for substantial greenhouse gas (GHG) emissions, with dairy manure contributing approximately half of the total US livestock manure GHG emissions at 40 MMT CO_2-eq. per year [3]. The negative environmental impacts associated with manure management combined with the growing need for renewable energy sources has driven interest in waste-to-energy technologies that can use materials such as dairy manure as a feedstock. One such promising emerging technology for manure management is hydrothermal carbonization (HTC).

HTC is a thermochemical conversion process that uses water at high temperature and pressure to convert wet biomass, such as dairy manure, into a stable solid fuel known as hydrochar. During the HTC process, a portion of nutrients and soluble organic compounds present in the manure partition to the HTC aqueous product (HAP) [4]. Typical HTC temperatures range from 180 to 250 °C [5], with higher temperatures increasing the energy value of the hydrochar but decreasing the yield [6]. HTC is advantageous because it can utilize wet biomass, eliminating the need for an energy-intensive drying step prior to the reaction. Many large-scale dairy farms handle liquid manure, which can also be

processed directly by HTC. Previous studies have demonstrated the feasibility of HTC to convert dairy manure to hydrochar for energy recovery. Depending on the reaction conditions used, the energy value of the hydrochar can range from 19-22 MJ/kg, similar to lignite coal [6]. Energy recovery through HTC is advantageous from an environmental perspective when hydrochar is used for energy production in place of fossil coal [7].

However, further research is needed to treat the nutrient-rich HAP stream to reduce environmental impacts associated with nutrients, metals, and organic compounds [7–9]. The type and concentration of nutrients and organic compounds in HAP are highly dependent on the feedstock and reaction conditions [10]. Degradation of lignocellulosic biomass can produce sugars, amino acids, volatile fatty acids (VFAs), and alcohols, as well as potentially toxic compounds such as phenols, furfurals, and aldehydes [6,11–13]. Anaerobic digestion (AD) has been proposed as a treatment method for HAP to recover additional energy from the organic compounds [12,14]; however, HAP is also a rich source of nutrients. Typically, the majority of nitrogen (N) in manure is present in organic forms such as amino acids, with smaller fractions present as NH_3-N and NO_x-N [4,6], while phosphorus (P) is mostly present as PO_4^{3-}. However, the reaction conditions used for HTC affect the form and concentration of nutrients found in HAP [4,6]. Several methods have been proposed to treat HAP and recover nutrients for application as a fertilizer [15–17], mineral precipitation [18], and microalgae cultivation [19,20].

Microalgae have been widely used for nutrient recovery from a variety of wastewater sources, including municipal wastewater [21,22] and livestock manure [23–25]. Production of algae at the industrial scale is limited by the cost of supplying adequate water and nutrients; however, using wastewater sources such as manure that contain

adequate nutrients, organic carbon, and water can improve the sustainability of large-scale cultivation [26,27]. In addition, the choice of growth medium may impact the energy requirements of these large-scale production facilities [28]. Algae have the benefit of high biomass productivities and can be grown on nonarable land, reducing competition with conventional terrestrial crops [26]. In the context of large-scale farms, algae biomass is also a rich source of protein that can be incorporated into the cow diet, replacing or supplementing conventional protein sources such as soybean and canola [29–31]. Nutrient recovery via microalgae in manure waste streams has also been shown to reduce eutrophication impacts associated with N and P contamination of water resources [32–34].

Studies of algae cultivation in hydrothermal effluents are more limited, although several groups have reported that substantially diluted HAP (~1.7 mg-P/L) can support algae growth [19,20]. Belete et al. [19] achieved high nutrient removals in HAP derived from sewage sludge with >87% of TN and >97% of TP removed, and growth rates greater than a standard media (BG-11) were observed. Lower nutrient removals, with 45-60% of TN and 85-95% of TP removed, have also been reported [20]. In both studies, potentially inhibiting species formed during the HTC process were hypothesized to be sufficiently diluted so as not to interfere with algae growth; however, such large water inputs will lead to high freshwater demand for a full-scale process [32]. Aqueous products from hydrothermal liquefaction (HTL) have also been evaluated as a medium for algae growth [35–37]. While similar to HTC, HTL uses higher temperatures (250-375 °C) and pressures to convert wet biomass into a biocrude oil and a nutrient-rich aqueous phase [5]. Several species of microalgae have been successfully cultivated in HTL aqueous products from various feedstocks, predominantly other algal biomass, although substantial dilutions are

also required to support growth (1-40 mg-P/L) [35,36,38]. These studies emphasize application for biofuels and target higher lipid content to produce crude bio-oil [39]. Such results for both HTC and HTL effluents suggest that nutrient recovery from HAP derived from dairy manure may be a feasible treatment option, and cultivation of protein-rich biomass on-site would have the added benefit of direct reuse on farms as a cattle feed or supplement.

The goal of this study was to evaluate the performance of four common algae species using HAP derived from dairy manure as the sole nutrient source. First, the tolerance of each species to different concentrations of HAP was determined to identify the optimal concentration to support growth and the minimum possible dilution. Next, the nutrient removal efficiency was determined in the optimal HAP concentration along with total biomass productivity. In addition, the protein and carbohydrate content of the produced biomass was determined, along with the elemental composition, to evaluate the use of each species as a protein supplement. The results of this study are intended to inform alternative treatment methods for dairy manure as part of an integrated nutrient and energy recovery scheme.

2.3 Materials and Methods

2.3.1 HTC Aqueous Product

Fresh dairy manure was collected from lactating Jersey cows at a commercial dairy farm in Fallon, NV. Manure was air dried for two weeks under ambient conditions, then ground to particle sizes <1 mm using a Model 4 Wiley Mill (Thomas Scientific, Swedesboro, NJ) and stored in plastic bags at 4 °C until use. For the HTC reaction, dried

manure was rehydrated at a 1:10 mass ratio of solids to water using deionized water. The rehydrated manure slurry was added to a 1-L reactor (Parr Instrument Company, Moline, IL) and the system purged with N_2 gas. The slurry was constantly mixed at 100 RPM and the temperature was increased to 200 °C at a rate of 2 °C/min, then maintained at 200 °C for 10 min [40]. The pressure in the reactor was autogenously produced by the water vapor. After 10 min, the reactor was rapidly cooled to room temperature using an ice bath and fan. The gaseous products were vented and the solid-liquid slurry was vacuum filtered using Whatman 42 filter paper. The aqueous product was immediately prepared for algae cultivation by diluting with deionized water and autoclaving the solution. The buffered HAP dilutions were prepared by combining sterile, equal volumes of HAP at 2x the concentration with a buffer solution (324 mM $NaHCO_3$, 76 mM Na_2CO_3) to obtain the target HAP concentration with an equivalent buffer concentration to the Spirulina media, and to prevent precipitation during autoclaving.

2.3.2 Algae Inoculum Cultures

Four microalgae species cultures were obtained from the University of Texas at Austin Culture Collection of Algae: *Arthrospira maxima* (UTEX LB 2342), *Chlorella vulgaris* (UTEX 30), *Scenedesmus obliquus* (UTEX 393), and *Chlamydomonas reinhardtii* (UTEX 2243). Stock cultures were grown and maintained in media suggested by UTEX for each species. A. *maxima* was grown in Spirulina medium, a variation of Zarrouk's medium, at pH = 9.5 with the following composition: 162 mM $NaHCO_3$, 38 mM Na_2CO_3, 2.9 mM K_2HPO_4, 29.4 mM $NaNO_3$, 5.74 mM K_2SO_4, 17.7 mM NaCl, 0.81 mM $MgSO_4$, 0.27 mM $CaCl_2{\cdot}2H_2O$, 12 μM $Na_2EDTA{\cdot}2H_2O$, 10 μM H_3BO_3, 2.2 μM $FeCl_3{\cdot}6H_2O$, 1.3

μM $MnCl_2 \cdot 4H_2O$, 0.22 μM $ZnCl_2$, 0.16 μM $Na_2MoO_4 \cdot 2H_2O$, 0.15 μM $ZnSO_4 \cdot 7H_2O$, 0.13 μM $CoCl_2 \cdot 6H_2O$, 0.08 μM $CuSO_4 \cdot 5H_2O$, and 100 nM vitamin B_{12}. *C. vulgaris* and *S. obliquus* were grown in Proteose Peptone media by adding 1 g/L proteose peptone (BD 211684) to Bristol medium (2.94 mM $NaNO_3$, 0.17 mM $CaCl_2 \cdot 2H_2O$, 0.3 mM $MgSO_4 \cdot 7H_2O$, 0.43 mM K_2HPO_4, 1.29 mM KH_2PO_4, 0.43 mM NaCl). *C. reinhardtii* was prepared using P49 media: 0.16 mM $MgSO_4 \cdot 7H_2O$, 0.16 mM Na_2glycerophosphate$\cdot 5H_2O$, 0.67 mM KCl, 3.8 mM glycylglycine, 1.2 mM NH_4NO_3, 0.5 mM $CaCl_2 \cdot 2H_2O$, 0.2 g/L yeast extract, 0.4 g/L tryptone, 12 μM $Na_2EDTA \cdot 2H_2O$, 2.2 μM $FeCl_3 \cdot 6H_2O$, 1.3 μM $MnCl_2 \cdot 4H_2O$, 0.23 μM $ZnCl_2$, 0.10 μM $Na_2MoO_4 \cdot 2H_2O$, 0.050 μM $CoCl_2 \cdot 6H_2O$, 1.3 μM thiamine, 100 nM biotin, and 100 nM vitamin B_{12}.

2.3.3 Experimental Design

2.3.3.1 HAP Tolerance

Each algae species' tolerance to HAP was tested to identify the optimal HAP concentration for growth with HAP as the sole nutrient source. Batch cultivation experiments were carried out using 250-mL Erlenmeyer flasks with 100 mL working volume. Cultures were continuously mixed at 80 rpm using orbital shake tables. White lights (Sylvania Octron® Eco®, 17W) were set at 60 μmol/m^2/s to a 12-hour alternating light-dark sequence during all experiments. HAP solutions were autoclaved and diluted to the appropriate concentration using sterile deionized water. Four HAP dilutions were tested: 3% (4 mg-P/L, 45 mg-N/L), 5% (6 mg-P/L, 75 mg-N/L), 10% (12 mg-P/L, 150 mg-N/L), and 15% (18 mg-P/L, 225 mg-N/L), with each concentration tested in triplicate for each algae species. Phosphorus and nitrogen values are provided for comparison to other

studies. In addition, triplicate cultures of each species in the corresponding media were diluted to have the same phosphorus content as the 10% diluted HAP (~12 mg-P/L) and were grown for comparison as positive controls. The resulting TN concentrations for the *A. maxima* media, *C. vulgaris*/*S. obliquus* media, and *C. reinhardtii* media are 55 mg-N/L, 52 mg-N/L, and 150 mg-N/L respectively. A HAP blank (no inoculum) was measured for each concentration as a negative control. To prevent carryover of media nutrients, each culture was centrifuged at 4500g for 10 min and excess media solution was decanted. Algae was resuspended in sterilized deionized water and centrifuged again, then the rinsed algae were inoculated into HAP solutions. Experiments continued until the stationary phase was reached. Growth curves were obtained for each species in each HAP dilution and the length of the exponential phase was determined. The optimal HAP concentration for each species was determined using the observed specific growth rate.

2.3.3.2 Nutrient Uptake

Once the optimal HAP concentrations were determined through HAP tolerance tests, a second set of growth experiments was performed to determine nutrient removal from HAP. The same experimental setup for batch cultivation in flasks was used, with the optimal HAP concentration as the nutrient source for all species. At the end of the experiment, the biomass was harvested by centrifugation at 4500g for 10 min. Excess HAP solution was removed by decanting the liquid and resuspending the algae in sterilized deionized water and centrifuging again. After excess HAP solution was removed, samples were taken for protein and carbohydrate analysis. The remaining biomass was freeze dried to measure productivity. Elemental analysis was conducted on the dried pellet.

2.3.4 Analytical Methods

2.3.4.1 Algae Growth Measurements

Growth was monitored using optical density (OD) at 750 nm measured with a Hach DR6000 spectrophotometer (HACH, Loveland, OH). OD_{750} was measured twice per day during the exponential phase of the HAP tolerance tests and once per day during the nutrient uptake tests. Non-inoculated sterile media was used as a spectrophotometric blank for each culture at the corresponding HAP concentration. Observed specific growth rates, μ_{obs}, were determined by plotting the natural logarithm of the OD_{750} data and calculating the slope of the linear portion for each culture replicate (Eq. 2.1).

$$\mu_{obs} = \frac{\ln(OD_2) - \ln(OD_1)}{t_2 - t_1} \tag{2.1}$$

2.3.4.2 Nutrient Measurements

During the nutrient uptake experiments, total nitrogen (TN), total phosphorus (TP), NO_3^-, and NH_3were measured once per day to track consumption by the algae. Samples were taken from each culture and centrifuged to remove the algae biomass; the supernatant was used for nutrient measurements. The analysis was conducted spectrophotometrically using HACH kits (HACH, Loveland, Ohio). The kits for the TN, TP, NO_3^-, and NH_3 measurements are TNT 826, TNT 843, TNT 835, and TNT 830, respectively.

2.3.4.3 Protein, Carbohydrate, and CHNS Content

At the end of the nutrient uptake experiments, separated and rinsed biomass was resuspended in sterilized deionized water to analyze carbohydrate content in the biomass. Carbohydrates were quantified using a phenol-sulfuric method [41,42]. In this procedure, 0.5 mL of a 5% phenol mixture was added to 0.5 mL of the rinsed algae sample resuspended in DI water in a 5-mL glass test tube. Next, 2.5 mL of concentrated sulfuric acid was added to the mixture and the test tube was quickly capped and vortexed. The mixture was kept at 50 °C in a water bath for 30 min. Absorbance was read at 490 nm compared to a DI water blank carried through the same process, and glucose was used as a calibration standard. The crude protein content of the algae was calculated by multiplying the algae's nitrogen content by 4.44 [43]. The CHNS mass fractions of the algal pellet were determined using a Thermo Scientific FlashSmart Elemental Analyzer (Thermo Scientific, Waltham, MA).

2.4 Results and Discussion

2.4.1 HAP Tolerance

The growth of each algae species was measured in different HAP dilutions to determine the optimal concentration for growth. Based on OD_{750} measurements over 9 days of growth, all species were observed to grow in the 3% and 5% dilutions (Fig. 2.1). Growth of *C. vulgaris* (Fig. 2.1C) and *S. obliquus* (Fig. 2.1D) was observed in both 3% and 5%, with higher growth observed in both concentrations than in the standard media. This improved growth in HAP may be a result of increased N amounts and the presence of N as NH_4^+ in the HAP compared to the standard media. For both species, 3% diluted HAP had

a 1-day shorter lag phase than 5%, and *S. obliquus* had the longest lag phase of all four species, suggesting it is slowest to acclimate to HAP as a growth medium. A slight increase in OD_{750} was measured in the 10% HAP dilution for *C. vulgaris* on the last day of the experiment, while no growth was observed in 15% diluted HAP. *S. obliquus* did not show any growth in the 10% and 15% dilutions over the course of the experiment. *C. reinhardtii* grew in both 3% and 5% dilutions as well, although less growth was observed in these HAP concentrations than in the standard media (Fig. 2.1B). The *C. reinhardtii* standard media had the highest concentration of N as well as significant fractions of both NH_4^+ and NO_3^-. In addition, growth was observed in the 10% dilution after a 5-day lag phase, whereas growth was observed in the 3% and 5% dilutions after 1 day of lag, similar to the standard media. No growth of *C. reinhardtii* was observed in 15% diluted HAP within 9 days (Fig. 2.1B).

Similar results were observed with *C. vulgaris* and other *Coelastrella* and *Chlorella* strains in the literature. Belete et al. [19] compared growth of novel *Coelastrella* and *Chlorella* strains in BG-11 media to growth in diluted HAP derived from sewage sludge and supplemented with micronutrients. Both strains achieved higher biomass production in diluted HAP over 6 days of growth. Du et al. [20] compared growth of *C. vulgaris* in BG-11 media to several dilutions of HAP derived from *Nannochloropsis oculata* biomass. In this study, the highest growth was observed in the highest concentration of HAP, which was diluted 50x and had an initial concentration of 6.2 mg-P/L. The other HAP dilutions (100x and 200x) also performed better than BG-11 media over 6 days, indicating that HAP is a suitable nutrient source for *C. vulgaris* at these dilution levels.

Unlike *C. vulgaris*, *S. obliquus*, and *C. reinhardtii*, the growth curves for *A. maxima* (Fig. 2.1A) do not follow an exponential pattern typical of algae growth in a batch reactor, namely at higher HAP concentrations. In the 3% and 5% dilutions of HAP, *A. maxima* reaches stationary phase after 2 days of growth with no lag period observed, unlike the other three species. In the 10% and 15% dilutions, the OD_{750} measurements decrease during the first day and then increase substantially to maximums after 2 and 4 days, respectively. After reaching a maximum, the OD_{750} in 10% and 15% decrease for the remainder of the experiment, unlike the other species and the *A. maxima* grown on 3% and 5% that had slow increased growth trends after the exponential phase. The OD_{750} results observed with high HAP concentration were a result of co-precipitation of the HAP and buffer that prevented algal growth, as determined by a visual loss of green coloration during the experiment. The OD_{750} of the *A. maxima* grown in standard media increased consistently over the course of the experiment, catching up to the 3% and 5% OD_{750} values after 5 and 7 days, respectively. Inhibition at higher HAP concentrations is likely attributed to lignocellulosic byproducts such as furfural or hydroxymethylfurfural [44] that may inhibit algal growth and photosynthesis [45,46].

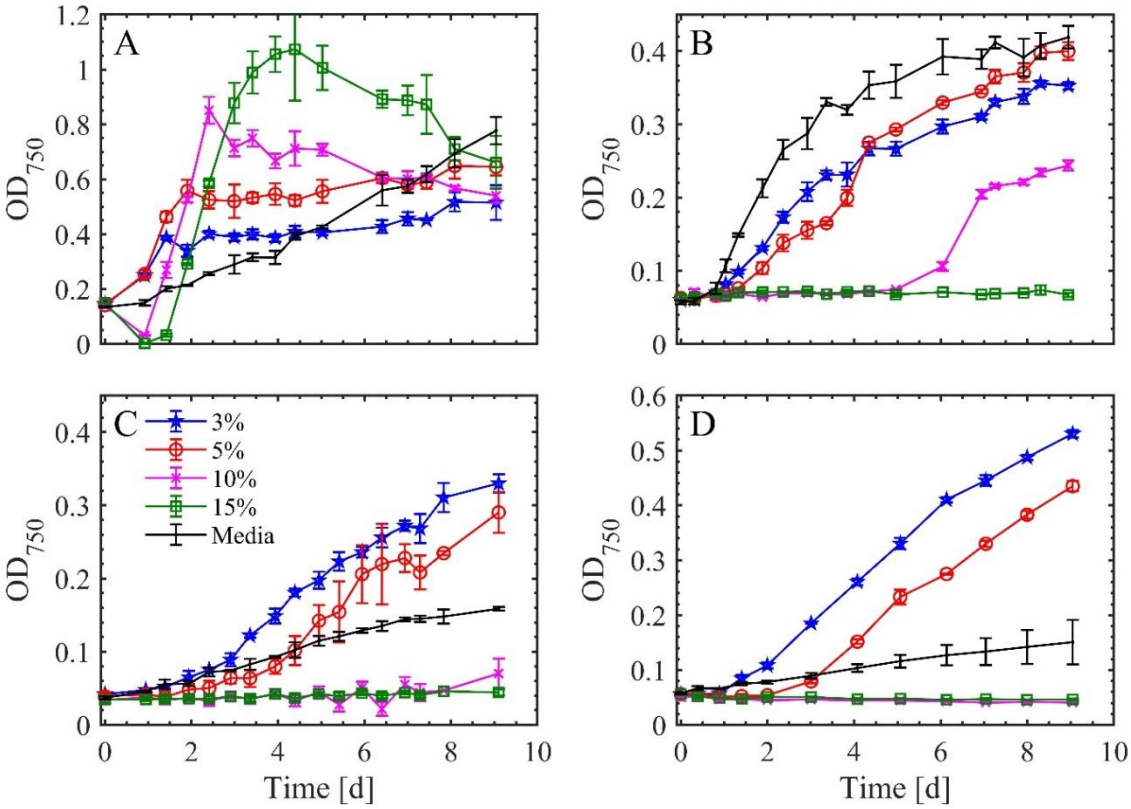

Figure 2.1: Growth curves in 3%, 5%, 10%, and 15% HAP dilutions for (A) *A. maxima,* (B) *C. reinhardtii,* (C) *C. vulgaris,* and (D) *S. obliquus.* Error bars represent the standard deviation of biological triplicates.

2.4.2 Biomass Growth

The observed specific growth rates, μ_{obs}, for each algae and each HAP concentration were calculated by plotting the natural logarithm of the OD_{750} measurements over time and calculating the slope (Eq. 2.1) of the linear portion of the graph. The specific growth rates for the 3%, 5%, and 10% dilutions were calculated for the species where growth was observed (Table 2.1). In standard media, the highest μ_{obs} was achieved by *C. reinhardtii* at 0.760 d^{-1}, followed by *A. maxima* at 0.240 d^{-1}, *C. vulgaris* at 0.228 d^{-1}, and *S. obliquus* at 0.127 d^{-1}. The μ_{obs} calculated for 3% and 5% HAP dilutions were higher than in standard media for all species except *C. reinhardtii*. Although *C. reinhardtii* and *C.*

vulgaris showed growth in 10% diluted HAP, a significant lag phase was observed for both species compared to media and the lower concentrations of HAP. Growth at 15% or higher HAP concentrations may be possible, but the cultures have long lag phases. Based on these results, 5% HAP was chosen as the best dilution for further testing because it consistently supported growth for all four species and required less water input than 3% HAP. The selected 5% HAP dilution corresponds to approximately 7.5 g of dry manure per L of algae pond, accounting for water volume lost during the HTC process [40].

Table 2.1: Observed specific growth rates, μ_{obs}, for the four algae species from tolerance tests in different dilutions of HAP. Error represents the standard deviation of biological triplicates.

	A. maxima	***C. reinhardtii***	***C. vulgaris***	***S. obliquus***
Media [d^{-1}]	0.240 ± 0.008	0.760 ± 0.053	0.228 ± 0.013	0.127 ± 0.012
HAP – 3% [d^{-1}]	0.683 ± 0.027	0.516 ± 0.021	0.400 ± 0.040	0.418 ± 0.011
HAP – 5% [d^{-1}]	0.756 ± 0.036	0.392 ± 0.023	0.336 ± 0.022	0.490 ± 0.018
HAP – 10% [d^{-1}]	-	0.506 ± 0.010	0.193 ± 0.013	-

The unique growth curves exhibited by *A. maxima* warrant additional exploration. *A. maxima* is unique from the other species in this study because its optimal growth pH is 8.5-10.5 [47]. To maintain this pH, sodium bicarbonate (13.61 g/L) and sodium carbonate (4.03 g/L) are added to the HAP to raise the pH to 9.5. These buffers were selected to match the concentration used in UTEX *Spirulina* media. While the basic pH was maintained over the course of the experiment, solid precipitates were observed in the HAP, accumulating on the bottom and sides of the flask. OD_{750} measurements operate under the assumption that the absorbance is proportional to the concentration of cells in the culture; however, precipitated solids may interfere with the absorbance or co-precipitate biomass. Therefore,

the OD_{750} trends of A. *maxima* (Fig. 2.1A) may be affected by precipitated solids, particularly at higher HAP concentrations. As significant precipitation was observed visually in the 10% and 15% HAP cultures, the increase in OD_{750} was not attributable to algal growth and thus growth rates under these conditions are not provided in Table 2.1. In an open pond cultivation system, elevated pH may help control contamination within the culture [48], but formation of precipitates could impact the biomass harvesting process or the final biomass product. In addition, other studies have shown that chemical additions in large-scale cultivation processes lead to considerable environmental impacts, such as increased carbon footprint and water consumption [32]. The other three algae species examined in this study do not require pH adjustment to grow in HAP and are not affected by precipitation over the course of growth, removing the need for chemical inputs and allowing for OD_{750} measurements of growth without complications.

2.4.3 Nutrient Uptake

The nutrient uptake experiments were performed using 5% diluted HAP, which was identified during the HAP tolerance tests as the optimal concentration for all species. The length of each experiment was five days to capture the behavior over the exponential phase. The maximum growth rates during this experiment (Table 2.2) were compared to the screening experiments (Table 2.1) and it was found that both *S. obliquus* and *C. vulgaris* grew slower during the nutrient screening experiment, while no statistical difference was found for *A. maxima* and *C. reinhardtii* ($\alpha = 0.05$). The slight difference for *C. vulgaris* and *S. obliquus* is likely attributed to the variation observed in HAP produced from different HTC reaction batches, which can have 10-20% variation in N or P concentration

[49]. All four species showed growth over the course of the experiment (Fig. 2.2A). *A. maxima* had the most growth, followed by *C. reinhardtii* and *C. vulgaris,* while *S. obliquus* had the least growth. The pH of each culture was measured once per day over the course of the experiment (Fig. 2.2B). The pH of *A. maxima* was maintained at 9.5 due to the bicarbonate buffer. No chemicals were used to control pH for the other three species so pH increased over time, with the species with the most growth having the largest pH increase (Fig. 2.2A), as expected. *C. reinhardtii* had the greatest pH increase from 5.2 to 8.0 at the end of the experiment, followed by *C. vulgaris,* which increased to a maximum of pH 7.5 after 4 days, then decreased to 7.3 on the fifth day. The pH of *S. obliquus* increased to 7.0, with most of the increase occurring on the last day of the experiment, mirroring the OD_{750} trend. Increasing pH is typically caused by consumption of CO_2 during photosynthesis [50], which explains why the pattern of pH increase mirrors the pattern of OD_{750} increases, except for the pH-controlled *A. maxima* culture.

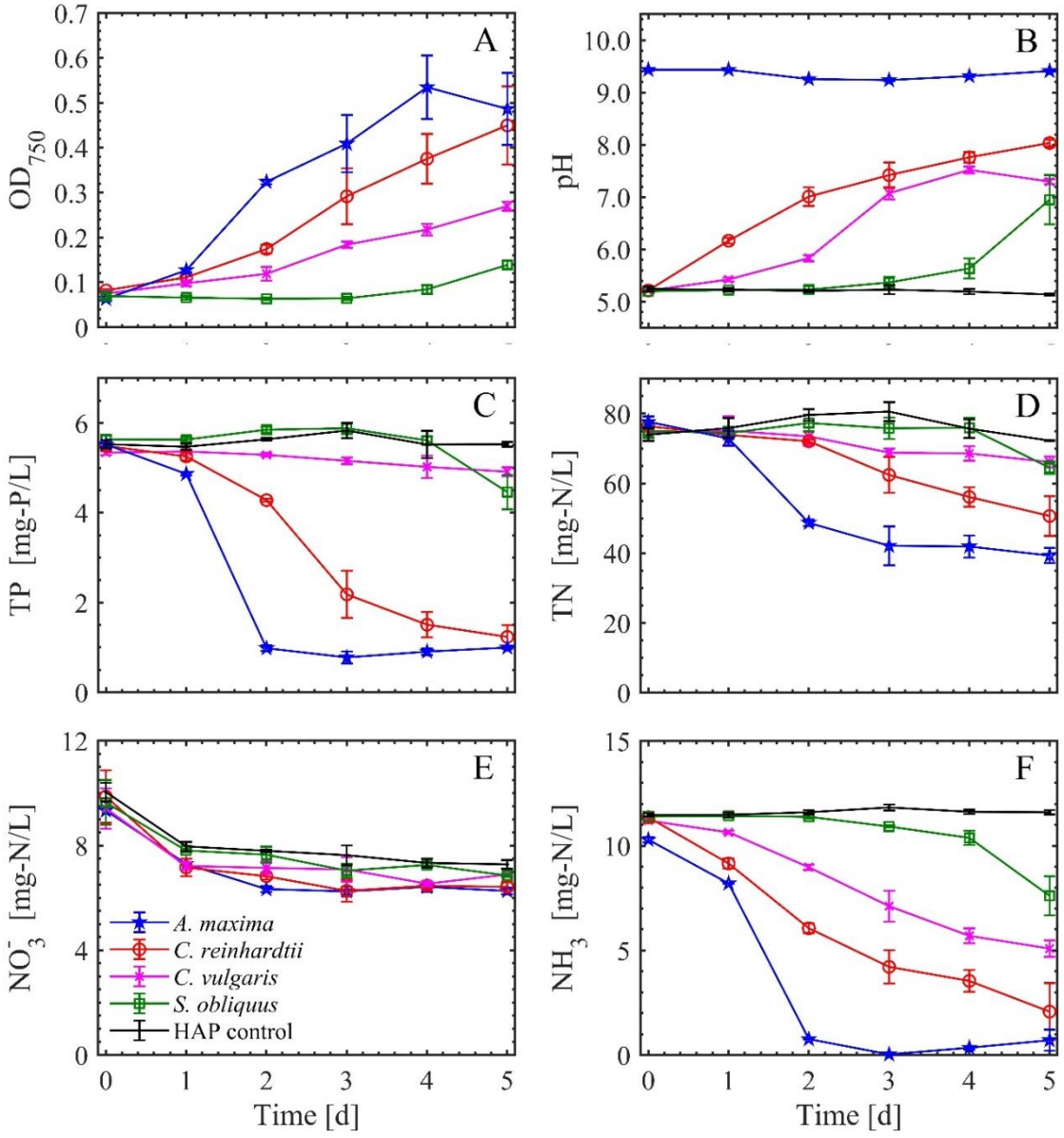

Figure 2.2: Results of the nutrient uptake study in 5% HAP dilution for the four algae species. (A) Growth curves, (B) pH, (C) TP concentration, (D) TN concentration, (E) NO_3^- concentration, and (F) NH_3 concentration.

Nutrient measurements were taken once per day to track consumption of P and different forms of N. Initially, 5% HAP contained approximately 70% organic N, 15%

NH_3-N, and 10% NO_3^--N, which is comparable to other studies characterizing HAP from dairy manure [4] as well as other HAP sources [19,51].

The amount of P consumed was dependent on the algae species (Fig. 2.2C). *A. maxima* consumed P the fastest but had little change after two days. After five days, *C. reinhardtii* and *A. maxima* had consumed ~80%. Neither *C. vulgaris* nor *S. obliquus* consumed significant amounts of P over the course of the experiment, although *S. obliquus* had a two-day lag phase. Despite demonstrating growth since the beginning of the experiment (based on OD_{750}, Fig. 2.2A), *C. vulgaris* had consumed the least P. By Day 5, the P concentration in the *S. obliquus* cultures had dropped below the *C. vulgaris* cultures despite having approximately half as much biomass (Table 2.2). In terms of nutrient remediation, *C. vulgaris* performed the worst.

Consumption of the different forms of N (Figs. 2.2D, 2.2E, and 2.2F) varied depending on the algae species and the culture pH. The trends of nutrient consumption generally paralleled those of overall algae growth, with *A. maxima* having the greatest removal and *S. obliquus* the least.

All species consumed at least a portion of the NH_3 present in HAP (Fig. 2.2F). *S. obliquus* consumed the least NH_3 with only 33% removal after five days of growth, with most of the consumption occurring on the last day. *C. vulgaris* and *C. reinhardtii* showed consistent decreases in NH_3 over five days, removing a total of 55% and 82% of the available NH_3, respectively. The highest NH_3 removal was achieved by *A. maxima* with 95% removal. Because *A. maxima* grows at elevated pH, some of the NH_3 removal could be due to volatilization; however, *A. maxima* showed the highest growth, so it is reasonable to expect the highest NH_3 removal to occur in this culture.

Unlike NH_3, NO_3^- was not substantially consumed by any species (Fig. 2.2E). The preferential consumption of NH_3 over NO_3^- has been observed in other growth conditions involving HAP [36,51]. NO_3^- removals ranged from 27-35% for all four species, however a 38% reduction in the NO_3^- concentration also occurred in the control HAP solution (no algae). Because this change also occurred in the control solution, the measured drop in NO_3^- concentration is likely due to an abiotic chemical change associated with the HAP. The NO_3^- concentrations did not significantly change after the first day, indicating that the algae do not consume NO_3^- during the rest of the growth period. The preferential consumption of NH_3 over NO_3^- is a possible explanation for the decreased growth of *C. reinhardtii* in HAP compared to its standard media (Table 2.1), as this was the only standard media with >1 mg-N/L of NH_3 present.

A. maxima had the highest TN removal of 49%, followed by *C. reinhardtii* with 34%, *S. obliquus* at 14%, and *C. vulgaris* had the lowest at only 11% (Fig. 2.2D). Consumption of organic N was calculated by subtracting NH_3 and NO_3^- from the TN concentration. *A. maxima*, *C. reinhardtii*, and *S. obliquus* removed 44%, 24% and 7.4% of the organic N respectively while *C. vulgaris* removed none. These results show that significant concentrations of N remain in HAP solution even after the exponential phase of growth, particularly organic N.

2.4.4 Algae Composition

After harvest, the algae were characterized based on their elemental makeup and nutritional content (Table 2.2). The CHNS results showed minor differences in the C and H content between species, however, the C to H ratio was consistent across the four species

ranging from 6.87 to 7.01; *A. maxima* had the highest C to H ratio, which is similar to what has been observed in other studies [38,52–54]. The N composition was used to estimate the protein fractions. *C. vulgaris* had the lowest protein content at 32.4% with *S. obliquus* at 38.9%. Both *A. maxima* and *C. reinhardtii* had higher protein content (>40%), indicating that these species may be better suited as protein supplements. The protein content also correlated with the organic N uptake potential, with the species more capable of using organic N having more protein.

The algae carbohydrate content was generally low, ranging from 6.5% for *C reinhardtii* to 12.6% for *S. obliquus* (Table 2.2), which agrees with what has been reported for algae cultivated on manure waste sources [55]. *C. reinhardtii* and *C. vulgaris* had significantly different protein fractions with statistically similar carbohydrate content. *A. maxima*, which had the most protein, had roughly 34% more carbohydrates than these two species.

From a nutritional perspective, both *A. maxima* and *C. reinhardtii* performed similarly demonstrating potential as a protein supplement. From a biomass production perspective, *A. maxima* had the highest specific growth rate; however, cultivation of this species requires the use of pH buffers, which is a potential concern for full-scale application from an environmental perspective [32]. *C. reinhardtii* had the second fastest growth rate and did not require a buffer for cultivation, while providing a biomass with a similar protein content to *A. maxima*.

Table 2.2: Specific growth rate, biomass productivity, and biomass composition data from the nutrient uptake experiment performed in 5% HAP. Error represents the standard deviation of biological triplicates.

	A. maxima	***C. reinhardtii***	***C. vulgaris***	***S. obliquus***
Growth rate [d^{-1}]	0.836 ± 0.088	0.411 ± 0.046	0.279 ± 0.027	0.387 ± 0.013
Productivity [mg/L*d]	93.2 ± 1.2	75.3 ± 7.2	52.0 ± 3.7	29.1 ± 1.7
Carbohydrate [%]	9.0 ± 0.4	6.5 ± 0.6	6.9 ± 0.8	12.6 ± 0.6
C	42.87 ± 0.86	47.18 ± 0.69	46.64 ± 0.07	49.65 ± 3.70
H	6.10 ± 0.10	6.80 ± 0.07	6.80 ± 0.03	7.20 ± 0.84
N	9.70 ± 0.22	9.84 ± 0.34	7.29 ± 0.05	8.76 ± 0.85
S	0.47 ± 0.01	0.58 ± 0.2	0.69 ± 0.02	0.40 ± 0.06
Protein [%]	43.1 ± 1.0	43.7 ± 1.5	32.4 ± 0.2	38.9 ± 3.7

2.5 Conclusions

All algae species tested were able to grow in 5% or lower concentrations of HAP. Minimal growth was observed in higher HAP concentrations, potentially due to inhibiting chemical compounds. Maximum specific growth rates and nutrient removals varied depending on the species. *A. maxima* showed the greatest removal of the nutrients measured, followed by *C. reinhardtii, C. vulgaris,* and *S. obliquus*. *A. maxima* and *C. reinhardtii* had similar protein content of near 43%, making these species an attractive option as a potential protein source for livestock feed. *A. maxima* was shown to grow faster than the other three algae species, but required a buffer for successful cultivation. Future work will investigate the feasibility of recycling the post-algae harvesting HAP-based media for additional cultivation cycles to improve nutrient uptake or reduce the required buffer input. Microalgae cultivation is a viable option for nutrient recovery from HAP, producing a useful, protein-rich biomass to supply to farms as an integrated resource recovery approach for dairy manure.

2.6 Works Cited

[1] R. MacDonald, J. M., Cessna, J., & Mosheim, Changing Structure, Financial Risks, and Government Policy for the U.S. Dairy Industry, (2016) 1–75.

[2] US EPA, Literature Review of Contaminants in Livestock and Poultry Manure and Implications for Water Quality, 2013. https://doi.org/10.1016/S1474-4422(13)70230-8.

[3] USEPA, Annexes to the Inventory of U . S . GHG Emissions and Sinks ANNEX 1 Key Category Analysis, (2017) 1–458.

[4] S. V. Qaramaleki, J.A. Villamil, A.F. Mohedano, C.J. Coronella, Factors Affecting Solubilization of Phosphorus and Nitrogen through Hydrothermal Carbonization of Animal Manure, ACS Sustain Chem Eng. 8 (2020) 12462–12470. https://doi.org/10.1021/acssuschemeng.0c03268.

[5] D. Lachos-Perez, P. César Torres-Mayanga, E.R. Abaide, G.L. Zabot, F. De Castilhos, Hydrothermal carbonization and Liquefaction: differences, progress, challenges, and opportunities, Bioresour Technol. 343 (2022). https://doi.org/10.1016/j.biortech.2021.126084.

[6] T.M. Reza, A. Freitas, X. Yang, S. Hiibel, H. Lin, C.J. Coronella, Hydrothermal carbonization (HTC) of cow manure: Carbon and nitrogen distributions in HTC products, Environ Prog Sustain Energy. 35 (2016) 1002–1011. https://doi.org/10.1002/ep.12312.

[7] N.D. Berge, L. Li, J.R.V. Flora, K.S. Ro, Assessing the environmental impact of energy production from hydrochar generated via hydrothermal carbonization of food wastes, Waste Management. 43 (2015) 203–217. https://doi.org/10.1016/j.wasman.2015.04.029.

[8] V. Benavente, A. Fullana, N.D. Berge, Life cycle analysis of hydrothermal carbonization of olive mill waste: Comparison with current management approaches, J Clean Prod. 142 (2017) 2637–2648. https://doi.org/10.1016/j.jclepro.2016.11.013.

[9] M.P. Maniscalco, M. Volpe, A. Messineo, Hydrothermal carbonization as a valuable tool for energy and environmental applications: A review, Energies (Basel). 13 (2020). https://doi.org/10.3390/en13164098.

[10] M. Langone, D. Basso, Process waters from hydrothermal carbonization of sludge: Characteristics and possible valorization pathways, Int J Environ Res Public Health. 17 (2020) 1–31. https://doi.org/10.3390/ijerph17186618.

[11] K. Nakason, B. Panyapinyopol, V. Kanokkantapong, N. Viriya-empikul, W. Kraithong, P. Pavasant, Hydrothermal carbonization of unwanted biomass materials: Effect of process temperature and retention time on hydrochar and liquid fraction, Journal of the Energy Institute. 91 (2018) 786–796. https://doi.org/10.1016/j.joei.2017.05.002.

[12] J.D. Marin-Batista, J.A. Villamil, S. V. Qaramaleki, C.J. Coronella, A.F. Mohedano, M.A. de la Rubia, Energy valorization of cow manure by hydrothermal carbonization and anaerobic digestion, Renew Energy. 160 (2020) 623–632. https://doi.org/10.1016/j.renene.2020.07.003.

[13] K. Wu, Y. Gao, G. Zhu, J. Zhu, Q. Yuan, Y. Chen, M. Cai, L. Feng, Characterization of dairy manure hydrochar and aqueous phase products generated by hydrothermal carbonization at different temperatures, J Anal Appl Pyrolysis. 127 (2017) 335–342. https://doi.org/10.1016/j.jaap.2017.07.017.

[14] M. Ahmed, G. Andreottola, S. Elagroudy, M.S. Negm, L. Fiori, Coupling hydrothermal carbonization and anaerobic digestion for sewage digestate management: Influence of hydrothermal treatment time on dewaterability and bio-methane production, J Environ Manage. 281 (2021) 111910. https://doi.org/10.1016/j.jenvman.2020.111910.

[15] W. Fan, L. Bryant, M. Srisupan, J. Trembly, An assessment of hydrothermal treatment of dairy waste as a tool for a sustainable phosphorus supply chain in comparison with commercial phosphatic fertilizers, Clean Technol Environ Policy. 20 (2018) 1467–1478. https://doi.org/10.1007/s10098-017-1440-z.

[16] V. Mau, J. Neumann, B. Wehrli, A. Gross, Nutrient Behavior in Hydrothermal Carbonization Aqueous Phase Following Recirculation and Reuse, Environ Sci Technol. 53 (2019) 10426–10434. https://doi.org/10.1021/acs.est.9b03080.

[17] K. McGaughy, M.T. Reza, Recovery of Macro and Micro-Nutrients by Hydrothermal Carbonization of Septage, J Agric Food Chem. 66 (2018) 1854–1862. https://doi.org/10.1021/acs.jafc.7b05667.

[18] C. Numviyimana, J. Warchoł, N. Khalaf, J.J. Leahy, K. Chojnacka, Phosphorus recovery as struvite from hydrothermal carbonization liquor of chemically produced dairy sludge by extraction and precipitation, J Environ Chem Eng. 10 (2022) 106947. https://doi.org/10.1016/j.jece.2021.106947.

[19] Y.Z. Belete, S. Leu, S. Boussiba, B. Zorin, C. Posten, L. Thomsen, S. Wang, A. Gross, R. Bernstein, Characterization and utilization of hydrothermal carbonization aqueous phase as nutrient source for microalgal growth, Bioresour Technol. 290 (2019) 121758. https://doi.org/10.1016/j.biortech.2019.121758.

[20] Z. Du, B. Hu, A. Shi, X. Ma, Y. Cheng, P. Chen, Y. Liu, X. Lin, R. Ruan, Cultivation of a microalga Chlorella vulgaris using recycled aqueous phase nutrients from hydrothermal carbonization process, Bioresour Technol. 126 (2012) 354–357. https://doi.org/10.1016/j.biortech.2012.09.062.

[21] S.R. Hiibel, M.S. Lemos, B.P. Kelly, J.C. Cushman, Evaluation of diverse microalgal species as potential biofuel feedstocks grown using municipal wastewater, Front Energy Res. 3 (2015) 1–8. https://doi.org/10.3389/fenrg.2015.00020.

[22] R. Craggs, J. Park, S. Heubeck, D. Sutherland, High rate algal pond systems for low-energy wastewater treatment, nutrient recovery and energy production, N Z J Bot. 52 (2014) 60–73. https://doi.org/10.1080/0028825X.2013.861855.

[23] L. Wang, Y. Li, P. Chen, M. Min, Y. Chen, J. Zhu, R.R. Ruan, Anaerobic digested dairy manure as a nutrient supplement for cultivation of oil-rich green microalgae Chlorella sp., Bioresour Technol. 101 (2010) 2623–2628. https://doi.org/10.1016/j.biortech.2009.10.062.

[24] J. Lv, Y. Liu, J. Feng, Q. Liu, F. Nan, S. Xie, Nutrients removal from undiluted cattle farm wastewater by the two-stage process of microalgae-based wastewater treatment, Bioresour Technol. 264 (2018) 311–318. https://doi.org/10.1016/j.biortech.2018.05.085.

[25] D. Nagarajan, A. Kusmayadi, H.W. Yen, C. Di Dong, D.J. Lee, J.S. Chang, Current advances in biological swine wastewater treatment using microalgae-based processes, Bioresour Technol. 289 (2019) 121718. https://doi.org/10.1016/j.biortech.2019.121718.

[26] A.F. Clarens, E.P. Resurreccion, M.A. White, L.M. Colosi, Environmental life cycle comparison of algae to other bioenergy feedstocks, Environ Sci Technol. 44 (2010) 1813–1819. https://doi.org/10.1021/es902838n.

[27] R. Slade, A. Bauen, Micro-algae cultivation for biofuels: Cost, energy balance, environmental impacts and future prospects, Biomass Bioenergy. 53 (2013) 29–38. https://doi.org/10.1016/j.biombioe.2012.12.019.

[28] E. Le, C. Park, S. Hiibel, Investigation of the Effect of Growth From Low to High Biomass Concentration Inside a Photobioreactor on Hydrodynamic Properties of Scenedesmus obliquus, J Energy Resour Technol. 134 (2012) 1–6. https://doi.org/10.1115/1.4005245.

[29] B.W.B. Holman, A.E.O. Malau-Aduli, Spirulina as a livestock supplement and animal feed, J Anim Physiol Anim Nutr (Berl). 97 (2013) 615–623. https://doi.org/10.1111/j.1439-0396.2012.01328.x.

[30] S.L. Lodge-Ivey, L.N. Tracey, A. Salazar, Ruminant nutrition symposium: The utility of lipid extracted algae as a protein source in forage or starch-based ruminant diets, J Anim Sci. 92 (2014) 1331–1342. https://doi.org/10.2527/jas.2013-7027.

[31] M.S. Madeira, C. Cardoso, P.A. Lopes, D. Coelho, C. Afonso, N.M. Bandarra, J.A.M. Prates, Microalgae as feed ingredients for livestock production and meat quality: A review, Livest Sci. 205 (2017) 111–121. https://doi.org/10.1016/j.livsci.2017.09.020.

[32] C.J. Glover, P.K. Cornejo, S.R. Hiibel, Life Cycle Assessment of Integrated Nutrient, Energy, and Water Recovery on Large-Scale Dairy Farms, Environ Eng Sci. 39 (2022) 811–820. https://doi.org/10.1089/ees.2021.0376.

[33] B.T. Higgins, A. Kendall, Life Cycle Environmental and Cost Impacts of Using an Algal Turf Scrubber to Treat Dairy Wastewater, J Ind Ecol. 16 (2012) 436–447. https://doi.org/10.1111/j.1530-9290.2011.00427.x.

[34] W. Wu, L.C. Cheng, J.S. Chang, Environmental life cycle comparisons of pig farming integrated with anaerobic digestion and algae-based wastewater treatment, J Environ Manage. 264 (2020) 110512. https://doi.org/10.1016/j.jenvman.2020.110512.

[35] P. Biller, A.B. Ross, S.C. Skill, A. Lea-Langton, B. Balasundaram, C. Hall, R. Riley, C.A. Llewellyn, Nutrient recycling of aqueous phase for microalgae cultivation from the hydrothermal liquefaction process, Algal Res. 1 (2012) 70–76. https://doi.org/10.1016/j.algal.2012.02.002.

[36] L. Garcia Alba, C. Torri, D. Fabbri, S.R.A. Kersten, D.W.F. Wim Brilman, Microalgae growth on the aqueous phase from Hydrothermal Liquefaction of the same microalgae, Chemical Engineering Journal. 228 (2013) 214–223. https://doi.org/10.1016/j.cej.2013.04.097.

[37] D. López Barreiro, M. Bauer, U. Hornung, C. Posten, A. Kruse, W. Prins, Cultivation of microalgae with recovered nutrients after hydrothermal liquefaction, Algal Res. 9 (2015) 99–106. https://doi.org/10.1016/j.algal.2015.03.007.

[38] U. Jena, N. Vaidyanathan, S. Chinnasamy, K.C. Das, Evaluation of microalgae cultivation using recovered aqueous co-product from thermochemical liquefaction of algal biomass, Bioresour Technol. 102 (2011) 3380–3387. https://doi.org/10.1016/j.biortech.2010.09.111.

[39] P. Biller, A.B. Ross, Potential yields and properties of oil from the hydrothermal liquefaction of microalgae with different biochemical content, Bioresour Technol. 102 (2011) 215–225. https://doi.org/10.1016/j.biortech.2010.06.028.

[40] N.A. Silva, S.R. Hiibel, Nutrient recovery of the hydrothermal carbonization aqueous product from dairy manure using membrane distillation, Environ Technol. 0 (2021) 1–10. https://doi.org/10.1080/09593330.2021.1995785.

[41] M. Dubois, K. Gilles, J.K. Hamilton, P.A. Rebers, F. Smith, A colorimetric method for the determination of sugars, Nature. (1951).

[42] M.D. Ruehl, S.R. Hiibel, Evaluation of organic carbon and microbial inoculum for bioremediation of acid mine drainage, Miner Eng. 157 (2020) 106554. https://doi.org/10.1016/j.mineng.2020.106554.

[43] C.V.G. López, M. del Carmen Cerón García, F.G.A. Fernández, C.S. Bustos, Y. Chisti, J.M.F. Sevilla, Protein measurements of microalgal and cyanobacterial biomass, Bioresour Technol. 101 (2010) 7587–7591. https://doi.org/10.1016/j.biortech.2010.04.077.

[44] E. Erdogan, B. Atila, J. Mumme, M.T. Reza, A. Toptas, M. Elibol, J. Yanik, Characterization of products from hydrothermal carbonization of orange pomace including anaerobic digestibility of process liquor, Bioresour Technol. 196 (2015) 35–42. https://doi.org/10.1016/j.biortech.2015.06.115.

[45] S. Yu, A. Forsberg, K. Kral, M. Pedersen, Furfural and hydroxymethylfurfural inhibition of growth and photosynthesisin spirulina, British Phycological Journal. 25 (1990) 141–148. https://doi.org/10.1080/00071619000650131.

[46] S.Z. Tarhan, A.T. Koçer, D. Özçimen, İ. Gökalp, Cultivation of green microalgae by recovering aqueous nutrients in hydrothermal carbonization process water of biomass wastes, Journal of Water Process Engineering. 40 (2021). https://doi.org/10.1016/j.jwpe.2020.101783.

[47] R.A. Soni, K. Sudhakar, R.S. Rana, Comparative study on the growth performance of Spirulina platensis on modifying culture media, Energy Reports. 5 (2019) 327–336. https://doi.org/10.1016/j.egyr.2019.02.009.

[48] A. Vonshak, S. Boussiba, A. Abeliovich, A. Richmond, Production of Spirulina biomass: Maintenance of monoalgal culture outdoors, Biotechnol Bioeng. 25 (1983) 341–349. https://doi.org/10.1002/bit.260250204.

[49] N.A. Silva, S.R. Hiibel, Nutrient recovery of the hydrothermal carbonization aqueous product from dairy manure using membrane distillation, Environ Technol. (2021) 1–10. https://doi.org/10.1080/09593330.2021.1995785.

[50] M.H. Gerardi, B. Lytle, Algae, Alkalinity, and pH, in: The Biology and Troubleshooting of Facultative Lagoons, 2015: pp. 105–109.

[51] C. Yao, Y. Pan, H. Lu, P. Wu, Y. Meng, X. Cao, S. Xue, Utilization of recovered nitrogen from hydrothermal carbonization process by Arthrospira platensis, Bioresour Technol. 212 (2016) 26–34. https://doi.org/10.1016/j.biortech.2016.03.166.

[52] W.H. Chen, Z.Y. Wu, J.S. Chang, Isothermal and non-isothermal torrefaction characteristics and kinetics of microalga Scenedesmus obliquus CNW-N, Bioresour Technol. 155 (2014) 245–251. https://doi.org/10.1016/j.biortech.2013.12.116.

[53] K. Kebelmann, A. Hornung, U. Karsten, G. Griffiths, Intermediate pyrolysis and product identification by TGA and Py-GC/MS of green microalgae and their extracted protein and lipid components, Biomass Bioenergy. 49 (2013) 38–48. https://doi.org/10.1016/j.biombioe.2012.12.006.

[54] L. Xu, D.W.F. Wim Brilman, J.A.M. Withag, G. Brem, S. Kersten, Assessment of a dry and a wet route for the production of biofuels from microalgae: Energy balance analysis, Bioresour Technol. 102 (2011) 5113–5122. https://doi.org/10.1016/j.biortech.2011.01.066.

[55] W.D. Lu, M.J. Lin, X.L. Guo, Z.Y. Lin, Cultivation of spirulina platensis using raw piggery wastewater for nutrients bioremediation and biomass production: Effect of ferrous sulfate supplementation, Desalination Water Treat. 175 (2020) 60–70. https://doi.org/10.5004/dwt.2020.24830.

3 MEMBRANE DISTILLATION AND ALGAL CULTIVATION OF HYDROTHERMAL CARBONIZATION AQUEOUS PRODUCT FOR WATER REUSE AND REMEDIATION

Silva, N. A. and Hiibel, S. R. (in review). *Separation Science and Technology*.

3.1 Abstract

With growing demand for more sustainable dairy manure management methods, a system involving hydrothermal carbonization (HTC), membrane distillation (MD), and algae cultivation for resource recovery from dairy manure was partially investigated in this study. Two algal species, *Arthrospira maxima* and *Chlamydomonas reinhardtii*, were cultivated on the hydrothermal aqueous product (HAP) of dairy manure, but the former requires a carbonate buffer for successful cultivation. The spent HAP after algae cultivation was treated using MD where the operational efficacy and distillate quality were assessed. Comparing the MD performance of the buffered HAP to the unbuffered HAP revealed the addition of the buffer decreased water flux and distillate quality, but cultivation with *A. maxima* reversed these effects and produced distillates with reduced COD, TN, and NH_3 concentrations. *C. reinhardtii* cultivation resulted in increased distillate COD and NH_3 concentrations compared to the unbuffered HAP. Fluorescence was used to broadly characterize the organic components of the feed and distillate streams. Regrowth experiments with *A. maxima* revealed the spent buffer can successfully be recycled, but fresh nutrients are required.

3.2 Introduction

Over recent years, the US dairy industry has consolidated into fewer facilities with larger herd sizes to streamline dairy production. Between 1987 and 2012, the median farm size increased from 80 to 900 cows [1]. Although larger farms are more cost-effective, they also lead to an increased localized manure concentration. Excess application of manure to nearby cropland risks soil nutrient accumulation and water eutrophication [2]. Large-scale farms commonly store the manure onsite until it can be used as a fertilizer, but the storage procedure is a major source of air pollutants [3]. Innovative technologies are needed to reduce environmental impacts and utilize the nutrients found in manure. A system partially investigated by this study is the combination of hydrothermal carbonization (HTC), membrane distillation (MD), and algae cultivation to treat the dairy manure on-site to produce a low-grade coal, clean water, and protein-rich algae that can supplement cattle's diet.

HTC is a thermal conversion process that uses the unique properties of water at high temperatures and pressures to convert wet biomass into a solid fuel called hydrochar. Depending on the HTC operating conditions, the energy value of the hydrochar can range from 19-22 MJ/kg [4]. HTC operating temperatures range from 180 to 250 °C, leading to self-induced high pressures associated with the water's vapor pressure. Dairy manure is a common feedstock for the HTC process due to its high carbon and moisture content and nutrient concentrations [5,6]. During the HTC process, a portion of the nutrients and soluble organics partition to the aqueous phase [7], called hydrothermal aqueous product (HAP). More phosphorus partitions into the aqueous phase at lower HTC operating temperatures, while the nitrogen concentrations remain roughly constant [7,8]. The

concentration and type of organic compounds formed by the HTC are dependent on the feedstock and reaction conditions [9]. Degradation of lignocellulosic biomass produces sugars, amino acids, volatile fatty acids (VFAs), and alcohols, as well as potentially toxic species such as phenols or furfurals [4,10]. The common focus of HTC studies is the production and optimization of the hydrochar, while the HAP is less frequently studied.

MD is a thermal separation process that can utilize low-grade waste heat sources because a small temperature gradient can drive separation [11,12], making it an ideal partner for the HTC process. MD uses a microporous, hydrophobic membrane to separate two streams of different temperatures, where vapor will pass through the pores at a rate roughly proportional to its partial pressure difference. In the case of desalination, near 100% rejection of salts can be achieved [13], but MD has also been used to treat oil-containing feed solutions such as polyphenol propolis extract [14] and various fruit juices [15–17]. The potential to treat HAP produced from dairy manure with a hydrophobic membrane has been demonstrated and found to reject most of the TOC, TN, and TP; however significant flux decline was also observed, primarily for HAP produced at higher temperatures [8]. Lower HTC reaction temperatures such as 200 °C also result in higher nutrient concentrations in the HAP. A pretreatment process, such as microalgae cultivation that could utilize the organic or nitrogenous species prior to MD treatment would improve distillate quality and decrease flux decline.

Microalgae are widely used for nutrient removal from a variety of waste streams, including manure [18], and several heterotrophic strains can use organic compounds as a carbon source. Production of algae at the industrial scale is limited by the cost of supplying nutrients; however, wastewater sources can contain nutrients, organic carbon, and water,

improving the sustainability of large-scale cultivation [19]. Nutrient recovery via microalgae in manure waste streams has been shown to reduce eutrophication impacts associated with N and P contamination of water resources [20,21]. Microalgae have the added benefit of high protein content, and because they can be grown on nonarable land they can be used as a food supplement that do not compete with crops. Microalgae have successfully been cultivated on a variety of HAP produced from other algae strains [22,23] or agricultural wastes [24]. For large-scale dairy facilities, the dairy manure can be used as an HTC feedstock and the microalgae can supplement the cow diet, replacing conventional protein sources derived from soybean or canola [25].

Several mixotrophic algae species have been cultivated on HAP produced from dairy manure, but dilution to 5% was required. Of the investigated strains, *Arthrospira maxima* and *Chlamydomonas reinhardtii* performed the best in terms of both protein/biomass production and nutrient remediation [26]. The two strains had similar protein content, but *A. maxima* was shown to grow faster and remediate more of the HAP nutrients. *A. maxima* also required a bicarbonate buffer to maintain a pH = 9.5 for successful cultivation [26]. The buffer helps with contamination prevention, which is a concern for scale-up, but causes other environmental concerns such as an increase in water demand for the buffer's production [27,28]. The spent, unbuffered HAP after *C. reinhardtii* cultivation may be used for irrigation where the remaining nutrients serve as a fertilizer; however, the *A. maxima* supernatant would not be suitable for direct application to cropland due to its high salt content from the added buffer. MD can concentrate the buffer and nutrients in the supernatant to recycle it back to the algae cultivation process and simultaneously produce clean water that can be used on-site.

The goal of this study was to assess MD's potential to treat HAP algal supernatants to produce clean water and a concentrate that can be recycled back into the cultivation process. *A. maxima* and *C. reinhardtii* were cultivated on HAP produced from dairy manure with the required dilutions or buffer. Each supernatant was treated with MD and compared to the performance of its uninoculated variant. The COD, TN, TP, and NH_3 of the feed, distillate, and concentrate were measured to assess the distillate quality. A regrowth experiment with the concentrated *A. maxima* supernatant was conducted to assess the potential of recycling the buffer during the cultivation process. Fluorescence excitation-emission matrices (EEM) were used to characterize the organic material found in the HAP, supernatants, and distillates.

3.3 Materials and Methods

3.3.1 HTC Aqueous Product

HAP was produced using dairy manure collected from a dairy in Fallon, NV. The manure was dried under ambient conditions for two weeks, then ground to particle sizes < 1 mm with a Wiley Mill (Model 4; Thomas Scientific, Swedesboro, NJ). Each HAP batch was produced from 100 g of milled manure with 1000 g of DI water. A 1-L reactor (Parr Instrument Company, Moline, IL) was pressurized to 20 bar and purged twice with nitrogen gas to remove oxygen. The temperature of the reactor was slowly increased at 2 °C/min to 200 °C. The reactor pressure is correlated with the vapor pressure of the water and reached ~15 bar. After 10 min at 200 °C, the reactor was rapidly cooled to room temperature via an ice bath and fan. Before opening the vessel, the gaseous products were vented off. The

HAP was then separated from the remaining solid-liquid slurry with vacuum filtration and Whatman 42 filter paper.

3.3.2 MD System

The bench-scale DCMD system (Fig. 3.1) follows a multi-pass design consisting of a feed loop and a distillate loop with an overflow drip component [29]. The excess distillate volume produced by transmembrane flux drips through the neck of a vacuum flask and into a capture flask on an analytical balance. Transmembrane flux (Eq. 3.1) was calculated using a backward difference estimation of the change in mass on the balance (Δm) over a time interval (Δt) assuming 1000 g/L as the water density (ρ).

$$J = \frac{\Delta m}{\rho \Delta t} \tag{3.1}$$

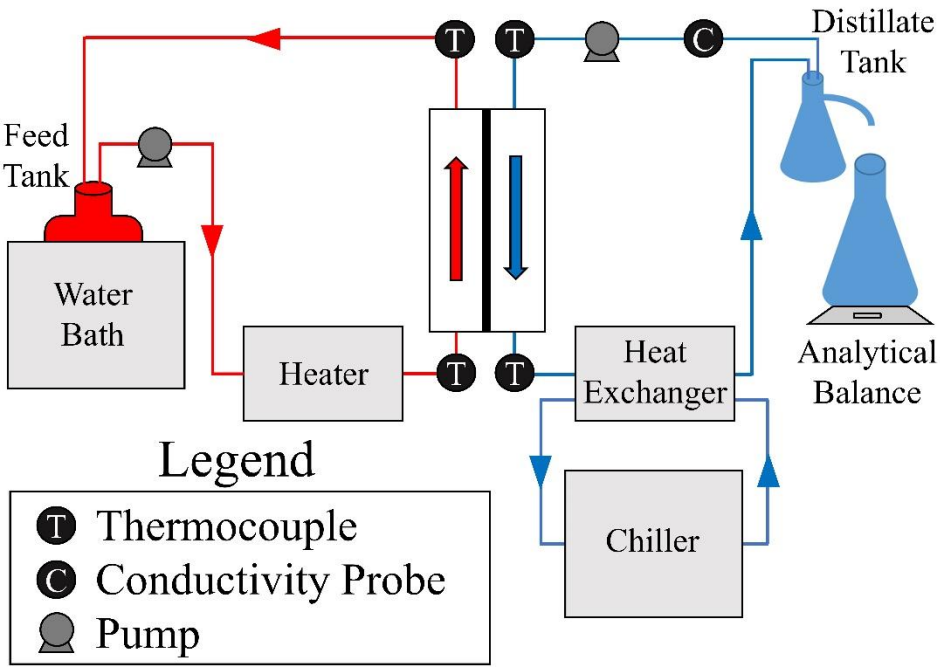

Figure 3.1: Schematic of the bench-scale DCMD system.

A total of four temperature probes were located around the membrane module; two at the entrance and two at the exit on both the feed and distillate loops. The feed temperature was maintained by a hot water bath set to 70 °C with an in-line heater (FLUENT, Watlow, St. Louis, MO) used for finer temperature control. The power of the heater was controlled by a LabView (Version 16.0, National Instruments, Austin, TX) PID controller to maintain 50.0 ± 0.5 °C at the feed inlet of the membrane module (SEPA cell, GE Osmonics, Minnetonka, MN). The distillate conductivity was monitored in real time throughout the experiment as a metric for distillate quality and an indicator for membrane failure. The feed and distillate loops were pumped using a dual-head peristaltic pump (Cole-Parmer, Vernon Hills, IL) at a rate of 600 mL/min. The LabView program recorded the four temperatures, distillate conductivity, and excess distillate mass in 2-min intervals. Each DCMD trial started with 1400 mL of feed and operated for 12 hr.

For each MD trial, a fresh polytetrafluoroethylene (PTFE) membrane (CLARCOR Inc., Franklin, TN) with an active area of 42.18 cm^2 was used. The membrane had a nominal pore size of 0.18 μm, thickness of 67 μm, and porosity of 80.1% [30]. To promote turbulence and improve mass transfer, cross-mesh plastic spacers were placed in the feed and distillate flow channels [31].

3.3.3 Algae Cultures

Arthrospira maxima (UTEX LB 2342) and *Chlamydomonas reinhardtii* (UTEX 2243) were obtained from UTEX (UTEX, Austin, TX) and grown on their respective suggested media to use as inoculum for the MD HAP experiments. The inoculum media for *A. maxima* was the UTEX Spirulina media: 162 mM $NaHCO_3$, 38 mM Na_2CO_3, 2.9

mM K_2HPO_4, 29.4 mM $NaNO_3$, 5.74 mM K_2SO_4, 17.7 mM NaCl, 0.81 mM $MgSO_4$, 0.27 mM $CaCl_2$, 12 μM Na_2EDTA, 10 μM H_3BO_3, 2.2 μM $FeCl_3$, 1.3 μM $MnCl_2$, 0.22 μM $ZnCl_2$, 0.16 μM Na_2MoO_4, 0.15 μM $ZnSO_4$, 0.13 μM $CoCl_2$, 0.08 μM $CuSO_4$, and 100 nM vitamin B_{12}. The bicarbonate buffer maintained pH near 9.5 to promote growth for the alkaliphilic *A. maxima*. The inoculum media for *C. reinhardtii* was the P49 media: 0.16 mM $MgSO_4$, 0.16 mM Na_2glycerophosphate, 0.67 mM KCl, 3.8 mM glycylglycine, 1.2 mM NH_4NO_3, 0.5 mM $CaCl_2$, 0.2 g/L yeast extract, 0.4 g/L tryptone, 12 μM Na_2EDTA, 2.2 μM $FeCl_3$, 1.3 μM $MnCl_2$, 0.23 μM $ZnCl_2$, 0.10 μM Na_2MoO_4, 0.050 μM $CoCl_2$, 1.3 μM thiamine, 100 nM biotin, and 100 nM vitamin B_{12}.

3.3.4 MD Feed Preparation

The unbuffered MD feed solutions were prepared by autoclaving 12 L of 5% HAP diluted with DI water. For the buffered HAP experiments, 6 L of 10% HAP were sterilely mixed with 6 L of the bicarbonate buffer (324 mM $NaHCO_3$/76 mM Na_2CO_3) post autoclave to produce a 5% HAP solution with buffer concentrations equal to the UTEX Spirulina media. Half of the resulting volume was used for the triplicate MD control experiments and the other half was used for algae cultivation. *C. reinhardtii* was cultivated on the unbuffered HAP and *A. maxima* on the buffered HAP.

The algae cultures were grown in four 2-L flasks with 1400 mL working volume. Cultures were mixed on shake tables at 100 rpm with white lights (Sylvania Octron® Eco®,17W) set to 60 μmol/m^2/s on a 12 hr light, 12 hr dark rotation. To reduce media carryover, inoculum cultures were centrifuged at 4500 x g for 10 min and the supernatant was decanted. The pellet was resuspended in sterile DI water and centrifuged again. The

DI rinse procedure was repeated twice before the pellet was suspended in the diluted HAP and used to inoculate.

The cultures were harvested in late exponential phase growth to simulate optimal continuous operation and the OD was estimated based on previous experimental work [26]. The cultures were harvested via centrifugation at 4500 x g for 10 min. After harvest, the supernatants were consolidated to eliminate variation associated with the biological replicates. The samples were stored at 4 °C until MD treatment. Triplicate MD experiments were conducted on the combined volume with a starting volume of 1400 mL for each trial.

3.3.5 Regrowth Experiment

A fourth MD trial was performed with a separate HAP batch for the *A. maxima* regrowth experiment. The *A. maxima* was cultivated, and the supernatant was treated by MD as previously described. A fresh HAP batch was produced to supplement a second algae growth stage. Three different growth conditions were tested during the second stage: (1) buffered 5% HAP using the fresh HAP batch, (2) recycled concentrated supernatant with fresh HAP added to achieve the same phosphorus concentration as the first stage, and (3) recycled concentrated supernatant diluted to have the same buffer concentration with no fresh HAP supplement. All three testing conditions result in the same buffer concentration; for cases (2) and (3) the buffer came from the concentrated supernatant. The second stage was inoculated from *A. maxima* grown on UTEX Spirulina media so the algal strain had no HAP acclimation.

3.3.6 Analytical Methods

3.3.6.1 Optical Density

Algae growth was tracked using optical density at 750 nm (OD_{750}) measured with a Hach DR6000 spectrophotometer (Hach, Loveland, OH). Each culture was blanked to its non-inoculated, sterile HAP mixture.

3.3.6.2 Nutrient Kits

The nutrients of the distillate, initial feed, and concentrated feed for each MD trial were measured spectrophotometrically using the lowest range kits provided by Hach (Loveland, CO). The COD, TN, TP, and NH_3 were measured using TNT 820 (ULR), TNT 826 (LR), TNT 843 (LR), and TNT 830 (ULR) respectively, with the necessary dilutions ranging from 1x to 200x.

The paired performance of the algae-MD treatment of MD for each nutrient was assessed using the total removal, R_i (Eq. 3.2). For each experiment $m_{i,d}$ was the mass of nutrient component i measured in the distillate stream and $m_{i,0}$ was the average mass of i measured in the feed stream for the respective control. For *A. maxima* and buffered HAP, $m_{i,0}$ was the mass measured in the buffered HAP feed; for *C. reinhardtii* and unbuffered HAP, $m_{i,0}$ was the mass measured in the unbuffered HAP.

$$R_i = 1 - \frac{m_{i,d}}{m_{i,0}} \tag{3.2}$$

3.3.6.3 Fluorescence

Excitation-emission matrix (EEM) spectra were obtained for each distillate, initial feed, and concentrated feed for each MD trial using a spectrofluorometer (RF-6000; Shimadzu, Kyoto, Japan). The excitation wavelengths ranged from 200 to 500 nm with a 1 nm step size and emission wavelengths ranged from 220 to 600 nm with a 2 nm step size. The instrument excitation and emission bandwidths were both set to 5.0 nm and the scan speed was 6000 nm/min. The instrument was autozeroed before each scan. The inner-filter effect was reduced by diluting the samples to absorbance < 0.05 [32]. First- and second-order Rayleigh and Raman scattering were removed during postprocessing by zeroing the regions and interpolating with a piecewise, shape-preserving cubic polynomial [33]. A 20 nm and 15 nm interpolation band were used for Rayleigh and Raman, respectively. Rayleigh scattering occurs when the excitation wavelength is equal to or twice (2^{nd} order) the emission wavelength. The Raman scattering wavelength was estimated using Eq. 3.3, where $\lambda_{EM,R}$ is the Raman wavelength [nm] at an excitation wavelength, λ_{EX} [34].

$$\lambda_{EM,R} = 1 \times 10^7 \left(\frac{1 \times 10^7}{\lambda_{EX}} - 3400 \right)^{-1} \tag{3.3}$$

The spectra were normalized to Raman units using the Raman peek of pure water at 350 nm excitation [35]. The EEM spectra were divided into five different regions for integration and characterization: Regions I and II correspond to aromatic compounds, Region III to fulvic acids, Region IV to biological byproducts, and Region V to humic acids [36]. Integration for Region *k* was done discretely using Eq. 3.4, where the intensities (I_{ij}) were summed across the excitation and emission indexes of the region.

$$\Phi_k = MF_k \sum_i \sum_j I_{ij} \Delta\lambda_{EX} \Delta\lambda_{EM} \quad (3.4)$$

The excitation step size ($\Delta\lambda_{EX}$) and emission step size ($\Delta\lambda_{EM}$) were 1 and 2 nm, respectively. The scaling factor, MF_k, was determined by the inverse of the fraction of projected area on the excitation emission plane [36]. After integrating the five regions, the volumes were normalized.

3.4 Results and Discussion

3.4.1 Algal Cultivation

The pH, COD, TN, TP, and NH_3 for each MD feed solution are shown in Table 3.1. The *A. maxima* culture and 5% buffered HAP came from the same HAP batch, while the *C. reinhardtii* culture came from the same batch as the 5% HAP. Only a small pH reduction was observed during the *A. maxima* cultivation, which was expected as the culture was buffered. *A. maxima* consumed 57% of the original COD, 51% of the TN, 77% of the TP, and ~100% of the NH_3 during cultivation. Although the solution is alkaline, the NH_3 reduction was mostly biotic as the sterile control under similar environmental conditions only lost 5% of the NH_3 to volatilization. During the *C. reinhardtii* cultivation, the pH increased as CO_2 was not added to the culture. Additionally, *C. reinhardtii* removed significantly fewer nutrients than *A. maxima* before it reached stationary phase, with only 20% of the initial COD, 15% of the TN, 57% of the TP, and 50% of the NH_3 consumed.

Table 3.1: The pH, COD, TN, TP, and NH_3 concentrations for the MD feed solutions.

	pH	**COD** [mg/L]	**TN** [mg-N/L]	**TP** [mg-P/L]	**NH_3** [mg-N/L]
5% buffered HAP	9.33 ± 0.01	1441 ± 54	74.7 ± 4.0	4.44 ± 0.06	9.60 ± 0.16
A. maxima	9.28 ± 0.01	612 ± 38	36.6 ± 0.4	1.04 ± 0.04	BDL
5% HAP	5.30 ± 0.06	1364 ± 68	74.1 ± 3.9	3.88 ± 0.09	9.50 ± 0.21
C. reinhardtii	8.03 ± 0.05	1096 ± 20	62.7 ± 1.7	1.66 ± 0.05	4.72 ± 0.03

3.4.2 MD Performance

The transmembrane flux and conductivity for MD treatment of the two algal supernatants are shown in Figure 3.2. A significant flux decline was observed at the start of the experiment with the buffered HAP. Unlike the unbuffered HAP, the initial flux was below 20 LMH and dropped to 13 LMH within 30 min; however, for the remainder of the experiment, the flux was relatively stable and only decreased by ~3 LMH. This indicates that most of the membrane fouling occurred quickly, likely caused by components of HAP that are hydrophobic under alkaline conditions. By comparing the two 5% HAP controls, it can be seen that the addition of the buffer to the HAP negatively affected the flux during MD operation (Fig. 3.2A). However, cultivation of *A. maxima* counteracted most of this effect as the supernatant flux closely resembled the unbuffered 5% HAP. Conversely, *C. reinhardtii* cultivation had minimal effect on MD operation as there was no noticeable difference in flux performance and no statistical difference in water produced during the 12 hr experiment ($p = 0.73$). Supernatants from both algae strains had similar or improved flux to their uninoculated controls.

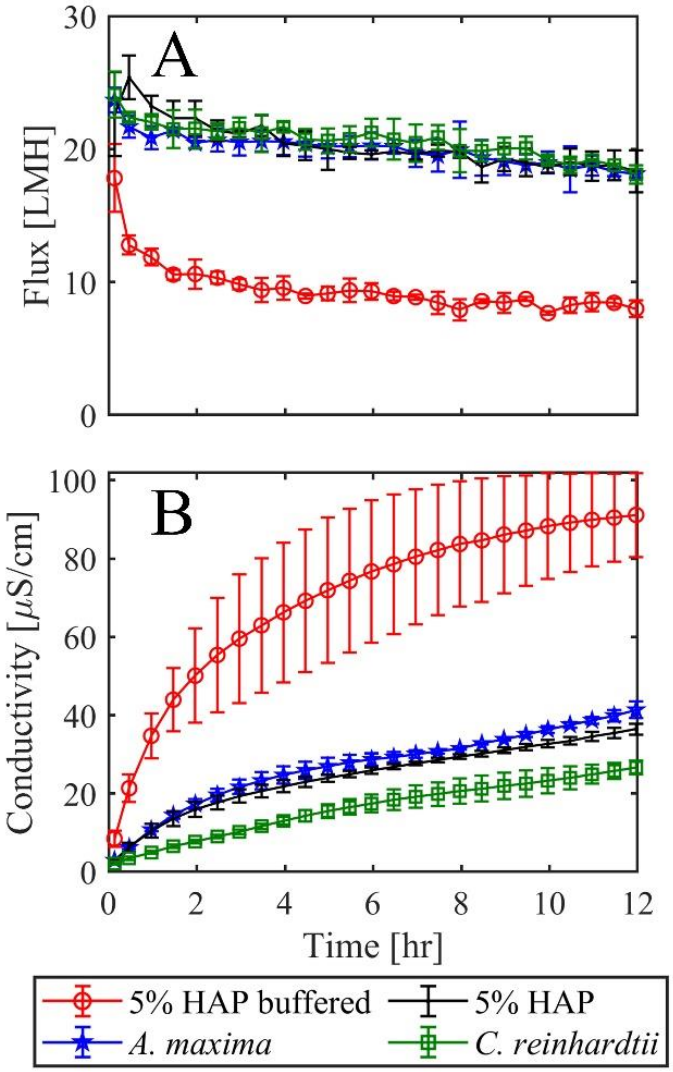

Figure 3.2: Transmembrane water flux (A) and distillate conductivity (B) for MD trials. Error bars represent the sample standard deviation of triplicates at the same time measurement.

The distillate conductivity (Fig. 3.2B) was measured in real time. Compared to the initial feed-side conductivity (~1 ms/cm unbuffered 5% HAP; ~50 ms/cm buffered 5% HAP), no dramatic increase in conductivity was observed, suggesting no membrane breakage or wetting occurred during treatment [29]. Both algae supernatants had lower conductivity than their respective control throughout the entirety of the experiment. The

buffered HAP had the highest conductivity, but the algae cultivation counteracted the adverse effects, lowering the conductivity to values similar to the unbuffered HAP. The increase in conductivity for the buffered scenarios suggests there are more volatile HAP species present under alkaline than acidic conditions, and that these then dissociate in the cleaner distillate side. Under alkaline conditions, species like NH_3 with a higher pKa will be unprotonated and are more likely to pass the membrane at the higher pHs [37]. After *A. maxima* cultivation, there was no NH_3 present, which contributes to the reduced conductivity in the distillate. The reduction of COD within the feed is another candidate. The distillate pHs ranged from 6.5 to 7.5 with no statistical difference between sample types using Tukey's Honest Significance Test ($\alpha = 0.05$). This suggests that there were near equal weak acids, such as carboxylic acids, that may have volatilized through the membrane.

3.4.3 MD Rejections

The total removals of COD, TN, TP, and NH_3, as determined by Eq. 3.2, are shown in Figure 3.3. NH_3 was a component of interest since it is a preferred nitrogen source for algae cultivation [26] as well as a volatile species that can be lost during MD treatment or pass through the membrane. Since all measurable NH_3 was consumed during *A. maxima* cultivation, there was none present when treating the *A. maxima* supernatant with MD, resulting in near 100% removal. In the case of buffered HAP, which had a starting pH of 9.3, the NH_3 was concentrated on the distillate side while the feed side concentration fell below detection limits due to any residual NH_3being lost to the atmosphere through the heated feed stream. For *C. reinhardtii*, 50% of the NH_3 was consumed during cultivation.

The supernatant pH was 8.0 (Table 3.1) and closer to NH_3 pKa than the HAP control. Due to the pH difference, more $NH_3$was detected in the *C. reinhardtii* distillates than in the unbuffered HAP distillates despite having lower initial feed concentrations. This resulted in a reduced calculated removal of NH_3 for the *C. reinhardtii* supernatant than the HAP control (Fig. 3.3). The TN present in the HAP can be divided into NH_3 and non- NH_3 N, which is predominantly organic N such as amino acids [26]. As seen in Table 3.1, only a small portion of the TN in the samples was NH_3. Although more NH_3 was present in the *C. reinhardtii* distillate, less TN was measured, indicating less non-NH_3 N passed the membrane during MD treatment. A similar analysis for *A. maxima* leads to the same conclusion, but the reduction of non-NH_3 N was to a lesser degree.

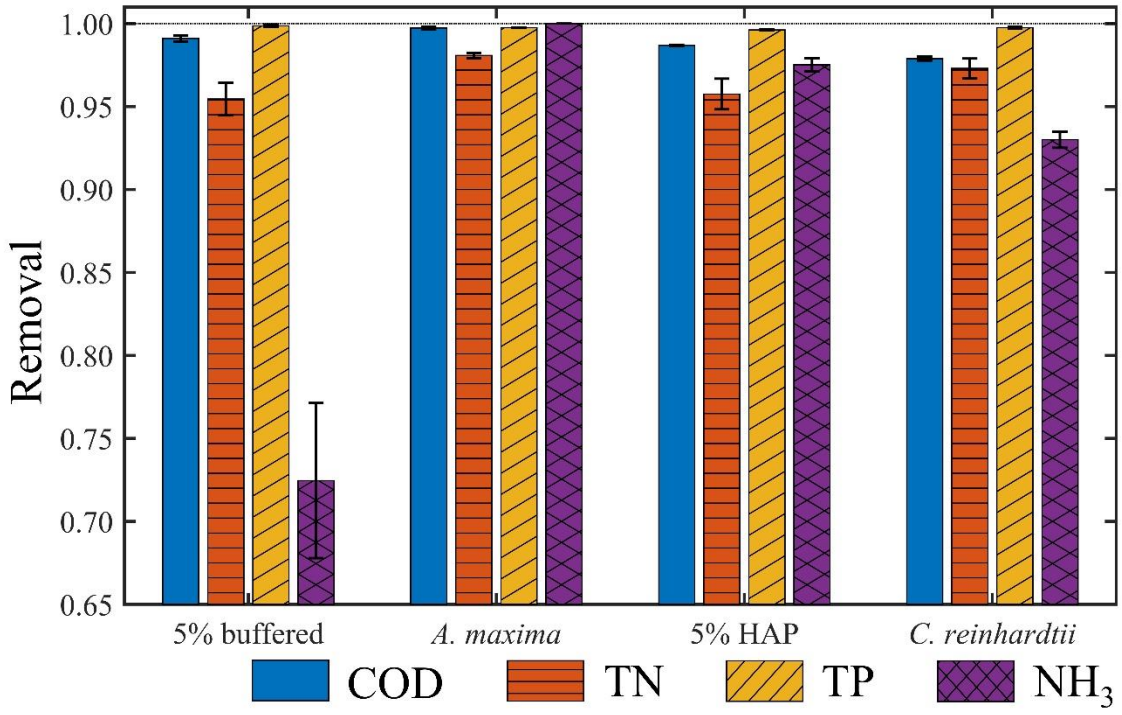

Figure 3.3: Total removal (Eq. 3.2) of COD, TN, TP, and NH_3 from the distillate stream measured after MD treatment. Error bars represent sample standard deviation of MD triplicates.

There were no significant trends in TP removal across sample types, with each demonstrating near 100% removal and distillate concentrations below detection limits. The phosphorus in HAP is predominantly phosphate [7], so near 100% rejection would be expected. Even if algae cultivation were not present in the process, the phosphorus would likely have been rejected by the membrane, similar to treatment of other non-volatile ions [13].

COD was used as a metric for the organic components in the HAP. The *A. maxima* cultivation consumed a significant amount of COD during cultivation (Table 3.1), resulting in increased overall removal of COD for the process (Fig. 3.3). Comparing the buffered samples, the COD concentration in the distillate was reduced from 37.7 to 5.3 mg/L, demonstrating that many of the organic species that pass through the membrane were consumed during *A. maxima* cultivation. Although *C. reinhardtii* also consumed COD during cultivation, a decreased removal was observed. The average COD concentration in the *C. reinhardtii* distillate (38.5 mg/L) was greater than the 5% HAP (24.3 mg/L), which is likely caused by two different mechanics: (1) more COD passes through the membrane under alkaline conditions as was seen when comparing the two HAP control distillates, and (2) the algae species excreted more simple organics that would pass through the membrane than were initially present in the HAP.

3.4.4 Fluorescence

HAP is a collection of various organics of different sizes and functional groups [4,10], thus fluorescence was used as a "fingerprint" to characterize the organic components of the HAP, supernatants, and distillates in terms of bulk properties. EEM

spectra with normalized integration of the five regions for each feed and distillate type are shown in Figure 3.4. The pH difference between the buffered samples (Figs. 3.4B and 3.4D) and unbuffered samples (Figs. 3.4F and 3.4H) strains a proper comparison across algae species. Based on Chen et al. [36], Regions I and II are predominantly simple aromatics such as tyrosine, Region IV are soluble biological byproduct-like substances, and Regions III and V correspond to fulvic- and humic-like substances, respectively [36]. The buffered feed solutions were composed of species from all 5 regions, with significant fractions in Region II (aromatics and biological byproducts). The effects of *A. maxima'*s cultivation can be seen by comparing the 5% buffered feed (Fig. 3.4B) to the *A. maxima* supernatant/feed (Fig. 3.4D). The most significant change was observed in Region I, which decreased by 16% when the *A. maxima* was cultivated, showing that *A. maxima* consumed many of the simple aromatics found in the HAP. The relative fraction of humic and fulvic acids increased, suggesting they were not a preferred carbon source for *A. maxima*. During *C. reinhardtii*'s cultivation, the relative fraction of humic and fulvic acid slightly decreased, suggesting it was preferentially consumed over other carbon sources. It has been seen that humic supplements offer a greater effect on the productivity for green algae like *C. reinhardtii* than blue-green algae like *A. maxima* [38]. Contrary to *A. maxima*, the simple aromatics associated with Region I increased after *C. reinhardtii* cultivation.

General conclusions for MD treatment of the samples are similar. MD performed well in terms of total removal by comparing the EEM total volume of the feeds to the distillates (Fig. 3.4). With this same comparison, both supernatants were of higher quality than their respective control and the supernatant distillates were of higher quality than their respective control distillates. For each feed solution, the humic and fulvic acids (Regions

III and V) were removed by MD with high efficiency due to their large size and low volatility. The most humic- and fulvic-like substances were detected in the distillate of the buffered HAP (Fig. 3.4A), while the least were observed in the distillate of the *A. maxima* supernatant. The species that were concentrated in the distillate were the simple aromatics associated with Region I. The aromatics associated with Region II were preferentially removed except for the treatment of unbuffered HAP, where the relative concentration in the feed and distillate were the same. Region IV biological byproducts were concentrated in the distillates except in the case of the *A. maxima* supernatant where it decreased slightly. The *C. reinhardtii* distillate had a higher biological byproducts concentration compared to its control, and the *A. maxima* had a reduced concentration, a similar trend to what was observed with the COD measurements.

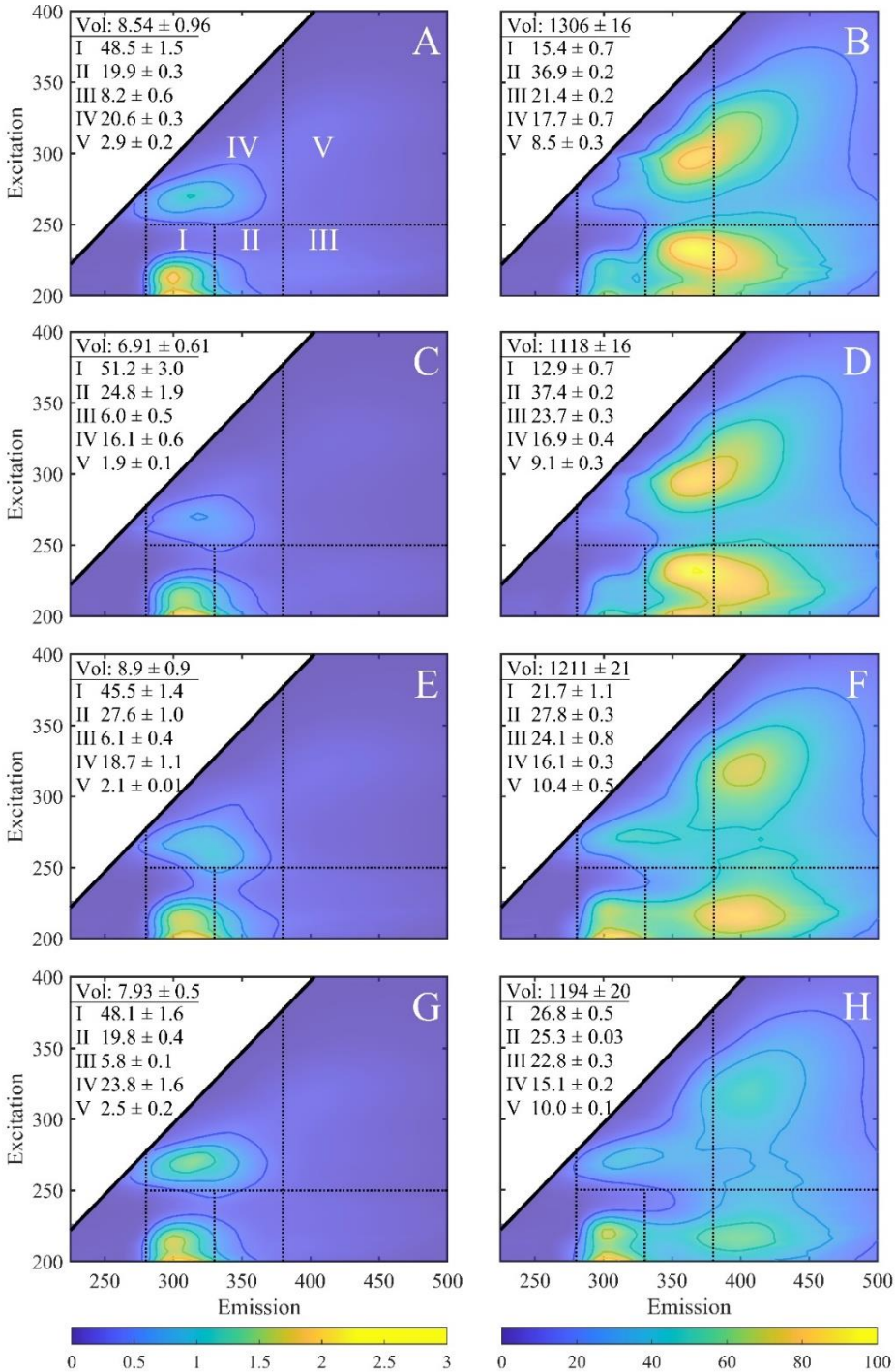

Figure 3.4: Fluorescence EEM for (A) buffered 5% HAP feed and (B) distillate, (C) *A. maxima* supernatant and (D) distillate, (E) unbuffered 5% HAP feed and (F) distillate, and (G) *C. reinhardtii* supernatant and (H) distillate. The dashed lines represent the different regions used for integration as described by Chen et al. [36]. The normalized volume percentage for each region is provided as a table within each subplot and the total volume is in the corner with units of 10^3 Raman*nm^2. Reported error represents the standard deviation of three MD replicates originating from consolidated four biological replicates.

3.4.5 Regrowth Experiment

A. maxima removed more nutrients than *C. reinhardtii* while having similar MD performance and an improved distillate quality, as measured through bulk measurements. An advantage to treating the *A. maxima* supernatant with MD would be to recycle the buffer back into the cultivation cycle, as the need for the buffer has been shown to increase the global warming potential and total water demand of the overall process [27,28]. The potential of buffer reuse was assessed in a two-stage regrowth experiment. In the first stage, *A. maxima* was cultivated with the buffered HAP concentrated by MD, and then the concentrate was used to cultivate a new batch of *A. maxima* in the second stage. The growth curves during the initial growth stage and the recycle growth stage are shown in Figure 3.5 and the nutrient concentrations were summarized in Table 3.2. For both the partial and total recycle, all the buffer was sourced from the spent HAP of Stage 1. Cultivation of *A. maxima* on a fresh HAP batch largely resembled the growth observed in Stage 1 despite having 35% more phosphorus. Cultivating *A. maxima* solely on the previously spent HAP resulted in the culture dying, as determined by the optical density gradually decreasing throughout the experiment and a visual loss of green coloration to the culture. The soluble nutrients also increased as the inoculated cells released more upon cell death and lysis. This is likely explained by the simple organics or NH_3 that would have supported heterotrophic growth being completely lost through the MD treatment. The partial recycle resulted in a successfully growing *A. maxima* culture with a growth rate similar to what was observed in Stage 1. The culture did not grow as long, likely due to reduced available nutrients (Table 3.2); the partial recycle had similar TN and TP concentrations as Stage 1, but a lower NH_3 concentration. Although the amount of TN and TP consumed was reduced after the recycle,

no additional buffer input was required. Notably, the culture also consumed the least amount of NH_3 (Table 3.2), suggesting there is a different mechanism limiting *A. maxima*'s growth. More rigorous experiments are required to optimize nutrient remediation with the applied recycle.

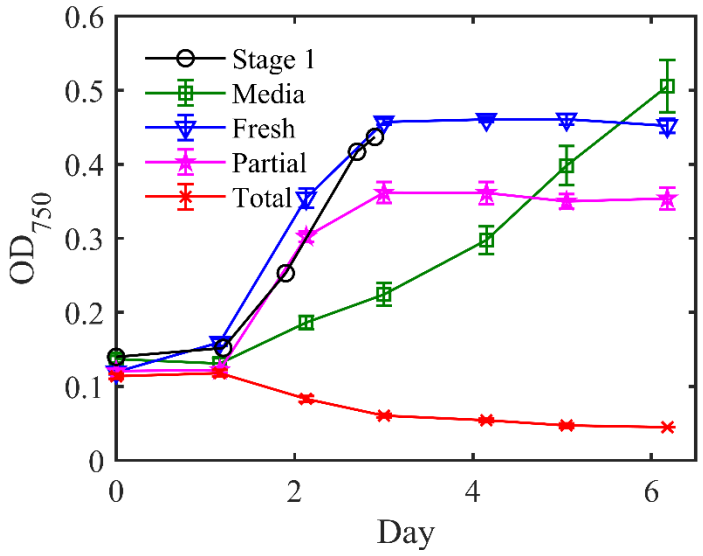

Figure 3.5: Growth curve for *A. maxima* during the regrowth experiment. Error bars represent the sample standard deviation of triplicates at the time measurement. There were no replicate measurements for Stage 1.

Table 3.2: The initial (I) and final (F) nutrient concentrations during the *A. maxima* regrowth experiment. BDL: below detection limit.

		COD [mg/L]	**TN** [mg-N/L]	**TP** [mg-P/L]	**NH_3** [mg-N/L]
Stage 1	I	1299	68.8	4.24	9.40
	F	697	43.4	1.37	BDL
Fresh	I	1313	65.7	5.73	9.21
	F	854	42.7	1.99	0.70
Partial	I	1248	68.1	4.25	4.95
	F	713	44.9	2.37	1.01
Total	I	693	37.4	1.38	BDL
	F	819	42.1	2.13	

3.5 Conclusion

MD treatment of the HAP was generally improved when treating the algal supernatants compared to treatment of the uninoculated media. No negative effects on water flux were observed when treating the algal supernatants while producing distillates with reduced conductivities. The cultivation of *A. maxima* resulted in reduced distillate concentrations of COD, TN, and NH_3, while the cultivation of *C. reinhardtii* resulted in increased distillate COD and NH_3 concentrations. In each case, the TP was removed by MD with near 100% effectiveness. The addition of the buffer to HAP reduced flux, increased distillate conductivities, and increased distillate nutrient concentrations; however, the cultivation of *A. maxima* counteracted these changes. Fluorescence revealed MD removed the humic- and fulvic-like substances in the HAP and suggests that the organics in the distillate are primarily simple aromatics and biological byproduct-like substances. The regrowth experiment on the concentrated algae supernatant revealed potential for recycling the buffer, but additional experiments are necessary to optimize the nutrient remediation in a recycle scenario. The proposed system could successfully extract value from the dairy manure, with the algae cultivation improving MD overall performance, but more details on the energetics of the HTC process and MD are required to investigate how much water the MD unit can treat.

3.6 Works Cited

[1] R. MacDonald, J. M., Cessna, J., & Mosheim, Changing Structure, Financial Risks, and Government Policy for the U.S. Dairy Industry, (2016) 1–75. https://www.ers.usda.gov/webdocs/publications/45519/56833_err205_errata.pdf?v=0.

[2] J.A. Burkholder, B. Libra, P. Weyer, S. Heathcote, D. Kolpin, P.S. Thorne, M. Wichman, Impacts of waste from concentrated animal feeding operations on water quality, Environ Health Perspect. 115 (2007) 308–312. https://doi.org/10.1289/ehp.8839.

[3] R.W. Todd, N.A. Cole, K.D. Casey, R. Hagevoort, B.W. Auvermann, Methane emissions from southern High Plains dairy wastewater lagoons in the summer, Anim Feed Sci Technol. 166–167 (2011) 575–580. https://doi.org/10.1016/j.anifeedsci.2011.04.040.

[4] T.M. Reza, A. Freitas, X. Yang, S. Hiibel, H. Lin, C.J. Coronella, Hydrothermal carbonization (HTC) of cow manure: Carbon and nitrogen distributions in HTC products, Environ Prog Sustain Energy. 35 (2016) 1002–1011. https://doi.org/10.1002/ep.12312.

[5] K. Wu, Y. Gao, G. Zhu, J. Zhu, Q. Yuan, Y. Chen, M. Cai, L. Feng, Characterization of dairy manure hydrochar and aqueous phase products generated by hydrothermal carbonization at different temperatures, J Anal Appl Pyrolysis. 127 (2017) 335–342. https://doi.org/10.1016/j.jaap.2017.07.017.

[6] Y.Z. Belete, V. Mau, R. Yahav Spitzer, R. Posmanik, D. Jassby, A. Iddya, N. Kassem, J.W. Tester, A. Gross, Hydrothermal carbonization of anaerobic digestate and manure from a dairy farm on energy recovery and the fate of nutrients, Bioresour Technol. 333 (2021) 125164. https://doi.org/10.1016/j.biortech.2021.125164.

[7] S. v. Qaramaleki, J.A. Villamil, A.F. Mohedano, C.J. Coronella, Factors Affecting Solubilization of Phosphorus and Nitrogen through Hydrothermal Carbonization of Animal Manure, ACS Sustain Chem Eng. 8 (2020) 12462–12470. https://doi.org/10.1021/acssuschemeng.0c03268.

[8] N.A. Silva, S.R. Hiibel, Nutrient recovery of the hydrothermal carbonization aqueous product from dairy manure using membrane distillation, Environ Technol. 0 (2021) 1–10. https://doi.org/10.1080/09593330.2021.1995785.

[9] M. Langone, D. Basso, Process waters from hydrothermal carbonization of sludge: Characteristics and possible valorization pathways, Int J Environ Res Public Health. 17 (2020) 1–31. https://doi.org/10.3390/ijerph17186618.

[10] K. Nakason, B. Panyapinyopol, V. Kanokkantapong, N. Viriya-empikul, W. Kraithong, P. Pavasant, Characteristics of hydrochar and liquid fraction from hydrothermal carbonization of cassava rhizome, Journal of the Energy Institute. 91 (2018) 184–193. https://doi.org/10.1016/j.joei.2017.01.002.

[11] R.D. Gustafson, S.R. Hiibel, A.E. Childress, Membrane distillation driven by intermittent and variable-temperature waste heat: System arrangements for water production and heat storage, Desalination. 448 (2018) 49–59. https://doi.org/10.1016/j.desal.2018.09.017.

[12] A. Alkhudhiri, N. Darwish, N. Hilal, Membrane distillation: A comprehensive review, Desalination. 287 (2012) 2–18. https://doi.org/10.1016/j.desal.2011.08.027.

[13] K.A. Salls, D. Won, E.P. Kolodziej, A.E. Childress, S.R. Hiibel, Evaluation of semi-volatile contaminant transport in a novel, gas-tight direct contact membrane distillation system, Desalination. 427 (2018) 35–41. https://doi.org/10.1016/j.desal.2017.11.001.

[14] N. Hamzah, C.P. Leo, Fouling evaluation on membrane distillation used for reducing solvent in polyphenol rich propolis extract, Chin J Chem Eng. 26 (2018) 477–483. https://doi.org/10.1016/j.cjche.2017.03.041.

[15] R. Bagger-Jørgensen, A.S. Meyer, M. Pinelo, C. Varming, G. Jonsson, Recovery of volatile fruit juice aroma compounds by membrane technology: Sweeping gas versus vacuum membrane distillation, Innovative Food Science and Emerging Technologies. 12 (2011) 388–397. https://doi.org/10.1016/j.ifset.2011.02.005.

[16] Á. Kozák, E. Békássy-Molnár, G. Vatai, Production of black-currant juice concentrate by using membrane distillation, Desalination. 241 (2009) 309–314. https://doi.org/10.1016/j.desal.2008.02.033.

[17] C.A. Quist-Jensen, F. Macedonio, C. Conidi, A. Cassano, S. Aljlil, O.A. Alharbi, E. Drioli, Direct contact membrane distillation for the concentration of clarified orange juice, J Food Eng. 187 (2016) 37–43. https://doi.org/10.1016/j.jfoodeng.2016.04.021.

[18] L. Wang, Y. Li, P. Chen, M. Min, Y. Chen, J. Zhu, R.R. Ruan, Anaerobic digested dairy manure as a nutrient supplement for cultivation of oil-rich green microalgae Chlorella sp., Bioresour Technol. 101 (2010) 2623–2628. https://doi.org/10.1016/j.biortech.2009.10.062.

[19] A.F. Clarens, E.P. Resurreccion, M.A. White, L.M. Colosi, Environmental life cycle comparison of algae to other bioenergy feedstocks, Environ Sci Technol. 44 (2010) 1813–1819. https://doi.org/10.1021/es902838n.

[20] B.T. Higgins, A. Kendall, Life Cycle Environmental and Cost Impacts of Using an Algal Turf Scrubber to Treat Dairy Wastewater, J Ind Ecol. 16 (2012) 436–447. https://doi.org/10.1111/j.1530-9290.2011.00427.x.

[21] W. Wu, L.C. Cheng, J.S. Chang, Environmental life cycle comparisons of pig farming integrated with anaerobic digestion and algae-based wastewater treatment, J Environ Manage. 264 (2020). https://doi.org/10.1016/j.jenvman.2020.110512.

[22] S.Z. Tarhan, A.T. Koçer, D. Özçimen, İ. Gökalp, Cultivation of green microalgae by recovering aqueous nutrients in hydrothermal carbonization process water of biomass wastes, Journal of Water Process Engineering. 40 (2021). https://doi.org/10.1016/j.jwpe.2020.101783.

[23] M. Tsarpali, N. Arora, J.N. Kuhn, G.P. Philippidis, Beneficial use of the aqueous phase generated during hydrothermal carbonization of algae as nutrient source for algae cultivation, Algal Res. 60 (2021) 102485. https://doi.org/10.1016/j.algal.2021.102485.

[24] S. Zora Tarhan, A.T. Koçer, D. Özçimen, I. Gökalp, Utilization of hydrothermal process water for microalgal growth, Eurasian Journal of Biological and Chemical Sciences. (2020) 42–47. https://doi.org/10.46239/ejbcs.733899.

[25] M.S. Madeira, C. Cardoso, P.A. Lopes, D. Coelho, C. Afonso, N.M. Bandarra, J.A.M. Prates, Microalgae as feed ingredients for livestock production and meat quality: A review, Livest Sci. 205 (2017) 111–121. https://doi.org/10.1016/j.livsci.2017.09.020.

[26] N.A. Silva, C.J. Glover, S.R. Hiibel, Nutrient Recovery by Microalgae in Aqueous Product of Hydrothermal Carbonization of Dairy Manure (in review), Cleaner Waste Systems. (n.d.).

[27] C.J. Glover, A. McDonnell, K.S. Rollins, S.R. Hiibel, P.K. Cornejo, Assessing the environmental impact of resource recovery from dairy manure, J Environ Manage. 330 (2023). https://doi.org/10.1016/j.jenvman.2022.117150.

[28] C.J. Glover, P.K. Cornejo, S.R. Hiibel, Life Cycle Assessment of Integrated Nutrient, Energy, and Water Recovery on Large-Scale Dairy Farms, Environ Eng Sci. 39 (2022) 811–820. https://doi.org/10.1089/ees.2021.0376.

[29] C.R. Taylor, P. Ahmadiannamini, S.R. Hiibel, Identifying pore wetting thresholds of surfactants in direct contact membrane distillation, Sep Purif Technol. 217 (2019) 17–23. https://doi.org/10.1016/j.seppur.2019.01.061.

[30] G. Rao, S.R. Hiibel, A.E. Childress, Simplified flux prediction in direct-contact membrane distillation using a membrane structural parameter, Desalination. 351 (2014) 151–162. https://doi.org/10.1016/j.desal.2014.07.006.

[31] C.P. Morrow, N.M. Furtaw, J.R. Murphy, A. Achilli, E.A. Marchand, S.R. Hiibel, A.E. Childress, Integrating an aerobic/anoxic osmotic membrane bioreactor with membrane distillation for potable reuse, Desalination. 432 (2018) 46–54. https://doi.org/10.1016/j.desal.2017.12.047.

[32] J.R. Lakowicz, Instrumentation for Fluorescence Spectroscopy, in: J.R. Lakowicz (Ed.), Principles of Fluorescence Spectroscopy, Springer US, Boston, MA, 2006: pp. 27–61. https://doi.org/10.1007/978-0-387-46312-4_2.

[33] M. Bahram, R. Bro, C. Stedmon, A. Afkhami, Handling of Rayleigh and Raman scatter for PARAFAC modeling of fluorescence data using interpolation, J Chemom. 20 (2006) 99–105. https://doi.org/10.1002/cem.978.

[34] G.W. Faris, R.A. Copeland, Wavelength dependence of the Raman cross section for liquid water, 1997.

[35] A.J. Lawaetz, C.A. Stedmon, Fluorescence intensity calibration using the Raman scatter peak of water, Appl Spectrosc. 63 (2009) 936–940. https://doi.org/10.1366/000370209788964548.

[36] W. Chen, P. Westerhoff, J.A. Leenheer, K. Booksh, Fluorescence Excitation-Emission Matrix Regional Integration to Quantify Spectra for Dissolved Organic Matter, Environ Sci Technol. 37 (2003) 5701–5710. https://doi.org/10.1021/es034354c.

[37] A. Zarebska, D.R. Nieto, K. v. Christensen, B. Norddahl, Ammonia recovery from agricultural wastes by membrane distillation: Fouling characterization and mechanism, Water Res. 56 (2014) 1–10. https://doi.org/10.1016/j.watres.2014.02.037.

[38] I.D. Pouneva, Effect of Humic Substances on the Growth of Microalgal Cultures, Russian Journal of Plant Physiology. 52 (2005) 410–413. https://doi.org/10.1007/s11183-005-0060-3.

4 CONCLUSIONS AND FUTURE WORK

4.1 Concluding Remarks

The number of CAFOs in the US dairy industry has been increasing over recent decades, leading to manure management concerns. Traditional methods of manure management have significant environmental impact in the form of greenhouse gas emissions and eutrophication potential. This work investigates an alternative treatment method for dairy manure management that incorporates hydrothermal carbonization, algae cultivation, and membrane distillation.

Initially, four algae were studied because of their high protein content and/or wastewater remediation potential: *Arthrospira maxima*, *Chlamydomonas reinhardtii*, *Chlorella vulgaris*, and *Scenedesmus obliquus*. The latter three species required dilutions for successful cultivation while the former required dilution and a pH buffer. At HAP concentrations higher than 5%, minimal growth was observed, and HAP precipitates formed that were further pronounced with the buffer. *A. maxima* had the highest removal of COD, TN, TP, and NH_3, as well as the fastest growth of the four strains, followed by *C. reinhardtii*. *A. maxima* and *C. reinhardtii* had similar protein contents near 43%, while the other two strains had both lower protein content and lower remediation potential. The results indicate that *A. maxima* and *C. reinhardtii* were the preferred strains as a cattle feed supplement and for nutrient remediation, with the former strain slightly outperforming the latter but requiring a bicarbonate buffer for cultivation.

In Chapter 3, the supernatants of *A. maxima* and *C. reinhardtii* were treated with MD. More detailed analysis of the HAP post-cultivation revealed the algae consumed COD, suggesting they could grow heterotrophically. However, the pH of the *C. reinhardtii*

culture increased so it predominantly grew autotrophically, while the pH of the *A. maxima* culture decreased slightly and consumed more COD, suggesting it grew more heterotrophically. During MD treatment, it was determined that the membrane flux was not negatively affected by the cultivation of either strain when compared to treatment of HAP. The inclusion of the buffer in the HAP resulted in reduced the flux, however cultivation with *A. maxima* negated this effect, with flux comparable to the unbuffered HAP. There was no statistical difference in flux between the unbuffered HAP and the *C. reinhardtii* supernatant. The distillate produced when treating *A. maxima* supernatant had lower concentrations of COD, TN, TP, and NH_3 than its control, while the distillate produced from *C. reinhardtii* supernatant had increased concentrations of COD and NH_3. From a MD perspective, *A. maxima* is preferred due to the improved distillate quality; however, the salts in the buffer prevent the concentrated supernatant from being used for irrigation. A simplified *A. maxima* regrowth experiment revealed cultivation using the recycled buffer is possible, but additional nutrients are required.

Cultivation with *A. maxima* on 5% HAP offers the most benefits for the dairy manure treatment system discussed in this work. This species utilized >90% of P and the most N of the algae investigated, greatly reducing eutrophication potential. *A. maxima* also grew the fastest, so fewer raceway ponds would be needed during scale-up to treat the same amount of manure. Additionally, MD treatment of *A. maxima* supernatant produced water with fewer contaminants while maintaining the same water production. The algae requires a bicarbonate buffer for successful cultivation. While this will reduce contamination that may be a concern during scale-up, the resulting high-salinity supernatant cannot be used for irrigation and would need to be treated further or sent to a wastewater treatment facility.

The recovered buffer can be recycled in future cultivation cycles thereby reducing the total buffer input required, but the operational details of recycling need to be investigated further.

4.2 Future Work

The work conducted has demonstrated the potential to use algae to remediate the HAP nutrients as well as the ability of MD to treat the supernatant. Preliminary energy balances between the HTC and MD processes revealed there is not enough waste heat to wholly treat the algal supernatant with MD; however, there is sufficient heat to replace the traditional RO unit output. Future efforts should be focused on further improvements to the system by reducing water usage and alleviating the complications associated with the bicarbonate buffer. *C. reinhardtii* should continue to be assessed along with *A. maxima* if further advancements improve its cultivation beyond the limitations of the buffer.

4.2.1 HAP Acclimation

When algae are constantly exposed to a particular wastewater, they may acclimate to the new environment. After acclimation to wastewater, *Arthrospira platensis* have been shown to remediate more nutrients and *Chlorella vulgaris* to grow faster than the unacclimated cultures [1]. Following a similar procedure, *C. reinhardtii* and *A. maxima* could acclimate to the HAP further increasing their remediation potential and reducing the footprint required for their cultivation. Another benefit to HAP acclimation is the potential to grow on higher HAP concentrations. By slowly acclimating the algae to HAP, the HAP concentration can gradually be increased. If the algae could reliably be cultivated on 10%

or higher HAP concentrations, the water input required for dilution would be halved or greater. In the case of *A. maxima* cultivation, the required buffer would also be halved.

4.2.2 Alternative Buffers

A bicarbonate buffer is advantageous for *A. maxima* cultivation because it aids in contamination prevention [2] and its pKa is near the optimal growth pH of 8.5-10.5 [3]. Additionally, it has been shown that $NaHCO_3$ has a positive effect on biomass production and protein content [4]. Traditionally, HCO_3^- is paired with Na^+; however, the salty HAP cannot be used in irrigation because the high salinity causes plant growth inhibition [5]. A $KHCO_3$ buffer may be used instead since it still provides soluble CO_3^{2-} and HCO_3^- ions. Potassium is used in fertilizer since it improves nitrogen metabolism in plants [6], so the buffered supernatant may be used in irrigation. It has been seen that growth is slightly reduced when using K_2CO_3 instead of Na_2CO_3 [7], so an additional economic analysis and LCA need to be conducted to see if the benefits outweigh the costs.

4.2.3 MD Longevity

The membrane experiments conducted in Chapter 3 only lasted for 12 hours and experiments from previous work were shorter. Long-term exposure to the algal supernatant is important for determining the limitations of MD treatment and the required membrane cleaning or replacement frequency. Prior to the work conducted in Chapter 3, a two-week experiment treating buffered 5% HAP with no algae cultivation was conducted in a modified DCMD system to identify the concentration factor (CF) limit of the membrane. The system had a feed tank with a float valve connected to an elevated feed tank to have a

continuous addition of the feed solution and keep a constant volume in the feed loop. The flux and conductivity of the experiment are summarized in Figure 4.1; near the end of the experiment, the conductivity gradually increased until a large conductivity spike occurred due to membrane failure, likely wetting. Membrane failure occurred around a 5.5 CF, but the cause was not thoroughly investigated. Previous work treated undiluted HAP with MD to a 2.5 CF (50 CF relative to diluted HAP) where the primary fouling was a calcium oxide salt [8]. The membrane failure was likely associated with the buffer. Since the $NaHCO_3$ and Na_2CO_3 concentrations were still below their solubility limit, the precipitation of the buffer salts with Ca^{2+} in the HAP is the most probable cause. As such, the potential to treat buffered algal supernatant to a high CF is limited.

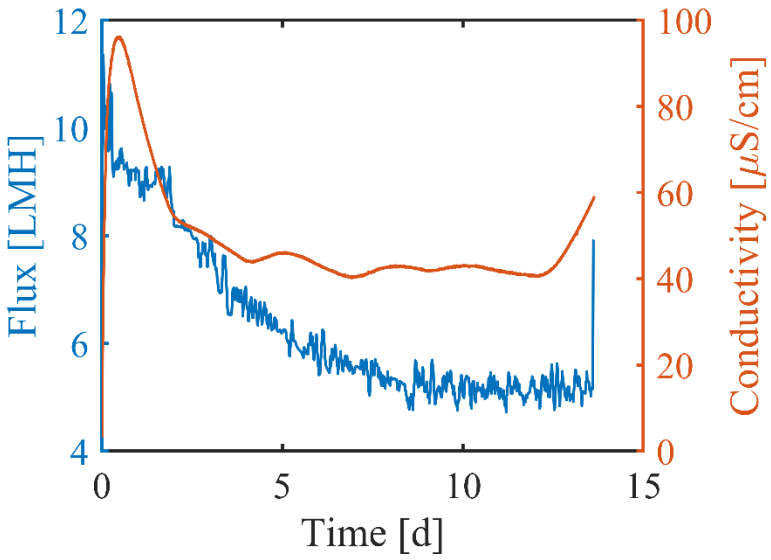

Figure 4.1: Flux and distillate conductivity during the treatment of buffered 5% HAP until membrane failure.

Mechanistically, all MD experiments have been run as a batch system with a constantly increasing CF. The DCMD schematic in Figure 4.2 is an alternative design that would restrict the CF by having a slow waste stream being pumped out of the feed tank.

Faster removal rates would result in lower CF. Using a steady state approximation, the CF can be estimated as a function of removal rate (R, m^3/hr) using Eq. 4.1 where Q is the rate of water distilling across the membrane in m^3/hr.

$$CF = \frac{Q - R}{R} \tag{4.1}$$

Long-term operation would reveal how constant exposure to the HAP and buffer affects MD operation without being confounded to the concentration effects associated with a changing CF.

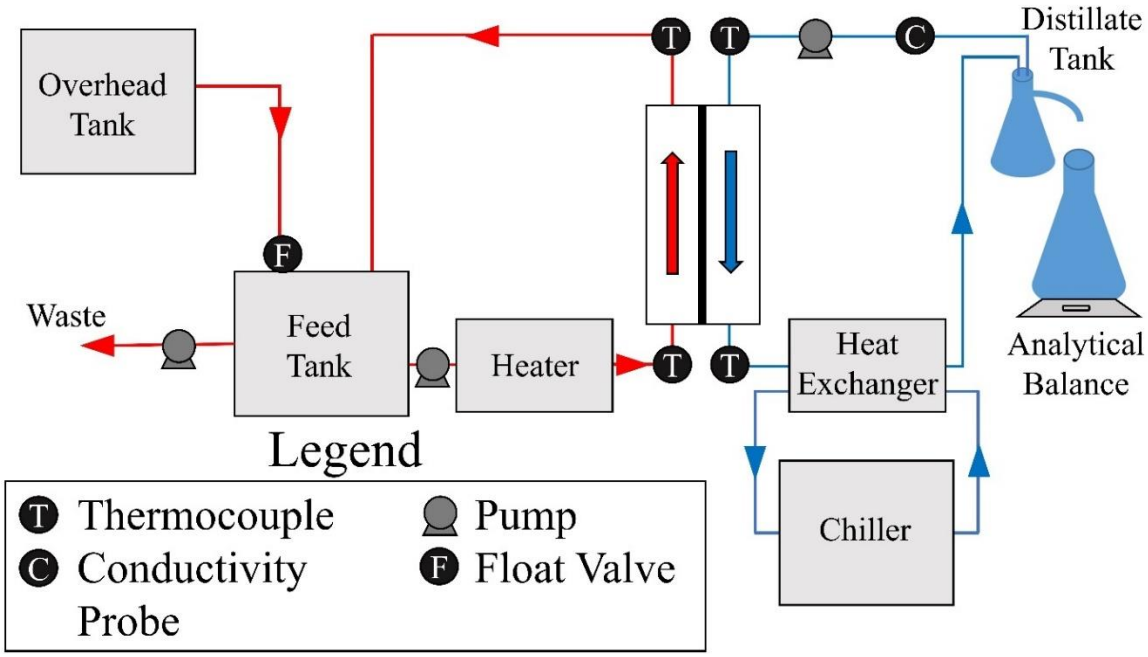

Figure 4.2: DCMD schematic with overhead tank and waste removal stream for constant CF operation.

4.2.4 Supernatant Recycling

In Chapter 3, a simplified recycling experiment was conducted that demonstrated the concentrated supernatant can be recycled back to the cultivation process, but extra nutrients were necessary. A 100% recycling rate is not possible even if only repeated once.

Preliminary energetics reveal MD will not be able to treat all the supernatant without an extra energy source, so there are several ways a recycle loop can be implemented between algae cultivation and MD, as demonstrated in Figure 4.3. Variation A is the method used in Chapter 3 and is limited by how much of the supernatant MD can treat, but offers the flexibility associated with concentrated nutrients or buffer. In Variation B, algae cultivation and the recycle loop are isolated from MD, but results in two waste streams. Variation C is a hybrid of A and B that is not limited by MD output, results in a single waste stream, but is a highly interconnected system. Based on the results of the simplified recycle experiment, Variation B is recommended. MD treatment volatilized NH_3 and COD, which are both beneficial for algae cultivation, so it is better to recycle prior to MD. Additionally, removing the interaction between MD and algae cultivation would decouple the system and allow for operational flexibility of both systems. If further energetic analysis or other improvements occur that help MD treat more of the supernatant, Variation A and C should be considered.

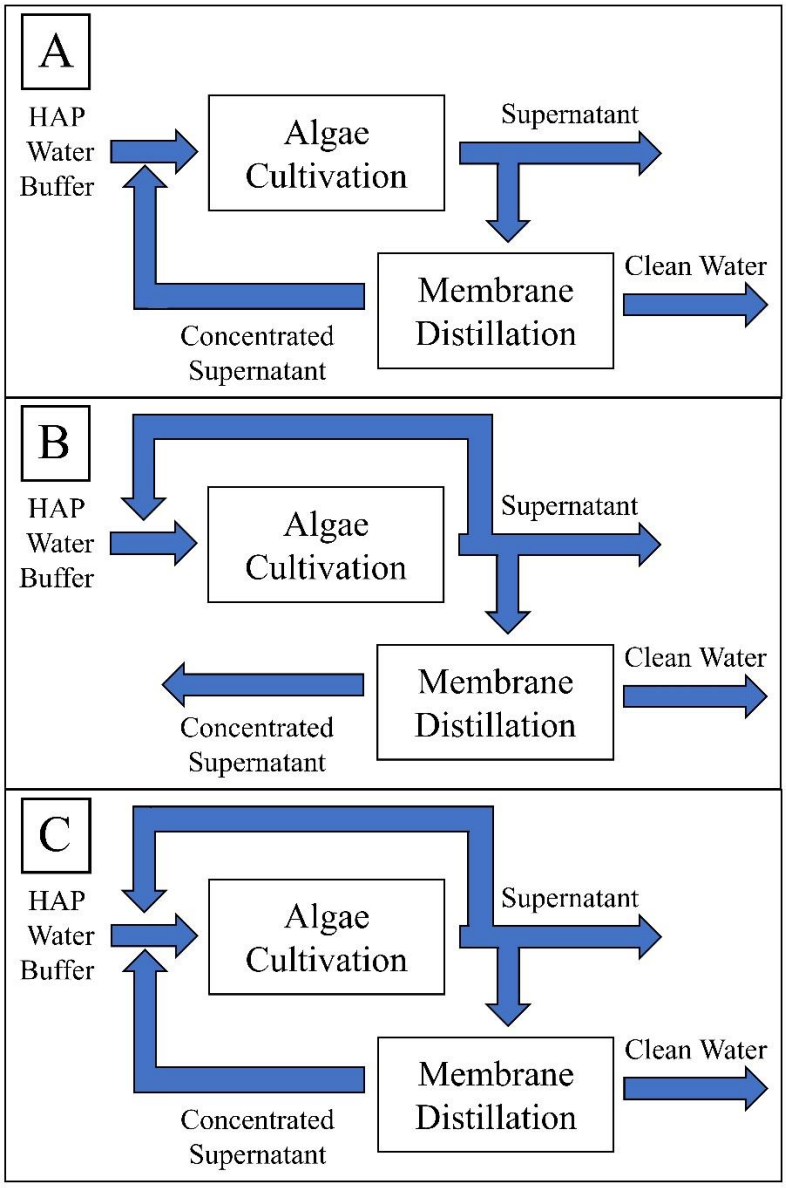

Figure 4.3: Supernatant recycle orientations: (A) recycle from MD concentrate, (B) recycle of supernatant, and (C) recycle from both MD concentrate and supernatant.

A properly implemented recycle loop would reuse some of the buffer and remediate more nutrients, but potentially decreases growth rates and increases footprint. The benefits and disadvantages associated with recycling should be assessed in another LCA. Since algae cultivation occurs as a batch system, the option to do a set number of recycles is

available. The results of the simple recycle experiment showed the growth mechanism is more complicated than what was suspected from the Chapter 2 results. During the regrowth cycle, NH_3 was not completely consumed like what was seen during Stage 1 and previous growth studies. The mechanism is likely a self-inhibiting biological byproduct or an unmeasured limiting nutrient. In Chapter 2, most algae could successfully be cultivated in 5% HAP but could not reliably be grown on 10% HAP. The inhibition at higher concentrations may have been excess nutrients, like NH_3 [9], or a toxic compound in the HAP. A recycling rate must be selected where there are sufficient nutrients for cultivation but does not result in an excessive concentration of potentially toxic compounds.

The recycle associated with Variation B, means the design variables are the initial HAP concentration, the recycle rate, and the HAP concentration of the replenishing stream. Algae cultivation with a 50% recycle rate with an initial and replenishing stream of 5% HAP feed means after the first growth stage, there would be fewer nutrients than in the initial 5% HAP. A fully consumed limiting species would converge to a concentration resembling 2.5% HAP and the concentration of a toxic inert remains at 5%. Likewise, an initial cultivation on 5% HAP with a 50% recycle replenished by 10% HAP would maintain ~5% of the limiting nutrient and the toxic inert would converge towards 10%. Comparative cultivation of a 5% HAP solution with 5% and 10% replenishing stream alongside cultivation on 2.5%, 5% and 10% HAP would identify if the growth is limited by a nutrient or the presence of a toxic or inhibiting compound. Figure 4.4 represents hypothetical growth trends for a species that cannot be cultivated on 10% HAP. The extent of the algae growth will be limited by the concentration of the limiting nutrient and the growth rate would be inhibited by the concentration of a toxic compound(s). Extra measurements

would be necessary to identify a limiting factor, although it is assumed that NH_3 is still frequently a limiting species. In addition to the measurements made in Chapter 2, measuring TOC and TKN would be beneficial to see if a different species is limited. The protein content of the culture should be measured by assay after each growth cycle. It was observed that the TN remediation per OD_{750} was higher for the Partial culture than the Fresh culture, suggesting the protein content changed under the different growth conditions. For maximum benefit of recycling the residual liquids after harvest, the algae should first be acclimated to the HAP as they may grow faster or remediate more nutrients. The rate of nutrient remediation and protein production should be measured after each growth stage to identify the number of recycling stages that should be done before stopping and cultivating on fresh HAP. The NEWIR Manure project has demonstrated potential to reduce several environmental impacts associated with dairy manure management [10,11]. Further advancements that increase remediation potential or decrease water usage would improve its sustainability and provide more benefits to the farmers.

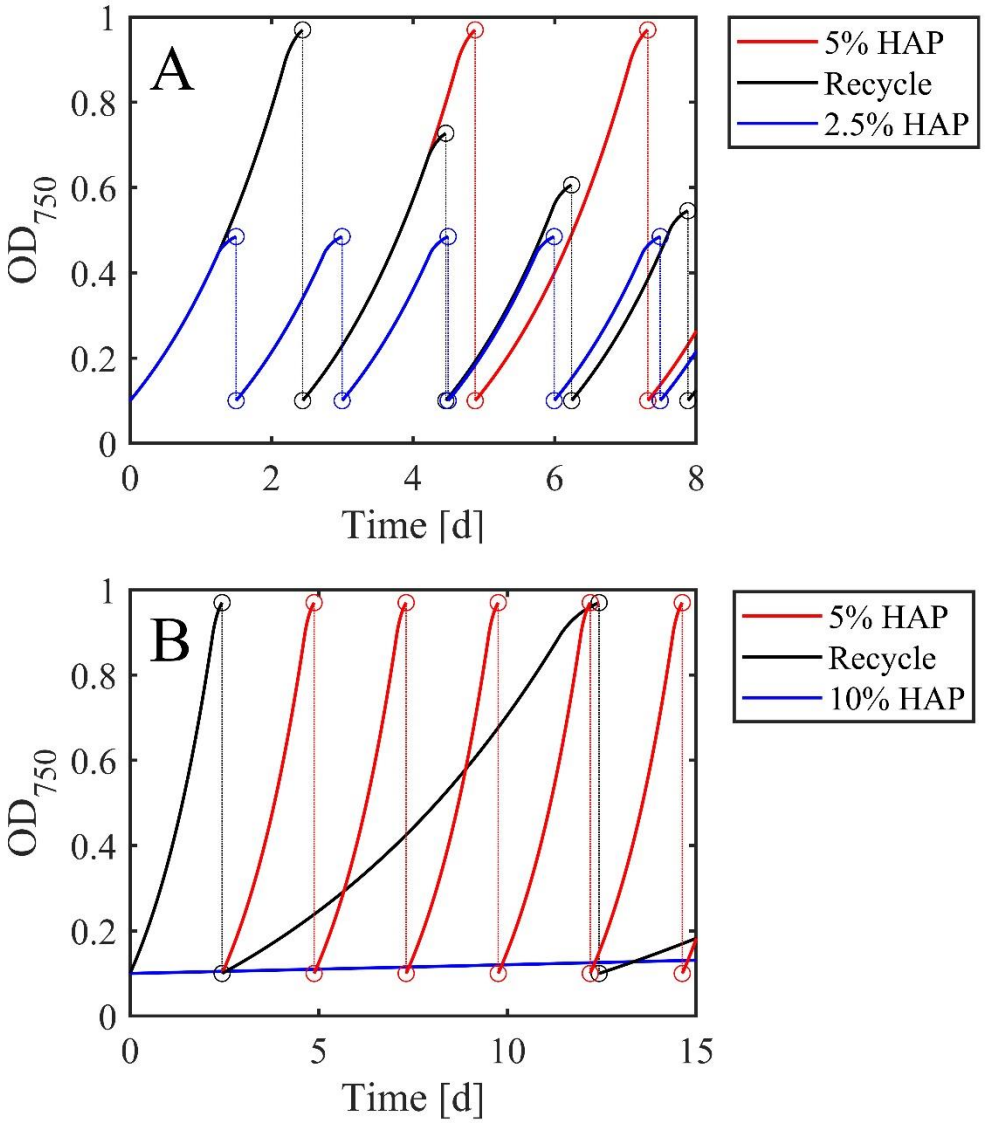

Figure 4.4: Hypothetical OD trends for (A) 50% recycle replenished with 5% HAP and (B) 50% recycle replenished with 10% HAP compared to repeated cultivation on 2.5%, 5%, and 10% HAP.

4.3 Works Cited

[1] R. Rezaei, A. Akbulut, S.L. Sanin, Effect of algae acclimation to the wastewater medium on the growth kinetics and nutrient removal capacity, Environ Monit Assess. 191 (2019). https://doi.org/10.1007/s10661-019-7856-7.

[2] Z. Zhu, G. Luan, X. Tan, H. Zhang, X. Lu, Rescuing ethanol photosynthetic production of cyanobacteria in non-sterilized outdoor cultivations with a bicarbonate-based pH-rising strategy, Biotechnol Biofuels. 10 (2017). https://doi.org/10.1186/s13068-017-0765-5.

[3] R.A. Soni, K. Sudhakar, R.S. Rana, Comparative study on the growth performance of Spirulina platensis on modifying culture media, Energy Reports. 5 (2019) 327–336. https://doi.org/10.1016/j.egyr.2019.02.009.

[4] P.F.R. Magwell, K.T. Djoudjeu, E. Minyaka, M.F. Tavea, O.W. Fotsop, R.F. Tagnikeu, A.M. Fofou, C.K.V. Darelle, C.U.D. Dzoyem, L.G. Lehman, Sodium Bicarbonate (NaHCO3) Increases Growth, Protein and Photosynthetic Pigments Production and Alters Carbohydrate Production of Spirulina platensis, Curr Microbiol. 80 (2023). https://doi.org/10.1007/s00284-022-03165-0.

[5] P. Shrivastava, R. Kumar, Soil salinity: A serious environmental issue and plant growth promoting bacteria as one of the tools for its alleviation, Saudi J Biol Sci. 22 (2015) 123–131. https://doi.org/10.1016/j.sjbs.2014.12.001.

[6] X. Xu, X. Du, F. Wang, J. Sha, Q. Chen, G. Tian, Z. Zhu, S. Ge, Y. Jiang, Effects of Potassium Levels on Plant Growth, Accumulation and Distribution of Carbon, and Nitrate Metabolism in Apple Dwarf Rootstock Seedlings, Front Plant Sci. 11 (2020). https://doi.org/10.3389/fpls.2020.00904.

[7] P. Zhang, Q. Sun, Y. Dong, S. Lian, Effects of different bicarbonate on spirulina in CO2 absorption and microalgae conversion hybrid system, Front Bioeng Biotechnol. 10 (2023). https://doi.org/10.3389/fbioe.2022.1119111.

[8] N.A. Silva, S.R. Hiibel, Nutrient recovery of the hydrothermal carbonization aqueous product from dairy manure using membrane distillation, Environ Technol. 0 (2021) 1–10. https://doi.org/10.1080/09593330.2021.1995785.

[9] A. Abeliovich, Y. Azov, Toxicity of ammonia to algae in sewage oxidation ponds, Appl Environ Microbiol. 31 (1976) 801–806. https://doi.org/10.1128/aem.31.6.801-806.1976.

[10] C.J. Glover, P.K. Cornejo, S.R. Hiibel, Life Cycle Assessment of Integrated Nutrient, Energy, and Water Recovery on Large-Scale Dairy Farms, Environ Eng Sci. 39 (2022) 811–820. https://doi.org/10.1089/ees.2021.0376.

[11] C.J. Glover, A. McDonnell, K.S. Rollins, S.R. Hiibel, P.K. Cornejo, Assessing the environmental impact of resource recovery from dairy manure, J Environ Manage. 330 (2023). https://doi.org/10.1016/j.jenvman.2022.117150.

5 APPENDIX

5.1 MATLAB Script for Fluorescence Analysis

```
function DATAsm = remove_interference(EMmat,EXmat,DATA,band)
% remove_interference(EMMAT, EXMAT, DATA, BAND) smooths the DATA matrix
% about the first and second order Rayleigh and Raman scattering where the
% EXMAT and EMMAT matrices represent the excitation and emission values for
% the DATA matrix. The BAND is a vector of length 4 where the indices are
% the estimated emission wavelengths [1st order Rayleigh, 2nd order Rayleigh,
% 1st order Raman, 2nd order Raman].


EMspec = EMmat(:,1)';
EXspec = EXmat(1,:)';
DATAsm = DATA;

for i = 1:length(EXspec)

    temp = DATAsm(:,i);
    tempx = EMspec;

    % estimation for scatter wavelengths
    ind = [EXspec(i),2*EXspec(i), 1e7/(1e7/EXspec(i)-
3682),2*(1e7/(1e7/EXspec(i)-3682))];

    id = zeros(1,length(ind));
    % true peaks
    maxloc = EMspec(islocalmax(smooth(temp)));

% Identifying true peaks and zeroing band
    for j = 1:length(id)
        [~,idx] = min(abs(maxloc-ind(j)));
        if abs(maxloc(idx) - ind(j))<band(j)
            id(j) = maxloc(idx);
        else
            id(j) = ind(j);
        end
        tempx( ( (id(j)-band(j) < EMspec) + (EMspec < id(j)+band(j)) )== 2 ) =
0;
    end

% removing zero values
    tempy = temp;
    tempy(tempx==0) = [];
    tempx(tempx==0) = [];

% Adding edge zero values if minimum or maximum x value was removed
    if ~ismember(min(EMspec), tempx)
        tempx = [min(EMspec)-20, tempx];
        tempy = [0; tempy];
    end
    if ~ismember(max(EMspec), tempx)
```

```
        tempx = [tempx, max(EMspec)+20];
        tempy = [tempy; 0];
    end

    temp = pchip(tempx,tempy,EMspec);
    temp(temp<0) = 0;
    DATAsm(:,i) = temp;

end

DATAsm(EXmat>EMmat) = 0;
% NaN for data removal. Creates white triangle for figure.
DATAsm(EXmat>EMmat+10) = NaN;
```

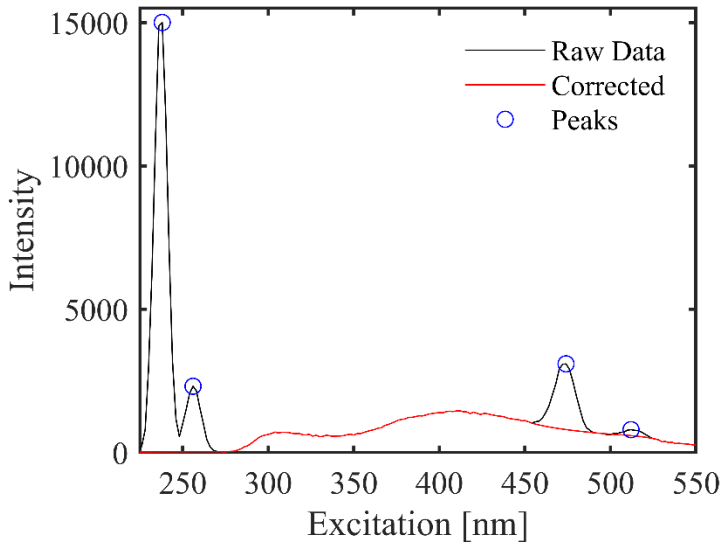

Figure 5.1: Example correction of the 1st and 2nd order Rayleigh and Raman scatter.